

## Supporting Information

### **Ketone-Functionalized Conjugated Organic Polymer Boosts Red-light-driven Molecular Oxygen-mediated Oxygenation**

Hao Zhang,<sup>\*a,b</sup> Tingting Yuan,<sup>a</sup> Nursaya Zhumabay,<sup>a</sup> Zhipeng Ruan,<sup>\*c</sup> Hai Qian<sup>\*b</sup>  
and Magnus Rueping<sup>\*a</sup>

*<sup>a</sup> KAUST Catalysis Center, KCC, King Abdullah University of Science and Technology, KAUST, Thuwal 23955-6900, Saudi Arabia. E-mail: magnus.rueping@kaust.edu.sa*

*<sup>b</sup> Department of Chemistry, School of Science, China Pharmaceutical University, Nanjing, 211198, P. R. China. E-mail: hzhang@cpu.edu.cn, qianhai24@163.com,*

*<sup>c</sup> Key Laboratory of Pharmaceutical Analysis and Laboratory Medicine (Putian University), Fujian Province University, 351100, Fujian, China. E-mail: rzp611@sina.com.*

Number of pages: 81

Number of figures: 24

Number of tables: 7

## Table of Contents

<b>1. General information</b> .....	<b>S3</b>
<b>2. Synthesis</b> .....	<b>S6</b>
2.1 Synthesis of TEP monomers (Scheme S1) .....	S6
2.2 Synthesis of POPs (Scheme S2) .....	S7
2.2 Synthesis of the substrates .....	S8
<b>3. Catalytic evaluation</b> .....	<b>S9</b>
3.1 General procedure .....	S9
3.2 Reaction comparison with L-proline as co-catalyst using acetone as solvent .....	S9
3.3 Catalyst recycling and catalyst stability study .....	S9
<b>4. Figure</b> .....	<b>S10</b>
<b>5. Table</b> .....	<b>S22</b>
<b>6. Reference</b> .....	<b>S26</b>
<b>7. NMR data</b> .....	<b>S27</b>
<b>8. NMR Spectra</b> .....	<b>S39</b>

## 1. General information

All required fine chemicals were purchased from commercial suppliers (abcr, Acros, Alfa Aesar, Fluka, Fluorochem, Merck, Sigma Aldrich, TCI, BLDPharm) and were used directly without further purification unless stated otherwise. All air and moisture sensitive reactions were carried out under nitrogen atmosphere inside the glovebox. Solvents were purchased and used as received.

**Liquid Nuclear Magnetic Resonance (NMR) spectra** for  $^1\text{H}$ ,  $^{13}\text{C}$  and  $^{19}\text{F}$  were recorded at room temperature using a Bruker AVANCE HD III 500M NMR spectrometer (500 MHz for  $^1\text{H}$ , 126 MHz for  $^{13}\text{C}$ , 471 MHz for  $^{19}\text{F}$ ) and Bruker AVANCE HD III 400M NMR spectrometer (400 MHz for  $^1\text{H}$ , 101 MHz for  $^{13}\text{C}$ , 377 MHz for  $^{19}\text{F}$ ). All chemical shifts are reported in  $\delta$ -scale as parts per million [ppm] (multiplicity, coupling constant  $J$ , number of protons) relative to the solvent residual peaks as the internal standard. Coupling constants  $J$  are given in Hertz [Hz]. Abbreviations used for signal multiplicity:  $^1\text{H}$ -NMR: b = broad, s = singlet, d = doublet, t = triplet, q = quartet, p = quintet, and m = multiplet. NMR spectrometer in  $\text{CDCl}_3$ , DMSO- $d_6$  solutions with internal solvent signals (for  $^1\text{H}$  and  $^{13}\text{C}$ ) as reference (7.26, 77.2 for  $\text{CDCl}_3$ , 2.50 and 39.5 for DMSO- $d_6$ ).

**Solid-state  $^{13}\text{C}$  cross-polarization MAS NMR spectra** (CP/MAS NMR) were carried out on Bruker AVANCE III 400WB Plus spectrophotometer at resonance frequencies of 100.6 MHz, and with a sample spinning rate of 10 kHz using 4 mm rotors, a contact time of 2 ms (ramp 100) and pulse delay of 3 s were applied.

All the NMR data were analyzed using commercially available software, Mestnova software (Mestrelab Research).

**X-ray Photoelectron Spectroscopy (XPS) studies** were conducted using a Kratos Axis Ultra DLD spectrometer with an Al  $K\alpha$  X-ray source operating at 150 W. The measurements were performed under ultra-high vacuum conditions ( $10^{-8}$  -  $10^{-9}$  mbar) with hybrid mode using electrostatic and magnetic lenses. High-resolution spectra were collected at a fixed analyzer pass energy of 20 eV. Charge neutralization was achieved with low-energy electrons for all samples. The C 1s spectrum line (284.8 eV for C-C aromatic carbon species) was used for binding energy correction. Powder samples were immobilized on Cu conductive tape from SPI supplies and placed on the sample holder. The samples were evacuated overnight until an ultra-high vacuum was reached. The data were analyzed using commercially available software, Avantage 6.60.

**UV-vis diffuse reflectance spectra (UV-vis DRS)** were collected using a JASCO V-670 UV-Vis-NIR spectrophotometer equipped with a 60 mm  $\text{BaSO}_4$ -coated integrating sphere and a PMT/PbS detector in the acquisition range of 300 - 900 nm at room temperature.  $\text{BaSO}_4$  (99.99 %, Sigma-Aldrich) was used as a reference. Optical bandgap values were estimated by using Tauc plot analysis of optical diffuse reflectance spectra.

**Attenuated total reflection fourier transform Infrared (ATR-FTIR) spectra** were recorded on an Thermo Scientific Nicolet iS20 FTIR Spectrometer with a diamond Smart iTX ATR accessory using 64 scans and  $4\text{ cm}^{-1}$  resolution at a mid-IR range of  $525\text{-}4000\text{ cm}^{-1}$ .

**Thermal gravimetric analyses (TGA)** were performed under N<sub>2</sub> gas flow (25 mL/min) with a heating rate of 10 °C/min from 40 to 800 °C using a TA Discovery TGA 5500 thermal analyzer.

**Field-emission Scanning Electron Microscopy (FE-SEM).** The SEM images and map scans were collected on a Zeiss Merlin FE-SEM (Carl Zeiss, Merlin compact, Germany) microscope. Samples were activated and coated with iridium to ~ 5 nm thickness in a Denton Desk III TSC Sputter Coater (Moorestown, NJ) before imaging.

**Transmission Electron Microscope (TEM).** The microstructure of the samples was characterized using a Titan Themis Z G3 Cs-Corrected TEM microscope operated at 200 kV.

**Gas sorption measurements** were obtained with Micromeritics ASAP 2420 automated surface area and porosimetry system at 77 K controlled by liquid N<sub>2</sub>. The samples were outgassed at 120 °C for 8 h before the measurements. Surface areas were calculated from the adsorption data using Brunauer-Emmett-Teller (BET) methods. The pore-size-distribution curves were obtained from the adsorption branches using 2D-NLDFT (N<sub>2</sub>-carbon finite pores, As=6) method with SAIEUS 3.0 program.

**The Powder X-ray diffraction patterns (PXRD)** were obtained on the Bruker D8 Advanced diffractometer, equipped with a copper tube operating at 40 kV and 40 mA. The diffractograms were obtained by scanning the 2θ range from 3 to 80°, with a step size of 0.020° and a time per step of 1 s.

**The inductively coupled plasma optical emission spectrometer (ICP-OES) analysis** was performed using an Agilent 5110 synchronous vertical dual view ICP-OES analyzer (Agilent Technologies, Santa Clara, CA, USA) with an autosampler to determine the Pd and Cu content of the samples. The samples (5 mg was used) was firstly digested by HNO<sub>3</sub>/HCl (1/3 mL; HNO<sub>3</sub>: 65%, HCl: 37%) solvent in the ultraCLAVE microwave digestion system.

**Gas chromatography analyses (GC-FID)** were carried out on an SHIMADZU GC-2014 system equipped using a flame ionization detector.

**Gas chromatography- mass spectrometer (GC-MS)** data were performed on Agilent Technologies 7890A GC system with 5975C inert XL MS Detector.

Column: Agilent J&W GC HP-5 capillary column (30 m × 320 μm × 0.25 μm film thickness)

Temperature program: Starting temperature: 75 °C, Hold: 1 min, Ramp: 50 °C/min, End temperature: 300 °C. Hold: 4.5 min.

Heterogenous samples were filtered and diluted with ethyl acetate prior to injection.

**High resolution mass spectrometry (HRMS)** was recorded on a Thermo Scientific LTQ Orbitrap XL spectrometer.

**Electron Paramagnetic Resonance (EPR).** Electron paramagnetic resonance (EPR) was carried out on Bruker A300.

Photogenerated electron signal measurement: 5 mg powder samples were put into the glass tube and tested directly.

EPR trapping measurement: 2.5 mg powder samples was dispersed in 2 mL of MeCN. After ultrasonic oscillation for 30 min, 200  $\mu\text{L}$  of mixed solution was taken and 200  $\mu\text{L}$  100 mM 5,5-dimethyl-1-pyrroline N-oxide (DMPO for  $\text{O}_2^{\cdot-}$ ) or TEMPO (for  $^1\text{O}_2$ ) solution was added. After mixing and shaking, it was loaded into a capillary tube and then put into a glass tube for machine testing. After that, 0.2 mmol THIQ substrate was added to the above MeCN solution. The same procedures were followed for machine testing.

All tests were carried out at room temperature, divided into dark conditions and light 15 min conditions. The light source is a commercial 300 W Xenon lamp (PLS-SXE300+, PerfectLight Co., Ltd) equipped with 600 nm longpass filter.

**Photoelectrochemical and electrochemical characterizations.** Photoelectrochemical measurements were performed with a three-electrode system using a CHI 660E electrochemical workstation with an Ag/AgCl in a saturated KCl solution as the reference electrode and a Pt plate counter electrode. The working electrode was prepared as follows: 4 mg of sample was dispersed in 5% Naflon solution, 0.375 mL  $\text{H}_2\text{O}$  and 0.125 mL  $\text{C}_2\text{H}_5\text{OH}$  by sonication to get a slurry. The slurry (100  $\mu\text{L}$ ) was coated on ITO glass with a fixed area of 1  $\text{cm}^2$ . The working electrodes were dried under vacuum at 60  $^\circ\text{C}$  for 12 h. A 0.1 M  $\text{Na}_2\text{SO}_4$  (pH = 7) was used as the electrolyte.

The transient photocurrent density was measured at open circuit voltage irradiated by a commercial 300 W Xenon lamp (PLS-SXE300+, PerfectLight Co., Ltd) equipped with 600 nm longpass filter. The light automatically turned on and off by an shutter controller (PFS40A, PerfectLight Co., Ltd) at a time interval of 50 s.

Electrochemical impedance spectroscopy (EIS) was measured via an electrochemical workstation (CHI 660E) in the three-electrode cell in the presence of 0.1 M  $\text{Na}_2\text{SO}_4$  solution with 5 mV amplitude in the frequency range from 0.01 Hz to 100 kHz under open circuit potential conditions.

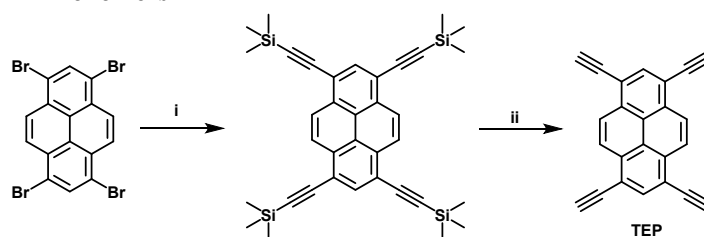
Mott–Schottky plots were obtained using an electrochemical workstation (CHI 660E) with 5 mV amplitude to evaluate the flat band potential. The frequencies were 500, 1000, and 1500 Hz.

#### **Computational Details:**

All the model units were first drawn in ChemDraw (20.0.0.41) and saved as MDL Molfile. The geometries of those molecules were then optimized with the MMFF94 force field using Avogadro (1.2.0). Then, sequential geometry optimizations and frequency calculations were performed by DFT using ORCA 5.0.4 with the B3LYP functional and the def2-SVP basis sets.<sup>1</sup> After that, TD-DFT was performed with the B3LYP functional and def2-TZVP basis set to compute the vertical transition energies. The optimized structures were also showed with Avogadro (1.2.0).

## 2. Synthesis

### 2.1 Synthesis of TEP monomers



**Scheme S1.** Synthesis of 1,3,6,8-tetraethynylpyrene (i) 6 equiv trimethylsilylethyne,  $[\text{PdCl}_2(\text{PPh}_3)_2]$ ,  $\text{PPh}_3$ ,  $\text{CuI}$ , toluene/triethylamine,  $80\text{ }^\circ\text{C}$ , 83%; ii) 8 equiv  $\text{K}_2\text{CO}_3$ , methanol, 92%.

TEP monomer has been synthesized according to the reported literature procedure.<sup>2</sup>

#### Synthesis of 1,3,6,8-tetrakis(trimethylsilylanylethynyl)pyrene :

1,3,6,8-Tetrabromopyrene (5.45 g, 10 mmol) was suspended in triethylamine (120 mL) and toluene (25 mL), and bis(triphenylphosphine)palladium(ii) dichloride (1.36 g, 1.9 mmol), copper(i) iodide (730 mg, 3.9 mmol), and triphenylphosphine (1.01 g, 3.9 mmol) were added. The flask was evacuated and flushed with  $\text{N}_2$ . While stirring, the reaction mixture was heated to  $60\text{ }^\circ\text{C}$  and trimethylsilylethyne (5.8 mL, 58 mmol) was injected through a septum. After 15 min of stirring at this temperature the reaction was heated to  $80\text{ }^\circ\text{C}$  and stirred overnight under  $\text{N}_2$  atmosphere. The cooled reaction mixture was diluted with  $\text{CH}_2\text{Cl}_2$  and extracted with water. The organic phase was dried over  $\text{MgSO}_4$ , and the solvent was removed under reduced pressure. The crude product was purified by column chromatography (silica gel, petroleum ether) to afford the product as an orange solid (4.9 g, 83%).

$^1\text{H}$  NMR (400 MHz, Chloroform-*d*)  $\delta$  8.60 (s, 2H), 8.31 (s, 1H), 0.38 (s, 18H).

$^{13}\text{C}$  NMR (101 MHz, Chloroform-*d*)  $\delta$  134.55, 132.05, 127.02, 123.63, 118.65, 102.79, 101.47.

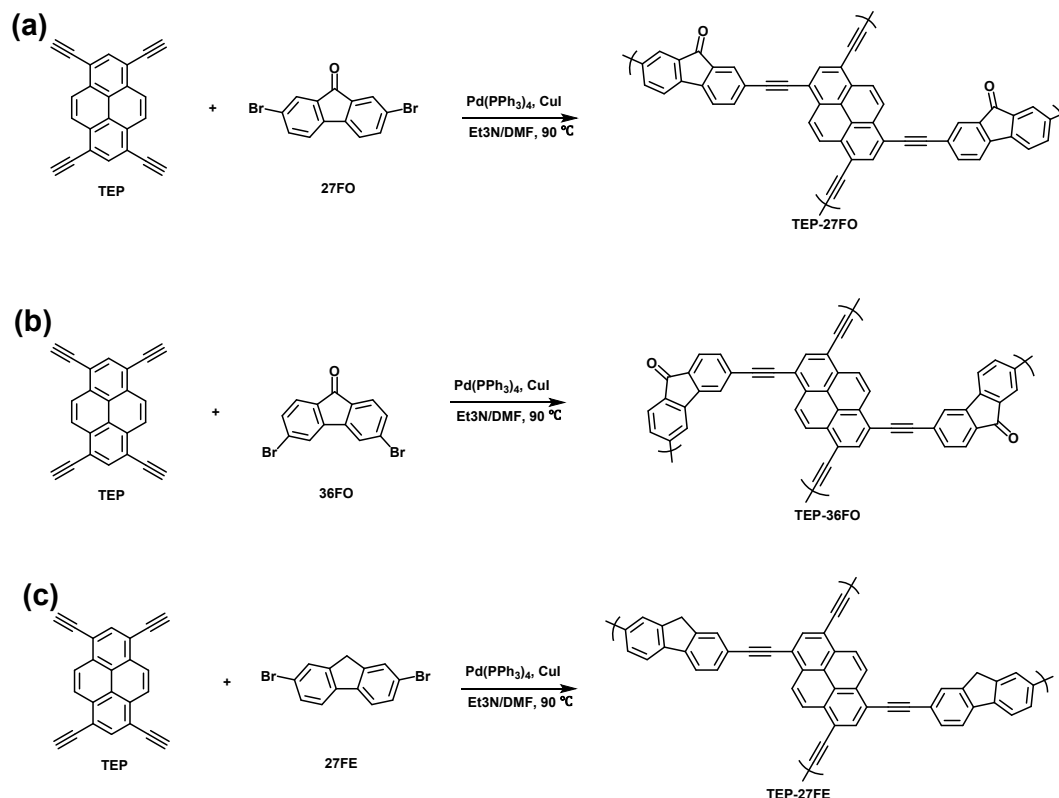
#### Synthesis of 1,3,6,8-tetrakis(trimethylsilylanylethynyl)pyrene (TEP) :

The synthesized 1,3,6,8-tetrakis(trimethylsilylanylethynyl)pyrene (3 g, 5 mmol) was suspended in methanol (250 mL).  $\text{K}_2\text{CO}_3$  (5.53 g, 40 mmol) was added and the reaction mixture stirred overnight and then poured into water (500 mL) and filtered. The filter was washed with water until the filtrate was neutral to afford the desired TEP as a slightly brown solid (1.37 g, 92%).

$^1\text{H}$  NMR (400 MHz, DMSO-*d*<sub>6</sub>)  $\delta$  8.60 (s, 4H), 8.36 (s, 2H), 4.97 (s, 4H).

$^{13}\text{C}$  NMR (101 MHz, DMSO-*d*<sub>6</sub>)  $\delta$  135.22, 131.97, 127.30, 122.39, 118.30, 88.74, 81.24.

## 2.2 Synthesis of POPs



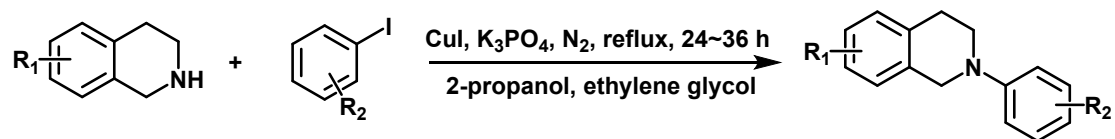
**Scheme S2.** Synthesis of (a) TEP-27FO, (b) TEP-36FO and (c) TEP-27FE by Sonogashira-Hagihara cross-coupling.

As shown in Scheme S2(a), TEP (44.8 mg, 0.15 mmol), 27FO (100.8 mg, 0.3 mmol), tetrakis(triphenylphosphine)palladium(0) (6 mg, 0.005 mmol), and CuI (0.9 mg, 0.0005 mmol) were added to a two-necked round-bottom flask. The flask was ex-changed between vacuum and N<sub>2</sub> for three cycles. Subsequently, a mixed solution of N,N-dimethylformamide (15 mL) and triethylamine (15 mL) was injected into the reaction flask. The reaction was performed at 90 °C under the protection of N<sub>2</sub> and stirred for 24 h. After cooling to room temperature, the solid product was collected via filtration. The product was stirred in 50 ml HCl (1 M) for 12 h and washed with water. Subsequently, the product was sequentially washed with excess methanol, toluene, chloroform, and acetone. After drying, the polymer was purified via Soxhlet extraction using methanol and THF for 24 h. Finally, the red powder (TEP-27FO, 80.3 mg, 86% yield) was obtained by drying the mixture in a vacuum oven (Scheme S2(a)).

The synthesis and post-treatment of TEP-36FO (83.5 mg, 82% yield) were similar to those of TEP-27FO, with the only difference being the substitution of 36FO (100.8 mg, 0.3 mmol) for 27FO (100.8 mg, 0.3 mmol) (Scheme S2(b)).

The synthesis and post-treatment of TEP-27FE (80.7 mg, 85% yeild) were similar to those of TEP-27FO, with the only difference being the substitution of 27FE (96.6 mg, 0.3 mmol) for 27FO (100.8 mg, 0.3 mmol) (Scheme S2(c)).

### 2.3 Synthesis of the substrates



Substrates were synthesized as reported.<sup>3,4</sup> A Schlenk tube (100 mL) was charged with Copper(I) iodide (200 mg, 1.0 mmol) and potassium phosphate (4.25 g, 20 mmol). The tube was evacuated and back filled with nitrogen. 2-Propanol (10.0 mL), ethylene glycol (20.0 mmol, 1.1 mL), substituted tetrahydroisoquinoline (15.0 mmol) and corresponding aryl iodide (10.0 mmol) were added successively via a micro-syringe at room temperature. The reaction mixture was heat to reflux at 85 °C under N<sub>2</sub> for 24 ~ 36 h. The reaction was monitored by TLC until the consumption of aryl iodide. After cooling to room temperature, water (20 mL) was added to quench the reaction. The mixture was extracted with CH<sub>2</sub>Cl<sub>2</sub> (3\*15 mL) and washed with brine (1\*15 mL). The organic phases were combined, dried over anhydrous MgSO<sub>4</sub> and concentrated under vacuum. The reaction crude was purified by column chromatography using petroleum ether and ethyl acetate as eluent.



### 3. Catalytic evaluation

#### 3.1 General procedure

A 5 mL cap vial equipped with a magnetic stirring bar was load with catalyst ( 2.5 mg for 0.1 mmol substrate), 1,5-diazabicyclo[4.3.0]non-5-ene (DBN) ( 0.15 mmol, 19  $\mu$ L, 1.5 eq.), the corresponding THIQ derivatives (0.1 mmol), MeCN (2 mL, 0.05M) and *n*-dodecane (0.1 mmol, 27  $\mu$ L) as the internal standard. In doing so, all solid compounds were added before capping the vial, whereas all liquid compounds were added via syringe after setting the capped vial under an O<sub>2</sub> atmosphere (highly viscous liquids were added before capping the vial as well). The reaction mixture was stirred under 1 bar of O<sub>2</sub> using an O<sub>2</sub>-filled balloon and under light irradiation using a 640 nm LEDs (Kessil PR160L-640nm-C (40 W Max) 100%) at 25-30 °C with Fan cooling. The reaction yield was monitored by withdrawing a small amount of the reaction mixture with a syringe and analyzing it by GC-FID. The crude product was purified by automated flash column chromatography using a petrol ether/ethyl acetate mixture.

#### 3.2 Reaction comparison with L-proline as co-catalyst using acetone as solvent

The reaction followed the above general procedure. The main differences are the addition of L-proline (0.01 mmol, 1 mg 10 mol%) a cocatalyst and the use of acetone as a solvent. The final isolate product 2aa is a pale yellow liquid (2aa, 24.5 mg, 83%).

<sup>1</sup>H NMR (500 MHz, Chloroform-*d*)  $\delta$  7.19 – 7.13 (m, 3H), 7.13 – 7.08 (m, 1H), 6.91 (d, *J* = 9.0 Hz, 2H), 6.85 – 6.78 (m, 2H), 5.24 (t, *J* = 6.4 Hz, 1H), 3.75 (s, 3H), 3.60 – 3.52 (m, 1H), 3.46 (ddd, *J* = 13.0, 10.3, 4.4 Hz, 1H), 3.00 (dq, *J* = 16.3, 5.3 Hz, 2H), 2.75 (ddd, *J* = 20.3, 12.0, 5.1 Hz, 2H), 2.06 (s, 3H).

<sup>13</sup>C NMR (126 MHz, Chloroform-*d*)  $\delta$  207.45, 153.31, 143.71, 138.28, 134.34, 128.96, 126.83, 126.65, 126.21, 118.44, 114.65, 56.00, 55.63, 49.99, 42.90, 30.90, 26.75.

#### 3.2 Catalyst recycling and catalyst stability study

Every cycle of the catalytic processes followed the above general procedure. After the completion of the reaction, the reaction mixture was filtered, the filtrate part was analyzed by GC-FID, and the filter part was washed with different solvents such as water, dichloromethane, methanol, and acetone. The filtered photocatalyst was dried at 80 °C under a high vacuum. The dried photocatalyst has been used for the next run directly. The stability of recycled photocatalyst was investigated using UV and IR spectroscopy.

#### 4. Figure

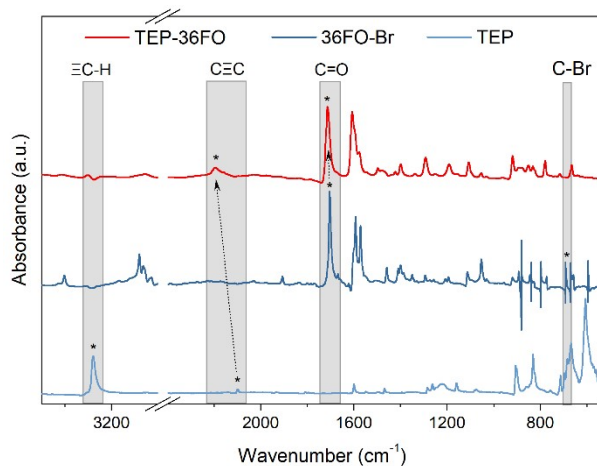


**Figure S1.** FT-IR spectra of **TEP-36FO** and its corresponding monomers. The characteristic bands at 2196 cm<sup>-1</sup> and 1711 cm<sup>-1</sup> corresponded to the stretching vibration of C≡C and C=O in **TEP-36FO**, respectively.

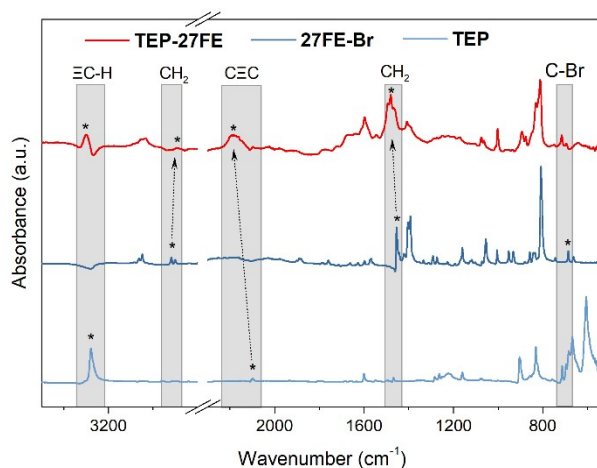


**Figure S2.** FT-IR spectra of **TEP-27FE** and its corresponding monomers. The characteristic bands at 2185 cm<sup>-1</sup> and 2891 cm<sup>-1</sup> corresponded to the stretching vibration of C≡C and C-H in the methylene group of **TEP-27FO**, respectively. The strong -CH<sub>2</sub>- in-plane bending vibration of the methylene group is also observed at 1480 cm<sup>-1</sup>. The observed peaks of ≡C-H and C-Br stretching vibration suggests the presence of residual incomplete polymerization.

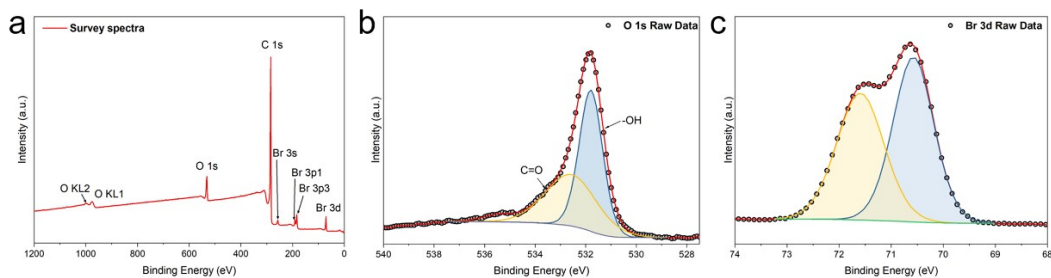


**Figure S3.** XPS spectra of **TEP-27FO**. (a) Survey scan XPS profile, high-resolution XPS spectra of (b) O 1s (c) Br 3d. In the C 1s spectra, since the binding energy of Br-C( $sp^2$ ), around 284.5 eV, overlaps with that of the triple bond carbon and its content is relatively low, peak fitting was not performed for it. The O 1s peaks can be divided into two peaks for absorbed -OH at 531.7 eV and C=O at 532.6 eV, respectively. The Br 3d spectra was fit to a doublet (70.57 eV and 71.59 eV,  $\Delta=1.04$  eV) corresponding to the Br 3d $_{5/2}$  and Br 3d $_{3/2}$  overlapping spin orbitals. In addition, no peaks assigning to possible metal residues including Pd 3d $_{5/2}$  (335-341 eV) and Cu 2p $_{3/2}$  (931~936 eV) were detected in the survey scan profile of XPS spectra. However, the ICP analysis indicated the presence of residual Pd and Cu in the polymers.

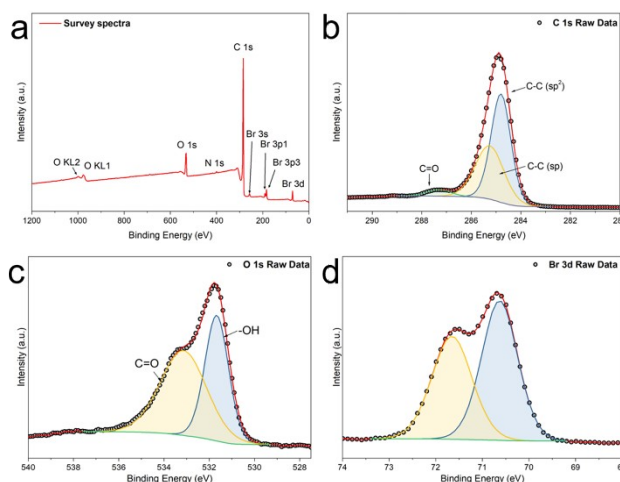


**Figure S4.** XPS spectra of **TEP-36FO**. (a) Survey scan XPS profile, high-resolution XPS spectra of (b) C 1s (c) O 1s (d) Br 3d. The C 1s peaks can be divided into three peaks for aromatic carbon at 284.8 eV, triple bond carbon at 285.3 eV and ketone carbon at 287.3 eV, respectively. In the C 1s spectra, since the binding energy of Br-C( $sp^2$ ), around 284.5 eV, overlaps with that of the triple bond carbon and its content is relatively low, peak fitting was not performed for it. The O 1s peaks can be divided into two peaks for absorbed -OH at 531.7 eV and C=O at 533.2 eV, respectively. The Br 3d spectra was fit to a doublet (70.63 eV and 71.67 eV,  $\Delta=1.04$  eV) corresponding to the Br 3d $_{5/2}$  and Br 3d $_{3/2}$  overlapping spin orbitals. In addition, no peaks assigning to possible metal residues including Pd 3d $_{5/2}$  (335-341 eV) and Cu 2p $_{3/2}$  (931~936 eV) were detected in the survey scan profile of XPS spectra. However, the ICP analysis indicated the presence of residual Pd and Cu in the polymers.

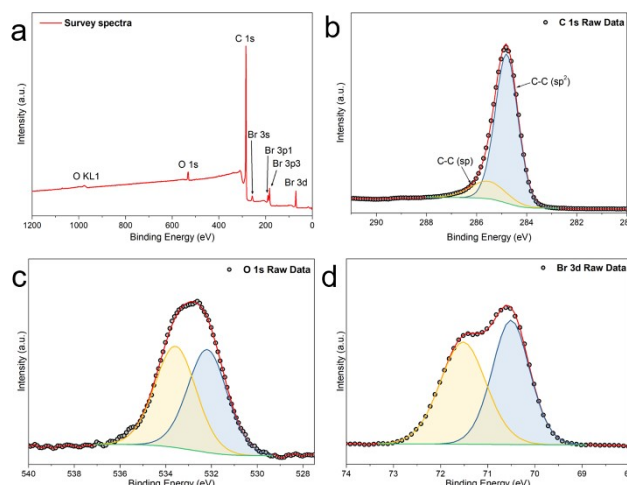


**Figure S5.** XPS spectra of **TEP-27FE**. (a) Survey scan XPS profile, high-resolution XPS spectra of (b) C 1s (c) O 1s (d) Br 3d. The C 1s peaks can be divided into two peaks for aromatic carbon at 284.8 eV, triple bond carbon at 285.6 eV, respectively. In the C 1s spectra, since the binding energy of Br-C( $sp^2$ ), around 284.5 eV, overlaps with that of the triple bond carbon and its content is relatively low, peak fitting was not performed for it. The O 1s peaks may be attributed to organic impurities introduced during the reaction process. The Br 3d spectra was fit to a doublet (70.49 eV and 71.53 eV,  $\Delta=1.04$  eV) corresponding to the Br  $3d_{5/2}$  and Br  $3d_{3/2}$  overlapping spin orbitals. In addition, no peaks assigning to possible metal residues including Pd  $3d_{5/2}$  (335-341 eV) and Cu  $2p_{3/2}$  (931-936 eV) were detected in the survey scan profile of XPS spectra. However, the ICP analysis indicated the presence of residual Pd and Cu in the polymers.

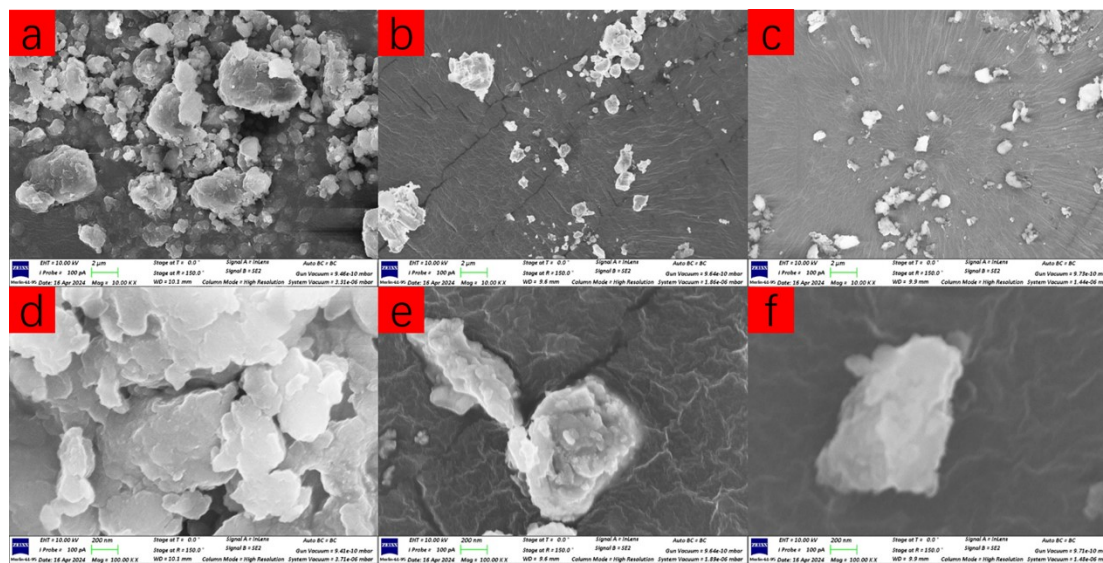


**Figure S6.** SEM images of (a, d) **TEP-27FO**, (b, e) **TEP-36FO**, (c, f) **TEP-27FE**. SEM images show the morphologies of three **TEP-X** POPs with a diameter of 2-4  $\mu\text{m}$ , which is assembled by numerous layered blocks.

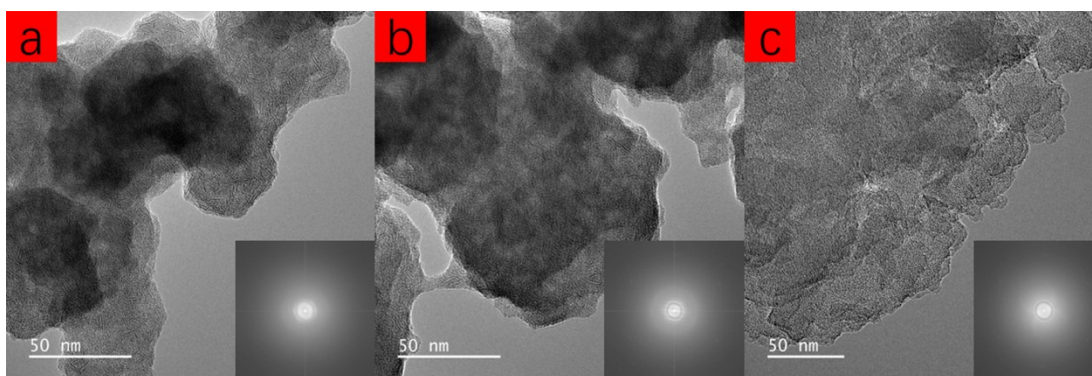


**Figure S7.** High resolution TEM images and corresponding FFT pattern of (a) **TEP-27FO**, (b) **TEP-36FO**, (c) **TEP-27FE**. The diffraction fingers can not be observed in the samples due to the relatively low crystallinity.

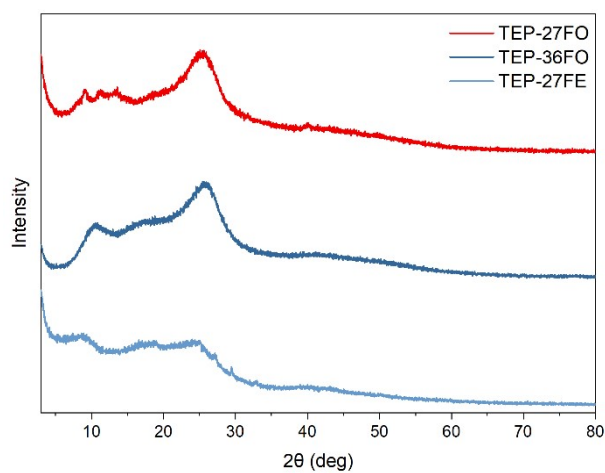


**Figure S8.** PXRD spectra of the **TEP-X** ( $X = 27\text{FO}$ ,  $36\text{FO}$  and  $27\text{FE}$ ) samples. The broad peak located at 25-30 degrees can be signed to (001) facet. The (001) facet originate from the  $\pi$ - $\pi$  stacking of 2D covalent layers.<sup>6</sup>

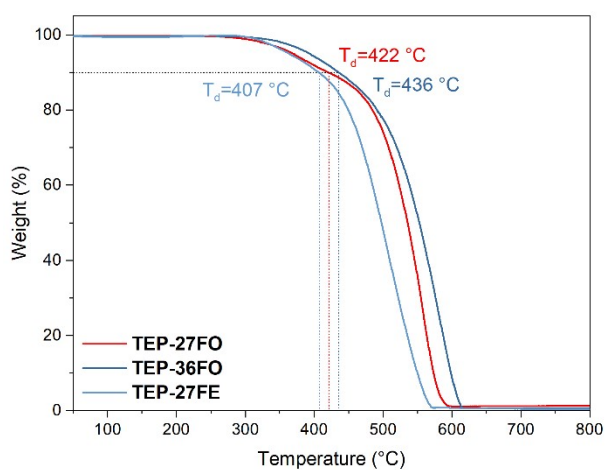


**Figure S9.** TGA curves of the **TEP-X** ( $X = 27\text{FO}$ ,  $36\text{FO}$  and  $27\text{FE}$ ) samples.

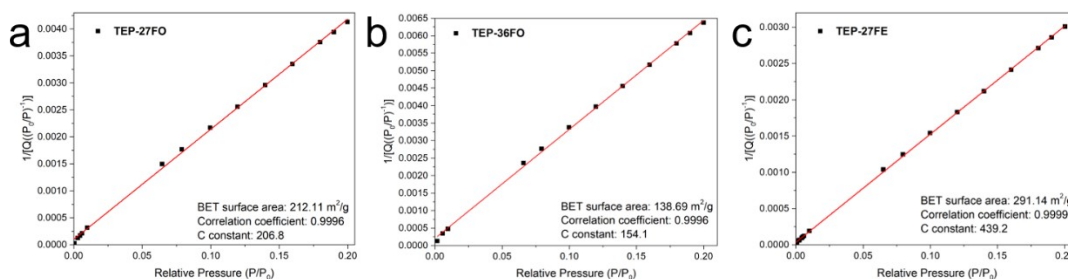


**Figure S10.** BET plot of (a) TEP-27FO, (b) TEP-36FO, (c) TEP-27FE.

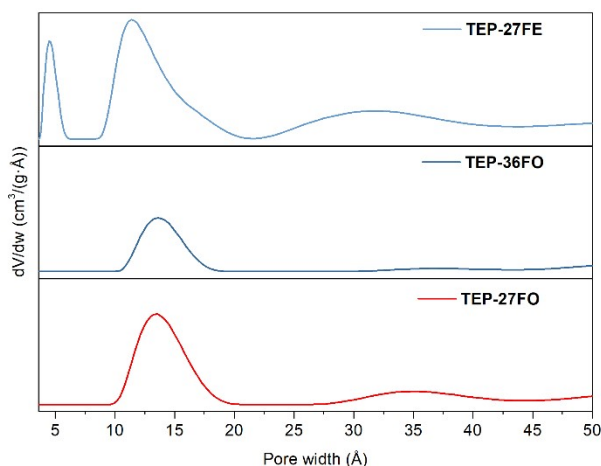


**Figure S11.** Pore size distributions of the TEP-X (X = 27FO, 36FO and 27FE) samples based on the calculation results of the NLDFT method. The additional ketone groups within the skeleton of TEP-27FO and TEP-36FO may work as pore-directing “anchors”, improving the stacking of the layers, which results in uniform pore size distribution.<sup>5</sup>

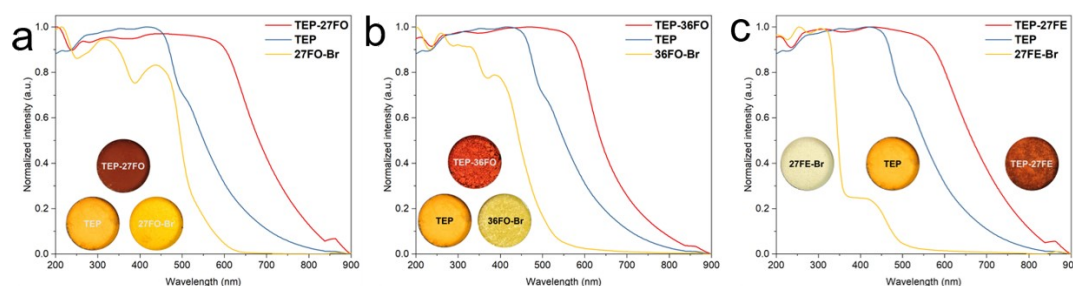


**Figure S12.** UV-vis absorption spectra of TEP-X (X = 27FO, 36FO and 27FE) powders and their corresponding reactant monomers (inset: digital photograph)



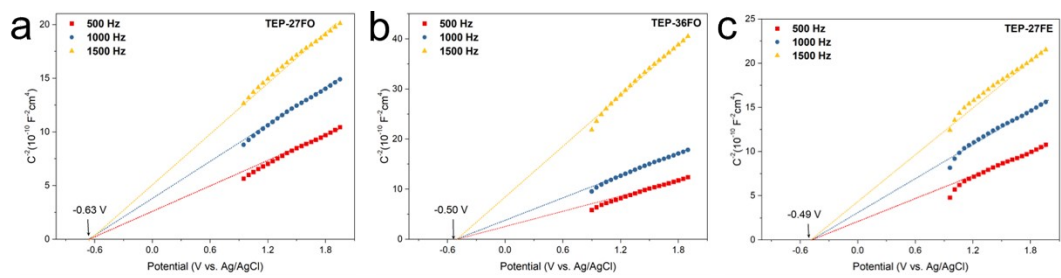


**Figure S13.** Mott-Schottky plots of (a) TEP-27FO, (b) TEP-36FO, (c) TEP-27FE at 500 Hz, 1000 Hz and 1500 Hz.

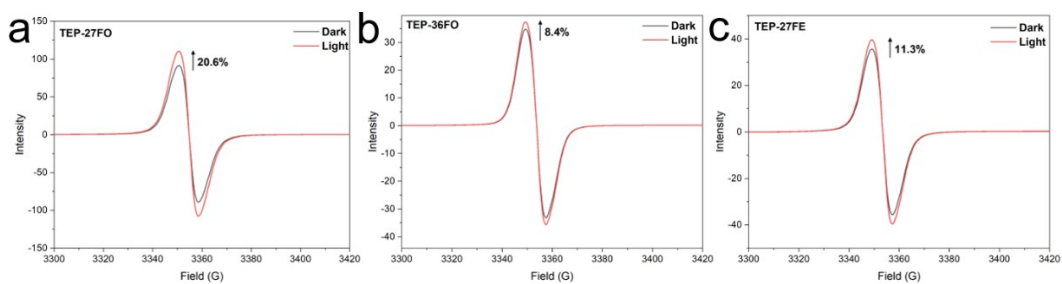


**Figure S14.** EPR spectra of (a) TEP-27FO, (b) TEP-36FO, (c) TEP-27FE under dark and after red light (>600 nm) irradiation for 15 min.

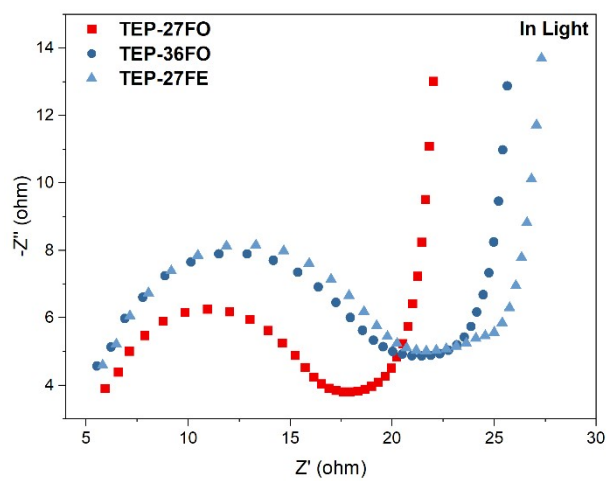


**Figure S15.** EIS Nyquist plots collected in the red light irradiation (> 600 nm)

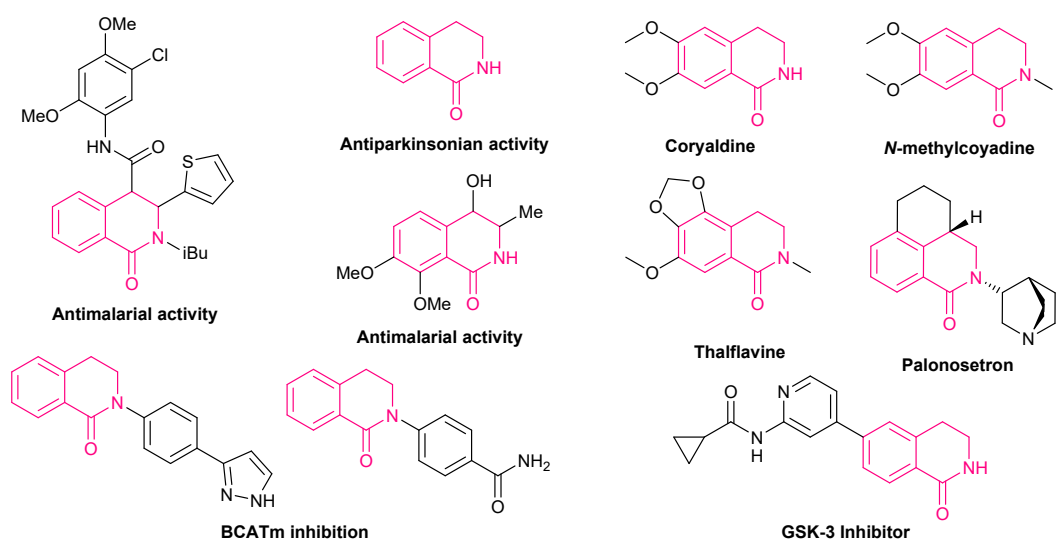
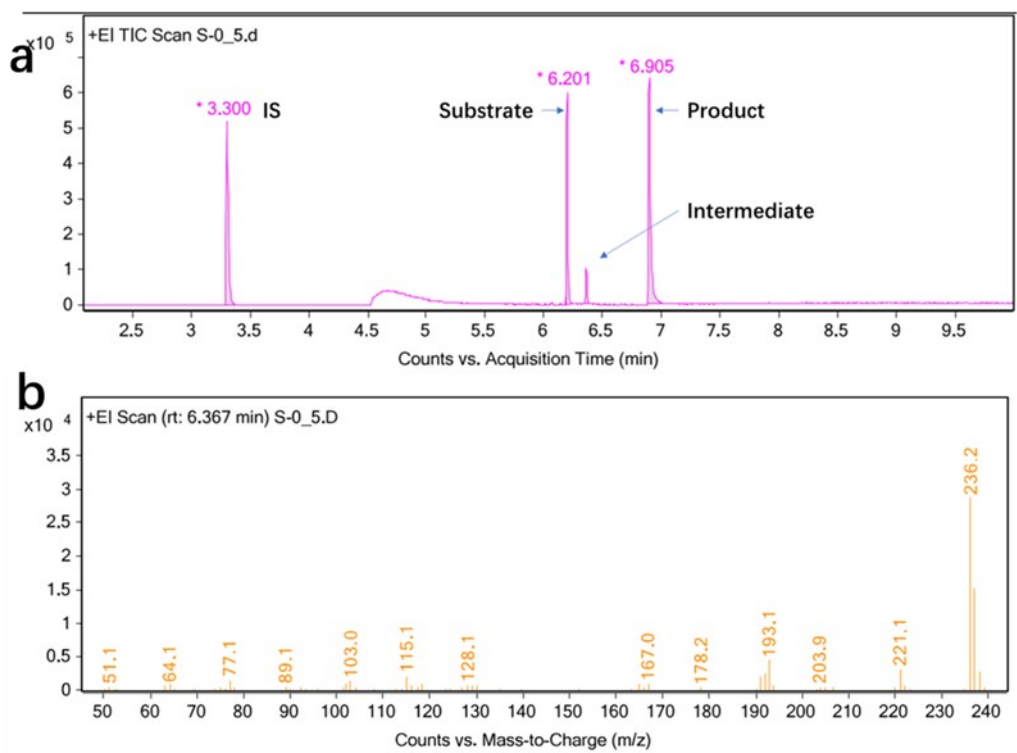


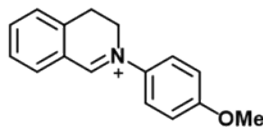
**Figure S16.** Representative biologically active compounds containing 3,4-dihydroisoquinolone cores





**Peak List**

m/z	z	Abund
77.1		1429
103		1406
115.1		2113
191.1		1966
192.1		2441
193.1	1	4448
221.1	1	3145
236.2		28664
237.1	1	15233
238.2	1	2624



**Chemical Formula:** C<sub>16</sub>H<sub>16</sub>NO<sup>+</sup>

**Exact Mass:** 238.12

**m/z:** 238.12 (100.0%), 239.13 (17.5%), 240.13 (1.6%)

**Figure S17.** Gas chromatography-mass spectrometry (GC-MS) analysis of the reaction solution after 0.5 hours under standard conditions. (a) GC spectra (b) MS spectra of intermediate component at 6.367min.

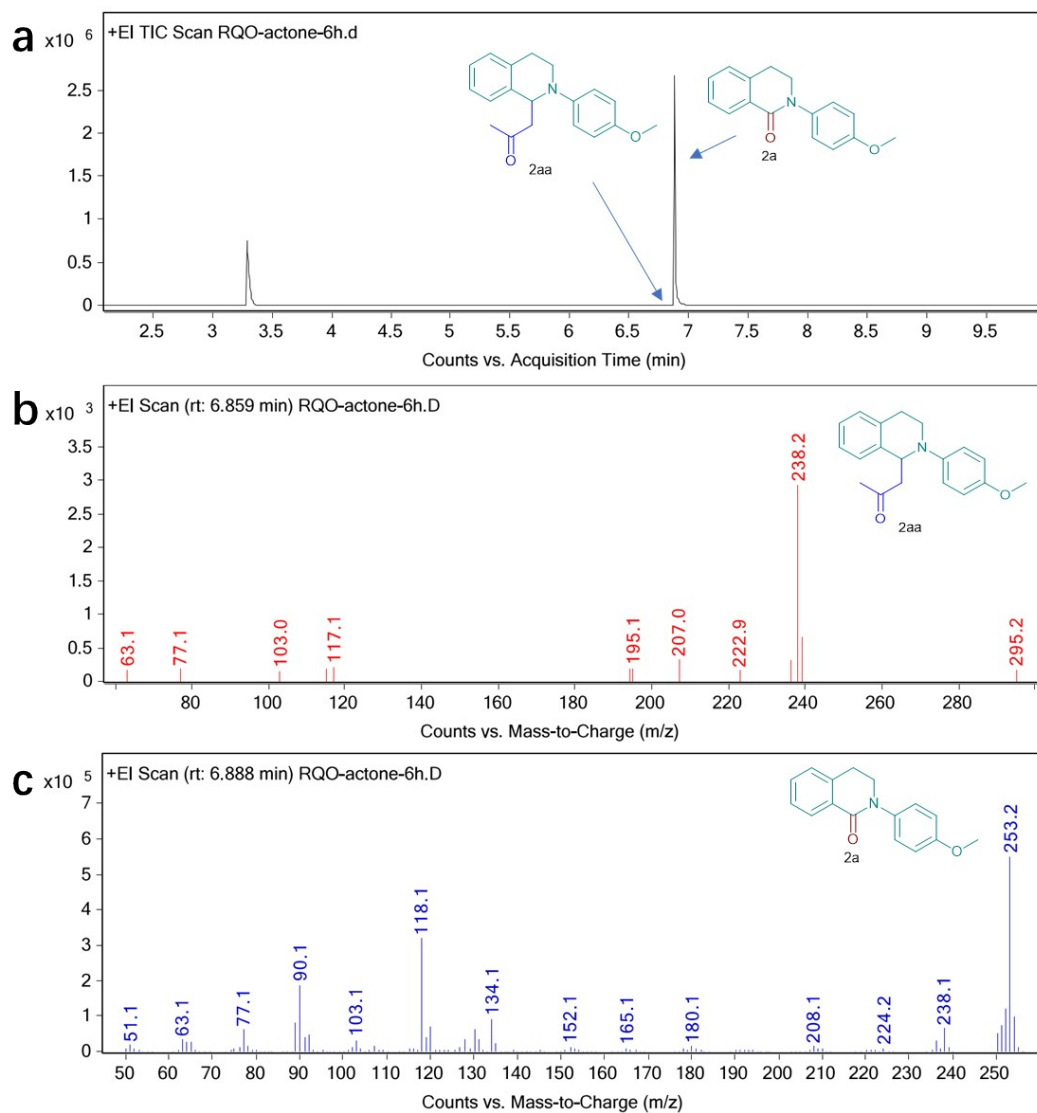


**Figure S18.** Gas chromatography-mass spectrometry (GC-MS) analysis of the reaction without L-proline as co-catalyst under acetone as solvent.

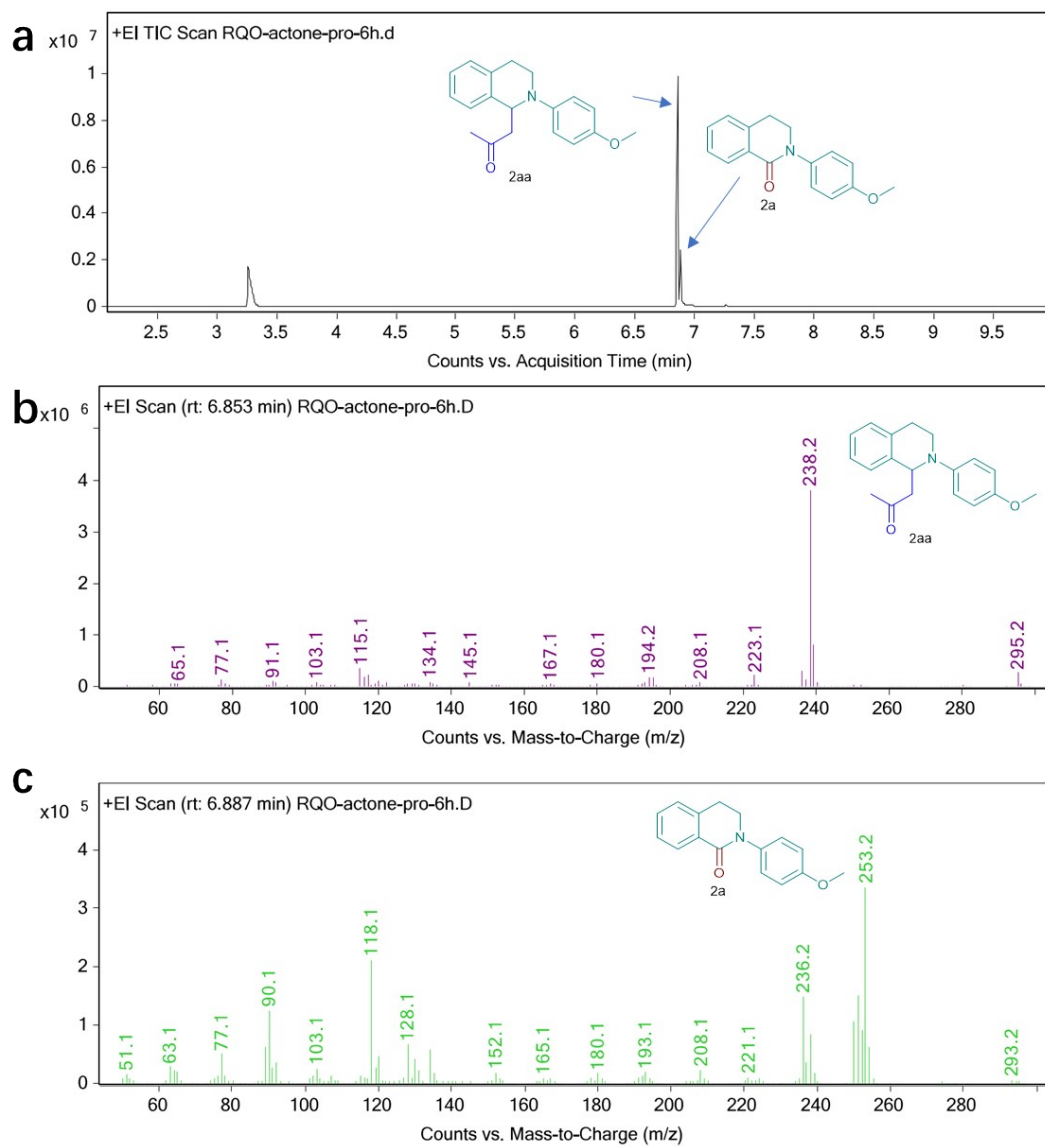


**Figure S19.** Gas chromatography-mass spectrometry (GC-MS) analysis of the reaction with L-proline as co-catalyst under acetone as solvent.

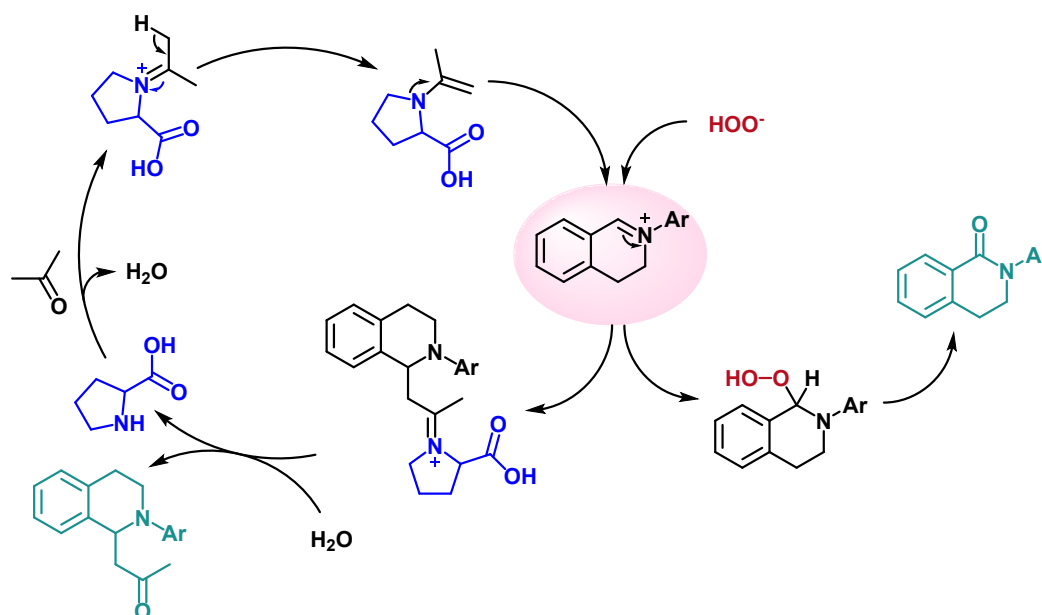


**Figure S20.** Proposed catalytic mechanism of cross-dehydrogenative coupling (CDC) reaction between N-aryl THIQ and acetone catalyzed by L-proline

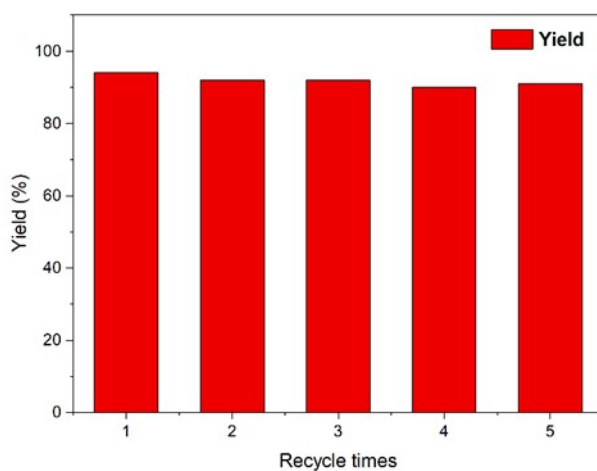


**Figure S21.** Recycling performance of TEP-27FO in direct  $\alpha$ -oxidation of THIQ under 640 nm red light irradiation

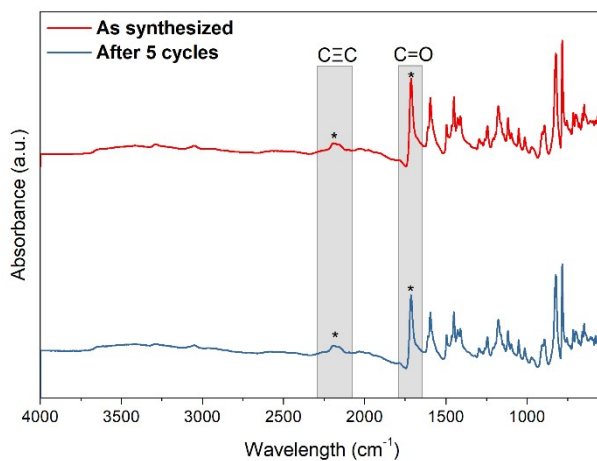


**Figure S22.** FTIR spectra of **TEP-27FO** as synthesized and collected after one cycle and five cycles.

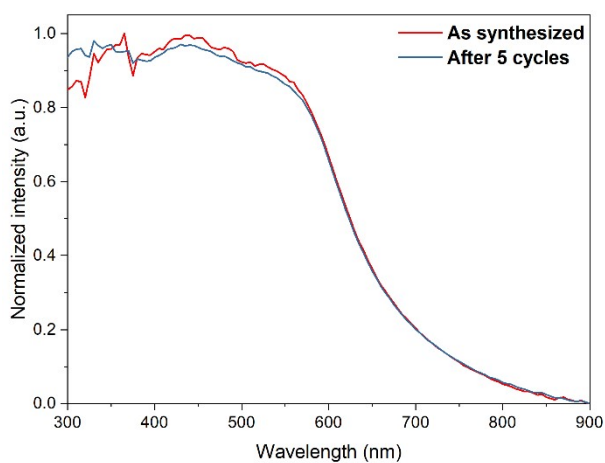


**Figure S23.** UV-Vis absorption spectra of **TEP-27FO** as synthesized and collected after one cycle and five cycles.

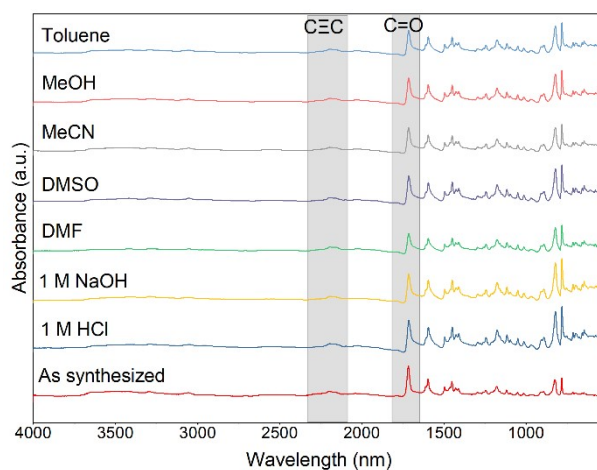
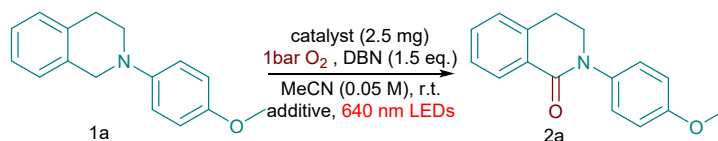


**Figure S24.** FTIR spectra of **TEP-27FO** in acidic and basic solutions and in organic solvents for 48 h..

## 5. Table

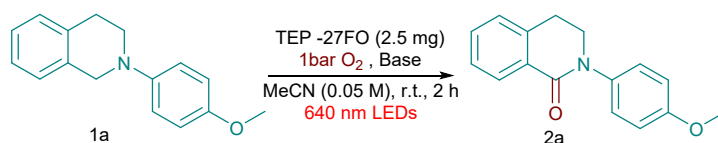
**Table S1.** Screening experiments <sup>a</sup>



Entry	Catalyst	Additive	Time	GC Yield (%) <sup>b</sup>
1	TEP-36FO	-	12 h	93
2	TEP-27FE	-	8 h	92
3	TEP-27FO	TEMPO (2 eq.)	2 h	92
4	TEP-27FO	BHT (2 eq.)	2 h	95
5	TEP-27FO	CuCl <sub>2</sub> (2 eq.)	2 h	3
6	TEP-27FO	TEOA (2 eq.)	2 h	8
7	TEP-27FO	BQ (2 eq.)	2 h	28
8	TEP-27FO	t-butanol (2 eq.)	2 h	89
9	TEP-27FO	NaN <sub>3</sub> (2 eq.)	2 h	83
10	TEP-27FO	Pd(Ph <sub>3</sub> P) <sub>2</sub> Cl <sub>2</sub> (0.1 eq)	2 h	12
11	TEP-27FO	CuI (0.1 eq.)	2 h	5

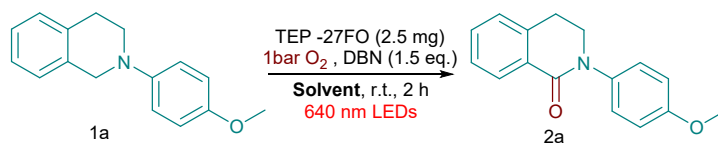
<sup>a</sup> Reaction conditions: 0.1 mmol of substrate, 2.5 mg of catalyst, 1.5 equiv of DBN, 2 mL of MeCN (0.05 M), 640 nm Kessil LEDs lamp with fan cooling, room temperature (25 – 30 °C) <sup>b</sup> GC yield using *n*-dodecane as the internal standard. “ND” means not detected

**Table S2.** Screening experiments of base <sup>a</sup>



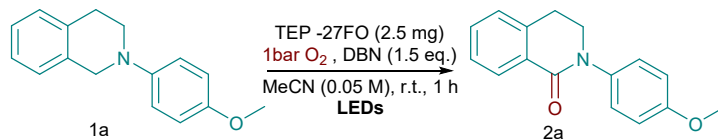
Entry	Base	GC Yield (%) <sup>b</sup>
1	DBN (1.5 eq)	94
2	DBU (1.5 eq)	70
3	TEA (1.5 eq)	49
4	2,6-lutidine (1.5 eq)	75
5	Na <sub>2</sub> CO <sub>3</sub> (1.5 eq)	11
6	DIPEA (1.5 eq)	72
7	K <sub>3</sub> PO <sub>4</sub> (1.5 eq)	Trace
8	DBN (0.5 eq)	52
9	DBN (1.0 eq)	83
10	DBN (2.0 eq)	92

<sup>a</sup> Reaction conditions: 0.1 mmol of substrate, 2.5 mg of TEP-27FO, 2 mL of MeCN (0.05 M), 640 nm Kessil LEDs lamp with fan cooling, room temperature (25 – 30 °C), 2 hours <sup>b</sup> GC yield using *n*-dodecane as the internal standard.

**Table S3.** Screening experiments of solvents <sup>a</sup>

Entry	Solvent	GC Yield (%) <sup>b</sup>
1	MeCN (0.05 M)	94
2	DMSO (0.05 M)	51
3	DMF (0.05 M)	49
4	DMA (0.05 M)	53
5	MeOH (0.05 M)	Trace
6	Toluene (0.05 M)	32
7	THF (0.05 M)	63
8	Acetone (0.05 M)	52
9	MeCN (0.02 M)	83
10	MeCN (0.1 M)	67
11	MeCN (0.2 M)	40

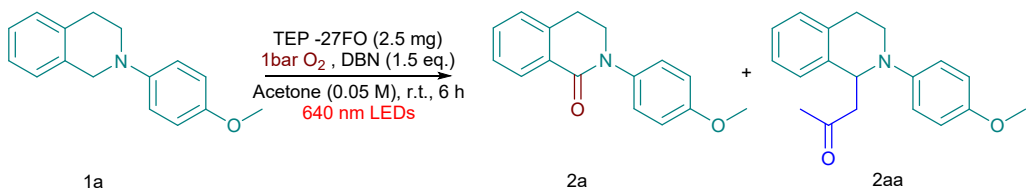
<sup>a</sup> Reaction conditions: 0.1 mmol of substrate, 2.5 mg of TEP-27FO, 1.5 equiv of DBN, 640 nm Kessil LEDs lamp with fan cooling, room temperature (25 – 30 °C), 2 hours <sup>b</sup> GC yield using *n*-dodecane as the internal standard.

**Table S4.** Screening experiments of LEDs with different wavelength and different power <sup>a</sup>

Entry	LEDs	GC Yield (%) <sup>b</sup>
1	Kessil PR160L-640nm-C (40 W Max) 100%	62
2	Kessil PR160L-640nm-C (40 W Max) 75%	52
3	Kessil PR160L-640nm-C (40 W Max) 50%	34
4	Kessil PR160L-640nm-C (40 W Max) 25%	21
5	Kessil PR160-390nm (40 W Max) 100%	83
6	Kessil PR160L-440nm (40 W Max) 100%	85
7	Kessil PR160L-525nm (40 W Max) 100%	70
8	Kessil PR160L-740nm-C (40 W Max) 100%	16

<sup>a</sup> Reaction conditions: 0.1 mmol of substrate, 2.5 mg of TEP-27FO, 1.5 equiv of DBN, 2 mL of MeCN (0.05 M), Kessil LEDs lamp with fan cooling, room temperature (25 – 30 °C), 1 hours <sup>b</sup> GC yield using *n*-dodecane as the internal standard.

**Table S5.** Reaction comparison with or without L-proline as co-catalyst under acetone as solvent <sup>a</sup>



Entry	Condition variations	GC-MS ratio of 2a/2aa(%)
1	None	100/trace
2	+ L-proline (5 mol%)	20/80

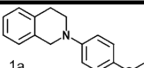
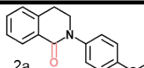
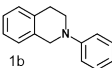
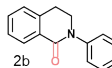
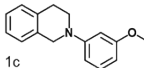
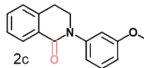
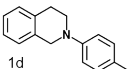
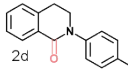
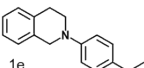
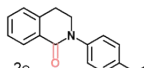
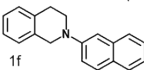
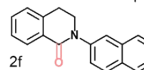
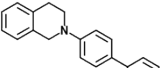
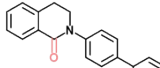
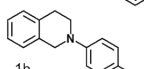
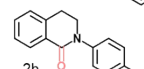
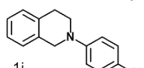
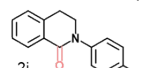
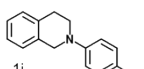
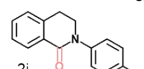
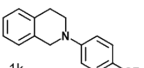
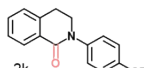
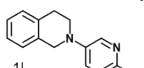
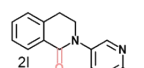
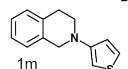
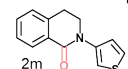
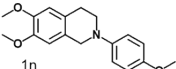
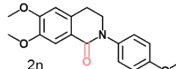
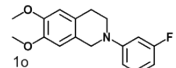
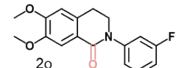
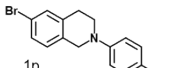
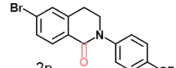
<sup>a</sup> Reaction conditions: 0.1 mmol of substrate, 2.5 mg of TEP-27FO, 1.5 equiv of DBN, 2 mL of MeCN (0.05 M), 640 nm Kessil LEDs lamp with fan cooling, room temperature (25 – 30 °C), 6 hours. GC-MS spectra are shown in Figure S18 and S19

**Table S6.** ICP-OES elemental analysis and the content of the element in **TEP-X**

Sample	Pd (wt.%)	Cu (wt.%)
TEP-27FO	0.0433	0.0036
TEP-36FO	0.0327	0.0027
TEP-27FE	0.0295	0.0037



**Table S7.** Scope of substituted-THIQ derivatives <sup>a</sup>

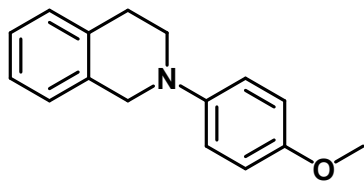
Entry	Substrate	Product	Time (h)	Yield (%)
1			2	94
2			4	91
3			4	89
4			4	87
5			4	88
6			4	85
7			4	85
8			12	78
9			8	83
10			8	85
11			8	83
12			12	86
13			12	79
14			2	81
15			12	73
16			12	70

## 6. Reference

- 1 F. Neese, *WIREs Comput Mol Sci*, 2022, **12**, e1606.
- 2 S. Bernhardt, M. Kastler, V. Enkelmann, M. Baumgarten and K. Müllen, *Chem. Eur. J*, 2006, **12**, 6117–6128.
- 3 A. H. Bansode and G. Suryavanshi, *Adv. Synth. Catal.*, 2021, **363**, 1390–1400.
- 4 T. Thatikonda, S. K. Deepake and U. Das, *Org. Lett.*, 2019, **21**, 2532–2535.
- 5 S. T. Emmerling, R. Schuldt, S. Bette, L. Yao, R. E. Dinnebier, J. Kästner and B. V. Lotsch, *J. Am. Chem. Soc.*, 2021, **143**, 15711–15722.
- 6 X. Chen, J. Gao and D. Jiang, *Chem. Lett.*, 2015, **44**, 1257–1259.

## 7. NMR data

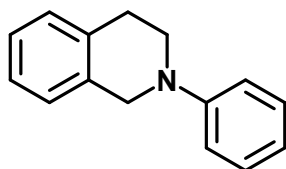
### 2-(4-methoxyphenyl)-1,2,3,4-tetrahydroisoquinoline (1a)



$^1\text{H}$  NMR (500 MHz, Chloroform-*d*)  $\delta$  7.21 – 7.12 (m, 4H), 7.02 – 6.97 (m, 2H), 6.88 (d,  $J = 8.9$  Hz, 2H), 4.31 (s, 2H), 3.79 (d,  $J = 1.0$  Hz, 3H), 3.46 (t,  $J = 5.8$  Hz, 2H), 3.00 (t,  $J = 5.9$  Hz, 2H).

$^{13}\text{C}$  NMR (126 MHz, Chloroform-*d*)  $\delta$  153.52, 145.39, 134.64, 134.57, 128.71, 126.53, 126.28, 125.93, 118.05, 114.59, 55.66, 52.70, 48.47, 29.14.

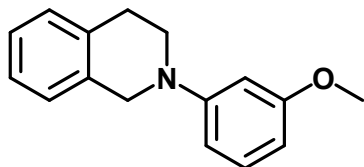
### 2-phenyl-1,2,3,4-tetrahydroisoquinoline (1b)



$^1\text{H}$  NMR (400 MHz, Chloroform-*d*)  $\delta$  7.33 (dd,  $J = 8.7, 7.2$  Hz, 2H), 7.25 – 7.17 (m, 4H), 7.05 – 7.00 (m, 2H), 6.86 (dd,  $J = 7.8, 6.7$  Hz, 1H), 4.45 (s, 2H), 3.60 (t,  $J = 5.9$  Hz, 2H), 3.02 (t,  $J = 5.8$  Hz, 2H).

$^{13}\text{C}$  NMR (101 MHz, Chloroform-*d*)  $\delta$  150.57, 134.90, 134.49, 129.23, 128.55, 126.56, 126.35, 126.05, 118.68, 115.17, 50.75, 46.54, 29.14.

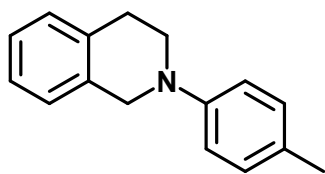
### 2-(3-methoxyphenyl)-1,2,3,4-tetrahydroisoquinoline (1c)



$^1\text{H}$  NMR (500 MHz, Chloroform-*d*)  $\delta$  7.18 (ddt,  $J = 9.6, 8.2, 6.4$  Hz, 5H), 6.60 (ddd,  $J = 8.3, 2.4, 1.0$  Hz, 1H), 6.54 – 6.51 (m, 1H), 6.40 (ddd,  $J = 8.1, 2.4, 1.0$  Hz, 1H), 4.42 (s, 2H), 3.82 (s, 3H), 3.59 – 3.54 (m, 2H), 2.99 (t,  $J = 5.9$  Hz, 2H).

$^{13}\text{C}$  NMR (126 MHz, Chloroform-*d*)  $\delta$  160.73, 151.89, 134.93, 134.42, 129.88, 128.48, 126.53, 126.36, 126.06, 107.91, 103.27, 101.51, 55.22, 50.62, 46.36, 29.13.

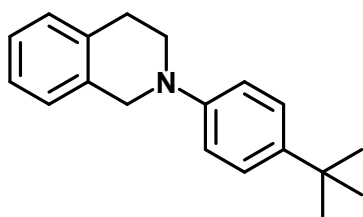
**2-(p-tolyl)-1,2,3,4-tetrahydroisoquinoline (1d)**



$^1\text{H}$  NMR (500 MHz, Chloroform-*d*)  $\delta$  7.23 – 7.16 (m, 4H), 7.13 (d,  $J$  = 8.2 Hz, 2H), 6.97 – 6.93 (m, 2H), 4.39 (s, 2H), 3.54 (t,  $J$  = 5.9 Hz, 2H), 3.01 (t,  $J$  = 5.9 Hz, 2H), 2.31 (s, 3H).

$^{13}\text{C}$  NMR (126 MHz, Chloroform-*d*)  $\delta$  148.68, 134.79, 134.62, 129.76, 128.64, 128.42, 126.58, 126.29, 125.98, 115.89, 51.52, 47.31, 29.13, 20.45.

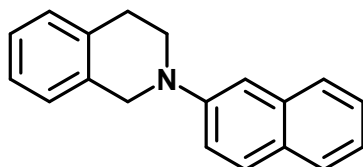
**2-(4-(tert-butyl)phenyl)-1,2,3,4-tetrahydroisoquinoline (1e)**



$^1\text{H}$  NMR (400 MHz, Chloroform-*d*)  $\delta$  7.38 – 7.33 (m, 2H), 7.25 – 7.15 (m, 4H), 7.05 – 6.94 (m, 2H), 4.42 (s, 2H), 3.57 (t,  $J$  = 5.9 Hz, 2H), 3.02 (t,  $J$  = 5.8 Hz, 2H), 1.35 (s, 9H).

$^{13}\text{C}$  NMR (101 MHz, Chloroform-*d*)  $\delta$  148.39, 141.57, 134.89, 134.63, 128.61, 126.59, 126.29, 126.03, 126.00, 115.13, 51.17, 46.80, 33.97, 31.55, 29.25.

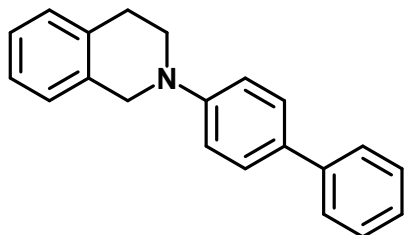
**2-(naphthalen-2-yl)-1,2,3,4-tetrahydroisoquinoline (1f)**



$^1\text{H}$  NMR (500 MHz, Chloroform-*d*)  $\delta$  7.81 – 7.70 (m, 3H), 7.46 – 7.40 (m, 1H), 7.38 (dd,  $J$  = 9.0, 2.5 Hz, 1H), 7.33 – 7.27 (m, 1H), 7.22 (dq,  $J$  = 12.3, 3.3 Hz, 5H), 4.54 (s, 2H), 3.69 (t,  $J$  = 5.9 Hz, 2H), 3.06 (t,  $J$  = 5.9 Hz, 2H).

$^{13}\text{C}$  NMR (126 MHz, Chloroform-*d*)  $\delta$  148.46, 134.81, 134.42, 128.86, 128.66, 128.08, 127.49, 126.62, 126.60, 126.43, 126.32, 126.12, 123.01, 118.75, 109.34, 51.12, 47.16, 29.24.

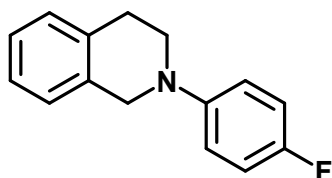
**2-([1,1'-biphenyl]-4-yl)-1,2,3,4-tetrahydroisoquinoline (1g)**



$^1\text{H}$  NMR (500 MHz, Chloroform-*d*)  $\delta$  7.62 – 7.53 (m, 4H), 7.42 (t,  $J$  = 7.6 Hz, 2H), 7.29 (t,  $J$  = 7.4 Hz, 1H), 7.25 – 7.17 (m, 4H), 7.09 – 7.03 (m, 2H), 4.49 (s, 2H), 3.63 (t,  $J$  = 5.8 Hz, 2H), 3.03 (t,  $J$  = 5.8 Hz, 2H).

$^{13}\text{C}$  NMR (126 MHz, Chloroform-*d*)  $\delta$  149.79, 141.04, 134.91, 134.37, 131.20, 128.71, 128.55, 127.85, 126.58, 126.46, 126.43, 126.30, 126.12, 115.07, 50.54, 46.29, 29.12.

**2-(4-fluorophenyl)-1,2,3,4-tetrahydroisoquinoline (1h)**

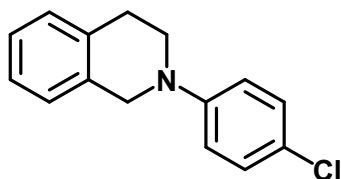


$^1\text{H}$  NMR (500 MHz, Chloroform-*d*)  $\delta$  7.23 – 7.11 (m, 4H), 7.03 – 6.91 (m, 4H), 4.34 (s, 2H), 3.49 (t,  $J$  = 5.9 Hz, 2H), 3.00 (t,  $J$  = 5.9 Hz, 2H).

$^{13}\text{C}$  NMR (126 MHz, Chloroform-*d*)  $\delta$  157.73, 155.84, 147.39, 134.55, 134.29, 128.65, 126.52, 126.42, 126.06, 117.22, 117.16, 115.69, 115.51, 51.93, 47.82, 29.03.

$^{19}\text{F}$  NMR (471 MHz, Chloroform-*d*)  $\delta$  -125.59.

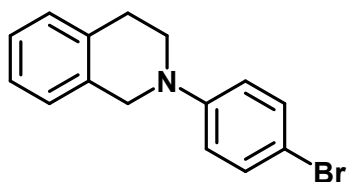
**2-(4-chlorophenyl)-1,2,3,4-tetrahydroisoquinoline (1i)**



$^1\text{H}$  NMR (500 MHz, Chloroform-*d*)  $\delta$  7.28 – 7.14 (m, 6H), 6.92 – 6.87 (m, 2H), 4.39 (s, 2H), 3.54 (t,  $J$  = 5.9 Hz, 2H), 2.99 (t,  $J$  = 5.9 Hz, 2H).

$^{13}\text{C}$  NMR (126 MHz, Chloroform-*d*)  $\delta$  149.09, 134.72, 134.11, 129.04, 128.55, 126.54, 126.52, 126.17, 123.34, 116.16, 50.65, 46.54, 28.98.

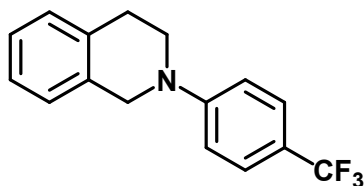
**2-(4-bromophenyl)-1,2,3,4-tetrahydroisoquinoline (1j)**



$^1\text{H}$  NMR (500 MHz, Chloroform-*d*)  $\delta$  7.41 – 7.34 (m, 2H), 7.24 – 7.12 (m, 4H), 6.87 – 6.81 (m, 2H), 4.38 (s, 2H), 3.54 (t,  $J = 5.9$  Hz, 2H), 2.99 (t,  $J = 5.9$  Hz, 2H).

$^{13}\text{C}$  NMR (126 MHz, Chloroform-*d*)  $\delta$  149.44, 134.73, 134.06, 131.92, 128.52, 126.53, 126.19, 116.49, 110.47, 50.45, 46.33, 28.96.

**2-(p-trifluoromethyl-phenyl)-1,2,3,4-tetrahydroisoquinoline (1k)**

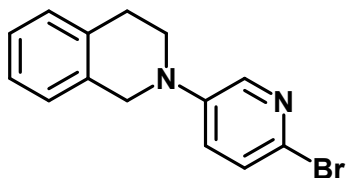


$^1\text{H}$  NMR (500 MHz, Chloroform-*d*)  $\delta$  7.51 (d,  $J = 8.6$  Hz, 1H), 7.25 – 7.16 (m, 2H), 6.94 (d,  $J = 8.6$  Hz, 1H), 4.49 (s, 1H), 3.64 (t,  $J = 5.9$  Hz, 1H), 3.00 (t,  $J = 5.9$  Hz, 1H).

$^{13}\text{C}$  NMR (126 MHz, Chloroform-*d*)  $\delta$  152.15, 134.93, 133.83, 128.35, 126.71, 126.53, 126.48, 126.45, 126.36, 112.95, 49.44, 45.23, 28.98.

$^{19}\text{F}$  NMR (471 MHz, Chloroform-*d*)  $\delta$  -61.04.

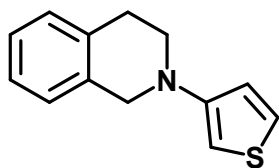
**2-(6-bromopyridin-3-yl)-1,2,3,4-tetrahydroisoquinoline (1l)**



$^1\text{H}$  NMR (500 MHz, Chloroform-*d*)  $\delta$  8.43 – 8.39 (m, 1H), 8.12 (d,  $J = 7.8$  Hz, 1H), 7.72 – 7.68 (m, 1H), 7.49 (td,  $J = 8.5, 7.7, 1.5$  Hz, 2H), 7.38 (t,  $J = 7.6$  Hz, 1H), 7.26 – 7.24 (m, 1H), 4.01 (td,  $J = 6.4, 1.5$  Hz, 2H), 3.17 (t,  $J = 6.4$  Hz, 2H).

$^{13}\text{C}$  NMR (126 MHz, Chloroform-*d*)  $\delta$  164.29, 145.89, 139.07, 138.21, 138.13, 135.37, 132.72, 128.89, 128.79, 127.78, 127.49, 127.18, 48.98, 28.40.

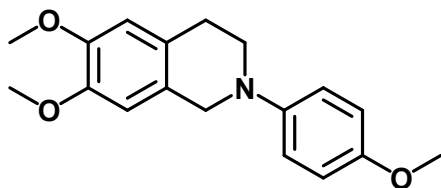
**2-(thiophen-3-yl)-1,2,3,4-tetrahydroisoquinoline (1m)**



$^1\text{H}$  NMR (400 MHz, Chloroform-*d*)  $\delta$  7.28 (s, 1H), 7.23 – 7.13 (m, 4H), 7.00 (dd,  $J$  = 5.2, 1.6 Hz, 1H), 6.27 (dd,  $J$  = 3.2, 1.6 Hz, 1H), 4.33 (s, 2H), 3.48 (t,  $J$  = 5.9 Hz, 2H), 3.01 (t,  $J$  = 5.9 Hz, 2H).

$^{13}\text{C}$  NMR (101 MHz, Chloroform-*d*)  $\delta$  151.93, 134.28, 134.00, 128.77, 126.55, 126.33, 126.00, 125.43, 120.15, 99.82, 52.57, 48.27, 28.99.

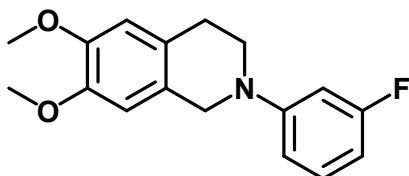
**6,7-dimethoxy-2-(4-methoxyphenyl)-1,2,3,4-tetrahydroisoquinoline (1n)**



$^1\text{H}$  NMR (500 MHz, Chloroform-*d*)  $\delta$  7.02 – 6.95 (m, 2H), 6.90 – 6.84 (m, 2H), 6.63 (d,  $J$  = 4.1 Hz, 2H), 4.22 (s, 2H), 3.86 (d,  $J$  = 3.0 Hz, 6H), 3.78 (s, 3H), 3.43 (t,  $J$  = 5.8 Hz, 2H), 2.89 (t,  $J$  = 5.8 Hz, 2H).

$^{13}\text{C}$  NMR (126 MHz, Chloroform-*d*)  $\delta$  153.52, 147.58, 147.45, 145.36, 126.41, 126.39, 118.17, 114.54, 111.44, 109.34, 55.98, 55.94, 55.63, 52.37, 48.63, 28.55.

**2-(3-fluorophenyl)-6,7-dimethoxy-1,2,3,4-tetrahydroisoquinoline (1o)**

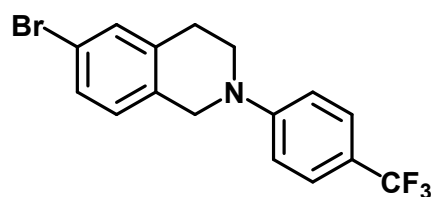


$^1\text{H}$  NMR (500 MHz, Chloroform-*d*)  $\delta$  7.20 (q,  $J$  = 7.9 Hz, 1H), 6.71 (dd,  $J$  = 8.3, 2.5 Hz, 1H), 6.66 (d,  $J$  = 3.0 Hz, 2H), 6.62 (dt,  $J$  = 12.6, 2.5 Hz, 1H), 6.49 (td,  $J$  = 8.2, 2.4 Hz, 1H), 4.33 (s, 2H), 3.87 (d,  $J$  = 3.3 Hz, 6H), 3.54 (t,  $J$  = 5.8 Hz, 2H), 2.89 (t,  $J$  = 5.8 Hz, 2H).

$^{13}\text{C}$  NMR (126 MHz, Chloroform-*d*)  $\delta$  165.01, 163.08, 152.09, 152.01, 147.71, 147.61, 130.21, 130.13, 126.63, 125.73, 111.30, 110.10, 110.08, 109.37, 104.71, 104.54, 101.66, 101.45, 56.01, 55.96, 49.92, 46.09, 28.42.

$^{19}\text{F}$  NMR (471 MHz, Chloroform-*d*)  $\delta$  -112.39.

**6-bromo-2-(4-(trifluoromethyl)phenyl)-1,2,3,4-tetrahydroisoquinoline (1p)**



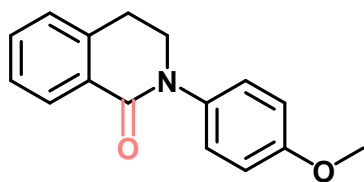
$^1\text{H}$  NMR (400 MHz, Chloroform-*d*)  $\delta$  7.54 – 7.47 (m, 2H), 7.34 (dq,  $J = 5.1, 2.1$  Hz, 2H), 7.05 (d,  $J = 8.7$  Hz, 1H), 6.93 (d,  $J = 8.6$  Hz, 2H), 4.42 (s, 2H), 3.61 (t,  $J = 5.9$  Hz, 2H), 2.96 (t,  $J = 5.8$  Hz, 2H).

$^{13}\text{C}$  NMR (101 MHz, Chloroform-*d*)  $\delta$  151.96, 137.10, 132.79, 131.25, 129.43, 128.16, 126.60, 126.57, 126.53, 126.49, 120.29, 113.20, 49.14, 45.03, 28.72.

$^{19}\text{F}$  NMR (377 MHz, Chloroform-*d*)  $\delta$  -61.15.



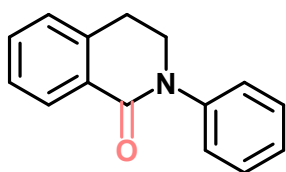
**2-(4-methoxyphenyl)-3,4-dihydroisoquinolin-1(2H)-one (2a)**



$^1\text{H}$  NMR (500 MHz, Chloroform-*d*)  $\delta$  8.15 (dd,  $J = 7.8, 1.5$  Hz, 1H), 7.45 (td,  $J = 7.5, 1.4$  Hz, 1H), 7.39 – 7.34 (m, 1H), 7.32 – 7.27 (m, 2H), 6.96 – 6.91 (m, 2H), 3.94 (t,  $J = 6.5$  Hz, 2H), 3.82 (s, 3H), 3.13 (t,  $J = 6.5$  Hz, 2H).

$^{13}\text{C}$  NMR (126 MHz, Chloroform-*d*)  $\delta$  164.47, 157.91, 138.40, 136.22, 132.02, 129.88, 128.77, 127.25, 127.03, 126.76, 114.34, 55.61, 49.80, 28.74.

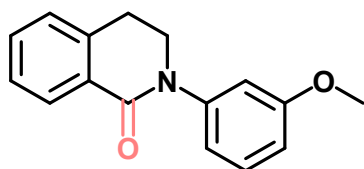
**2-phenyl-3,4-dihydroisoquinolin-1(2H)-one (2b)**



$^1\text{H}$  NMR (500 MHz, Chloroform-*d*)  $\delta$  8.17 (dd,  $J = 7.8, 1.4$  Hz, 1H), 7.47 (td,  $J = 7.5, 1.5$  Hz, 1H), 7.44 – 7.36 (m, 5H), 7.26 (ddd,  $J = 9.0, 5.6, 2.1$  Hz, 2H), 3.99 (t,  $J = 6.5$  Hz, 2H), 3.14 (t,  $J = 6.4$  Hz, 2H).

$^{13}\text{C}$  NMR (126 MHz, Chloroform-*d*)  $\delta$  164.22, 143.15, 138.35, 132.06, 129.75, 128.94, 128.76, 127.22, 126.98, 126.27, 125.35, 49.44, 28.65.

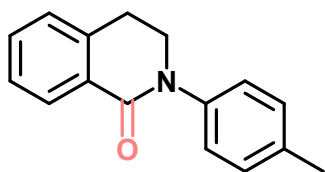
**2-(3-methoxyphenyl)-3,4-dihydroisoquinolin-1(2H)-one (2c)**



$^1\text{H}$  NMR (500 MHz, Chloroform-*d*)  $\delta$  8.16 (dd,  $J = 7.9, 1.4$  Hz, 1H), 7.46 (td,  $J = 7.5, 1.4$  Hz, 1H), 7.37 (td,  $J = 7.6, 1.3$  Hz, 1H), 7.35 – 7.29 (m, 1H), 7.26 – 7.22 (m, 1H), 6.99 – 6.94 (m, 2H), 6.81 (ddd,  $J = 8.4, 2.4, 1.0$  Hz, 1H), 3.97 (t,  $J = 6.5$  Hz, 2H), 3.82 (s, 3H), 3.13 (t,  $J = 6.4$  Hz, 2H).

$^{13}\text{C}$  NMR (126 MHz, Chloroform-*d*)  $\delta$  164.22, 160.00, 144.30, 138.33, 132.08, 129.73, 129.61, 128.76, 127.21, 126.99, 117.50, 112.18, 111.43, 55.41, 49.52, 28.64.

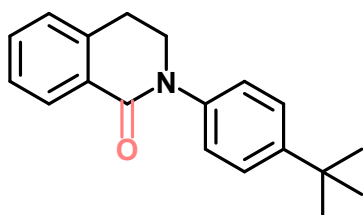
**2-(p-tolyl)-3,4-dihydroisoquinolin-1(2H)-one (2d)**



$^1\text{H}$  NMR (500 MHz, Chloroform-*d*)  $\delta$  8.16 (dd,  $J = 7.7, 1.4$  Hz, 1H), 7.45 (dd,  $J = 7.5, 1.5$  Hz, 1H), 7.38 (dd,  $J = 7.7, 1.3$  Hz, 1H), 7.29 – 7.18 (m, 5H), 3.96 (t,  $J = 6.5$  Hz, 2H), 3.13 (t,  $J = 6.5$  Hz, 2H), 2.37 (s, 3H).

$^{13}\text{C}$  NMR (126 MHz, Chloroform-*d*)  $\delta$  164.26, 140.60, 138.33, 136.07, 131.96, 129.83, 129.57, 128.73, 127.17, 126.95, 125.23, 49.54, 28.66, 21.07.

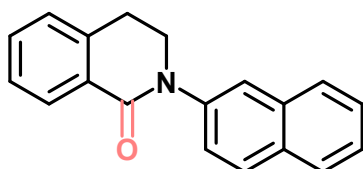
**2-(4-(tert-butyl)phenyl)-3,4-dihydroisoquinolin-1(2H)-one (2e)**



$^1\text{H}$  NMR (500 MHz, Chloroform-*d*)  $\delta$  8.16 (dd,  $J = 7.8, 1.4$  Hz, 1H), 7.48 – 7.41 (m, 3H), 7.37 (td,  $J = 7.6, 1.2$  Hz, 1H), 7.34 – 7.30 (m, 2H), 7.24 (d,  $J = 7.5$  Hz, 1H), 3.99 (t,  $J = 6.4$  Hz, 2H), 3.13 (t,  $J = 6.4$  Hz, 2H), 1.34 (s, 9H).

$^{13}\text{C}$  NMR (126 MHz, Chloroform-*d*)  $\delta$  164.25, 149.11, 140.44, 138.32, 131.96, 129.86, 128.76, 127.18, 126.92, 125.86, 124.75, 49.44, 34.55, 31.38, 28.66.

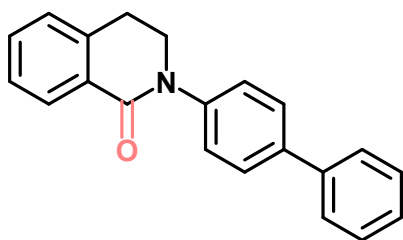
**2-(naphthalen-2-yl)-3,4-dihydroisoquinolin-1(2H)-one (2f)**



$^1\text{H}$  NMR (500 MHz, Chloroform-*d*)  $\delta$  8.20 (dd,  $J = 7.7, 1.4$  Hz, 1H), 7.91 – 7.77 (m, 4H), 7.59 (dd,  $J = 8.8, 2.1$  Hz, 1H), 7.52 – 7.45 (m, 3H), 7.40 (td,  $J = 7.6, 1.3$  Hz, 1H), 7.27 (d,  $J = 7.3$  Hz, 1H), 4.11 (t,  $J = 6.4$  Hz, 2H), 3.20 (t,  $J = 6.4$  Hz, 2H).

$^{13}\text{C}$  NMR (126 MHz, Chloroform-*d*)  $\delta$  164.46, 140.89, 138.38, 133.62, 132.15, 131.77, 129.73, 128.80, 128.54, 127.77, 127.67, 127.27, 127.03, 126.32, 125.90, 124.65, 122.61, 49.69, 28.73.

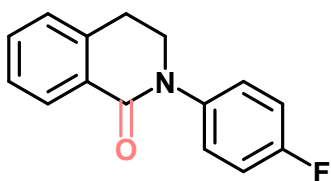
**2-([1,1'-biphenyl]-4-yl)-3,4-dihydroisoquinolin-1(2H)-one (2g)**



$^1\text{H}$  NMR (500 MHz, Chloroform-*d*)  $\delta$  8.19 (dd,  $J = 7.8, 1.5$  Hz, 1H), 7.67 – 7.57 (m, 4H), 7.51 – 7.43 (m, 5H), 7.42 – 7.33 (m, 2H), 4.04 (t,  $J = 6.4$  Hz, 2H), 3.17 (t,  $J = 6.4$  Hz, 2H).

$^{13}\text{C}$  NMR (126 MHz, Chloroform-*d*)  $\delta$  164.29, 142.31, 140.62, 139.14, 138.34, 132.13, 129.73, 128.82, 127.64, 127.35, 127.26, 127.13, 127.01, 125.51, 49.42, 28.65.

**2-(4-fluorophenyl)-3,4-dihydroisoquinolin-1(2H)-one (2h)**

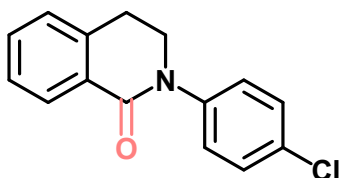


$^1\text{H}$  NMR (500 MHz, Chloroform-*d*)  $\delta$  8.15 (dd,  $J = 7.8, 1.5$  Hz, 1H), 7.47 (td,  $J = 7.5, 1.5$  Hz, 1H), 7.41 – 7.32 (m, 3H), 7.24 (d,  $J = 7.6$  Hz, 1H), 7.10 (t,  $J = 8.6$  Hz, 2H), 3.96 (t,  $J = 6.5$  Hz, 2H), 3.15 (t,  $J = 6.5$  Hz, 2H).

$^{13}\text{C}$  NMR (126 MHz, Chloroform-*d*)  $\delta$  164.38, 161.70, 159.75, 139.09, 139.07, 138.27, 132.17, 129.51, 128.75, 127.27, 127.15, 127.09, 127.02, 115.85, 115.67, 49.59, 28.60.

$^{19}\text{F}$  NMR (471 MHz, Chloroform-*d*)  $\delta$  -115.70.

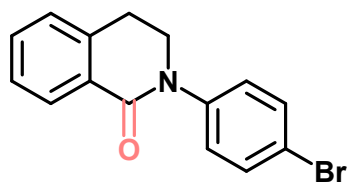
**2-(4-chlorophenyl)-3,4-dihydroisoquinolin-1(2H)-one (2i)**



$^1\text{H}$  NMR (500 MHz, Chloroform-*d*)  $\delta$  8.14 (d,  $J = 7.8$  Hz, 1H), 7.51 – 7.45 (m, 1H), 7.42 – 7.31 (m, 5H), 7.24 (d,  $J = 7.6$  Hz, 1H), 3.97 (t,  $J = 6.4$  Hz, 2H), 3.15 (t,  $J = 6.5$  Hz, 2H).

$^{13}\text{C}$  NMR (126 MHz, Chloroform-*d*)  $\delta$  164.23, 141.58, 138.25, 132.26, 131.59, 129.44, 129.00, 128.79, 127.31, 127.03, 126.57, 49.33, 28.56.

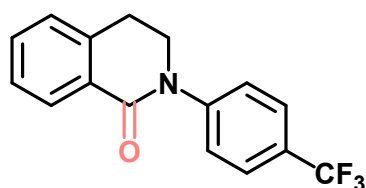
**2-(4-bromophenyl)-3,4-dihydroisoquinolin-1(2H)-one (2j)**



$^1\text{H}$  NMR (500 MHz, Chloroform-*d*)  $\delta$  8.14 (dd,  $J = 7.8, 1.4$  Hz, 1H), 7.55 – 7.50 (m, 2H), 7.47 (dd,  $J = 7.5, 1.4$  Hz, 1H), 7.38 (td,  $J = 7.6, 1.3$  Hz, 1H), 7.30 – 7.26 (m, 2H), 7.24 (d,  $J = 7.5$  Hz, 1H), 3.97 (t,  $J = 6.4$  Hz, 2H), 3.15 (t,  $J = 6.4$  Hz, 2H).

$^{13}\text{C}$  NMR (126 MHz, Chloroform-*d*)  $\delta$  164.18, 142.09, 138.24, 132.27, 131.96, 129.42, 128.80, 127.31, 127.03, 126.90, 119.46, 49.27, 28.55.

**2-(4-(trifluoromethyl)phenyl)-3,4-dihydroisoquinolin-1(2H)-one (2k)**

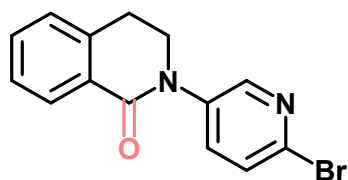


$^1\text{H}$  NMR (500 MHz, Chloroform-*d*)  $\delta$  8.16 (dd,  $J = 7.8, 1.4$  Hz, 1H), 7.67 (d,  $J = 8.4$  Hz, 2H), 7.54 (d,  $J = 8.4$  Hz, 2H), 7.50 (td,  $J = 7.5, 1.4$  Hz, 1H), 7.40 (td,  $J = 7.6, 1.2$  Hz, 1H), 7.26 (d,  $J = 7.6$  Hz, 1H), 4.03 (t,  $J = 6.4$  Hz, 2H), 3.17 (t,  $J = 6.4$  Hz, 2H).

$^{13}\text{C}$  NMR (126 MHz, Chloroform-*d*)  $\delta$  164.23, 146.08, 138.26, 132.47, 129.27, 128.90, 127.39, 127.08, 126.00, 125.97, 125.94, 125.91, 125.12, 49.11, 28.52.

$^{19}\text{F}$  NMR (471 MHz, Chloroform-*d*)  $\delta$  -62.36.

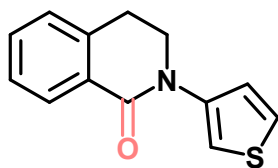
**2-(6-bromopyridin-3-yl)-3,4-dihydroisoquinolin-1(2H)-one (2l)**



$^1\text{H}$  NMR (500 MHz, Chloroform-*d*)  $\delta$  8.43 – 8.39 (m, 1H), 8.12 (d,  $J = 7.8$  Hz, 1H), 7.72 – 7.68 (m, 1H), 7.49 (td,  $J = 8.5, 7.7, 1.5$  Hz, 2H), 7.38 (t,  $J = 7.6$  Hz, 1H), 7.26 – 7.24 (m, 1H), 4.01 (td,  $J = 6.4, 1.5$  Hz, 2H), 3.17 (t,  $J = 6.4$  Hz, 2H).

$^{13}\text{C}$  NMR (126 MHz, Chloroform-*d*)  $\delta$  164.29, 145.89, 139.07, 138.21, 138.13, 135.37, 132.72, 128.89, 128.79, 127.78, 127.49, 127.18, 48.98, 28.40.

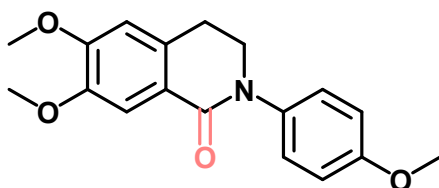
**2-(thiophen-3-yl)-3,4-dihydroisoquinolin-1(2H)-one (2m)**



$^1\text{H}$  NMR (400 MHz, Chloroform-*d*)  $\delta$  8.15 (dd,  $J = 7.8, 1.4$  Hz, 1H), 7.45 (dd,  $J = 7.3, 1.4$  Hz, 1H), 7.41 – 7.33 (m, 2H), 7.33 – 7.25 (m, 2H), 7.23 (d,  $J = 7.6$  Hz, 1H), 4.03 (t,  $J = 6.5$  Hz, 2H), 3.13 (t,  $J = 6.5$  Hz, 2H).

$^{13}\text{C}$  NMR (101 MHz, Chloroform-*d*)  $\delta$  163.54, 141.23, 137.98, 132.10, 129.70, 128.72, 127.29, 126.90, 124.17, 123.88, 113.97, 48.99, 28.32.

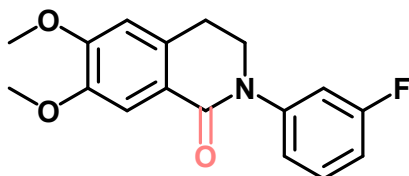
**6,7-dimethoxy-2-(4-methoxyphenyl)-3,4-dihydroisoquinolin-1(2H)-one (2n)**



$^1\text{H}$  NMR (400 MHz, Chloroform-*d*)  $\delta$  7.64 (s, 1H), 7.29 – 7.25 (m, 2H), 6.96 – 6.90 (m, 2H), 6.68 (s, 1H), 3.92 (dd,  $J = 8.0, 6.1$  Hz, 8H), 3.81 (s, 3H), 3.05 (t,  $J = 6.5$  Hz, 2H).

$^{13}\text{C}$  NMR (101 MHz, Chloroform-*d*)  $\delta$  164.42, 157.70, 152.03, 148.06, 136.31, 132.06, 126.67, 122.27, 114.19, 110.82, 109.22, 56.10, 55.51, 49.94, 28.28.

**2-(3-fluorophenyl)-6,7-dimethoxy-3,4-dihydroisoquinolin-1(2H)-one (2o)**

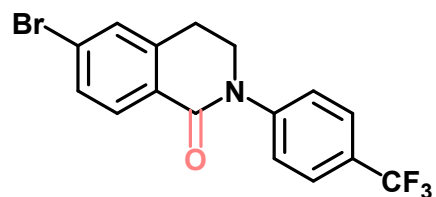


$^1\text{H}$  NMR (500 MHz, Chloroform-*d*)  $\delta$  7.64 (d,  $J = 1.2$  Hz, 1H), 7.38 – 7.32 (m, 1H), 7.16 (ddd,  $J = 10.5, 8.5, 2.3$  Hz, 2H), 6.94 (ddd,  $J = 10.7, 8.1, 2.7$  Hz, 1H), 6.69 (s, 1H), 3.99 – 3.92 (m, 8H), 3.07 (t,  $J = 6.5$  Hz, 2H).

$^{13}\text{C}$  NMR (126 MHz, Chloroform-*d*)  $\delta$  164.17, 152.37, 148.20, 144.73, 144.65, 132.11, 129.83, 129.76, 121.89, 120.60, 120.58, 112.93, 112.80, 112.76, 112.61, 110.87, 109.22, 56.12, 49.49, 28.19.

$^{19}\text{F}$  NMR (471 MHz, Chloroform-*d*)  $\delta$  -112.20.

**6-bromo-2-(4-(trifluoromethyl)phenyl)-3,4-dihydroisoquinolin-1(2H)-one (2p)**

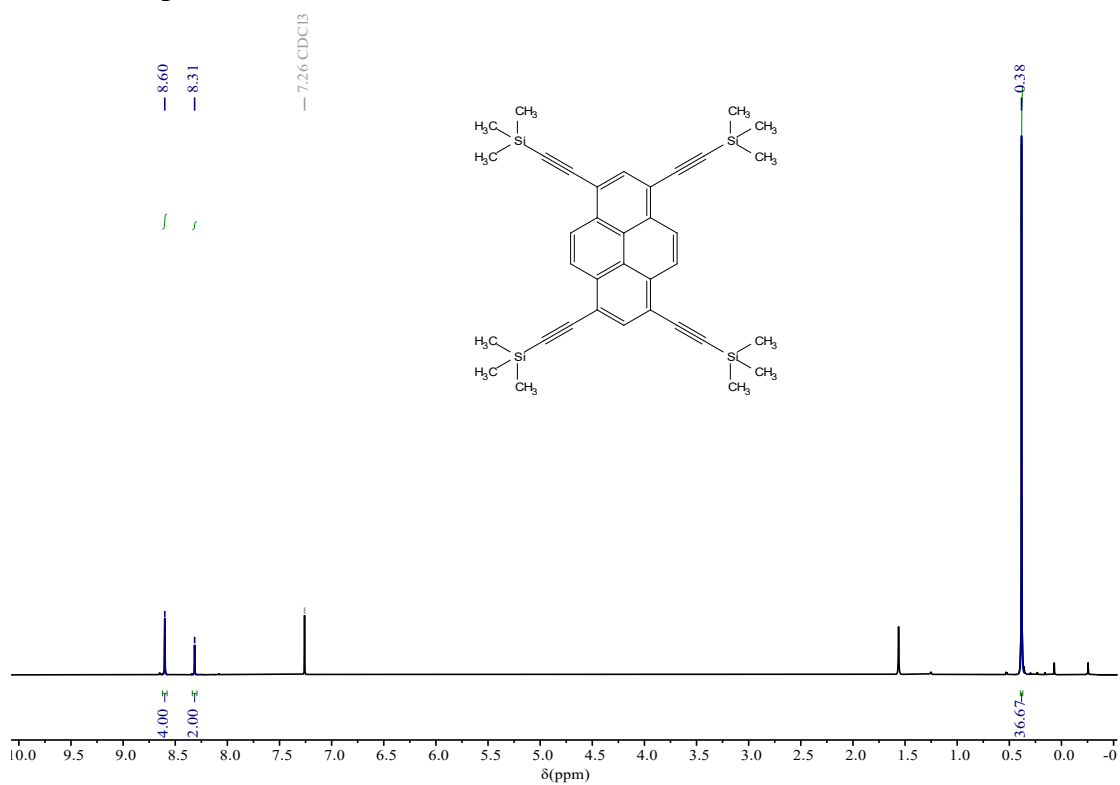


$^1\text{H}$  NMR (400 MHz, Chloroform-*d*)  $\delta$  8.01 (d,  $J = 8.3$  Hz, 1H), 7.67 (d,  $J = 8.3$  Hz, 2H), 7.52 (td,  $J = 5.6, 2.7$  Hz, 3H), 7.44 (d,  $J = 1.9$  Hz, 1H), 4.03 (t,  $J = 6.4$  Hz, 2H), 3.15 (t,  $J = 6.4$  Hz, 2H).

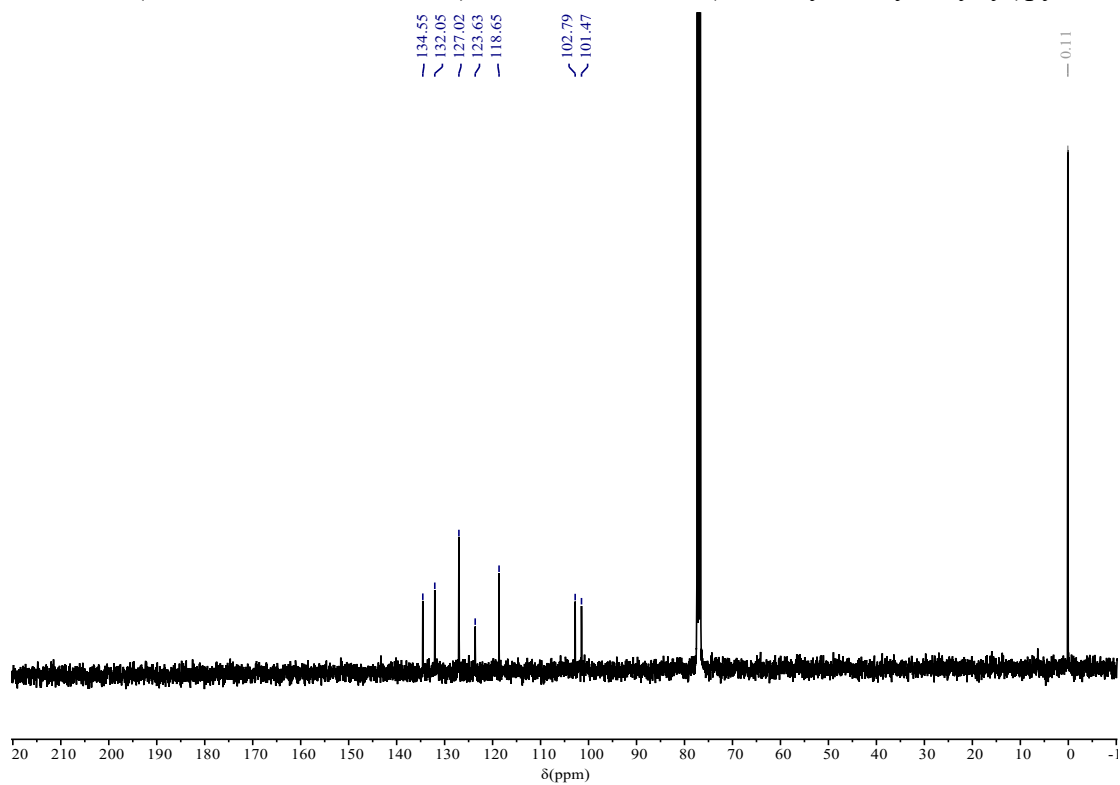
$^{13}\text{C}$  NMR (101 MHz, Chloroform-*d*)  $\delta$  163.55, 145.74, 140.02, 130.77, 130.66, 130.09, 128.19, 127.25, 126.10, 126.06, 126.03, 125.99, 125.09, 48.93, 28.26.

$^{19}\text{F}$  NMR (377 MHz, Chloroform-*d*)  $\delta$  -62.39.

## 8. NMR Spectra

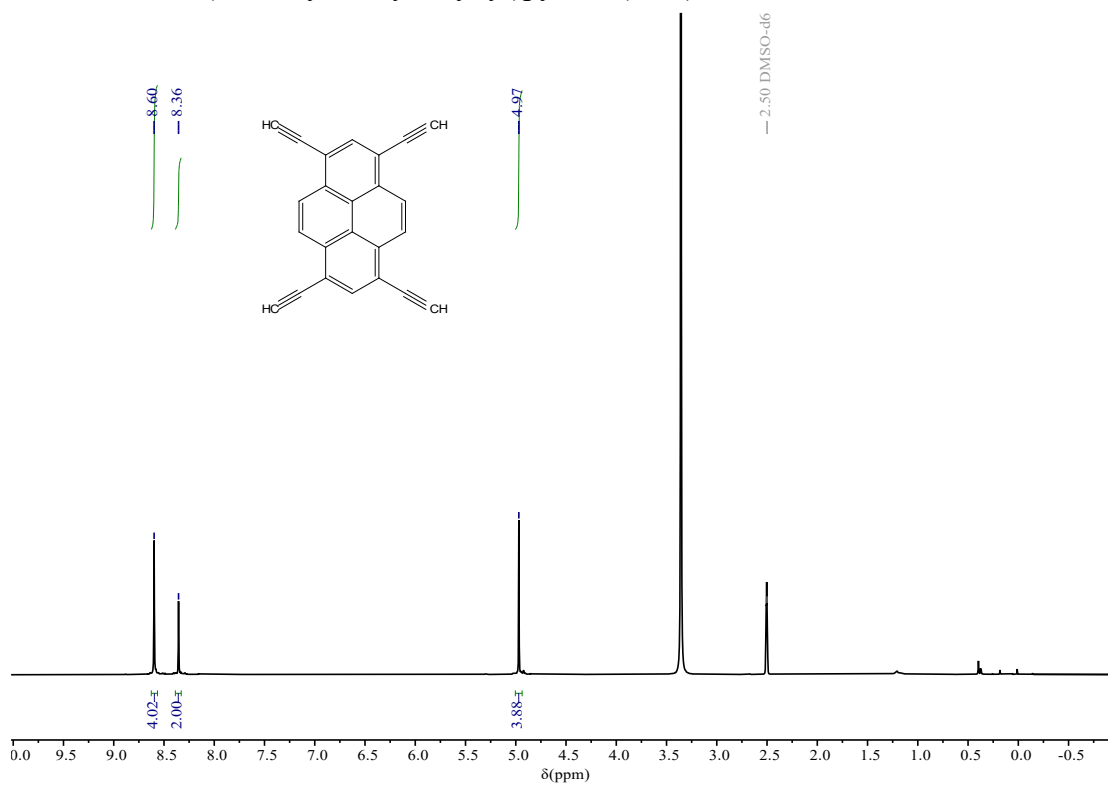


<sup>1</sup>H NMR (400 MHz, Chloroform-*d*) of 1,3,6,8-tetrakis(trimethylsilyl)ethynylpyrene

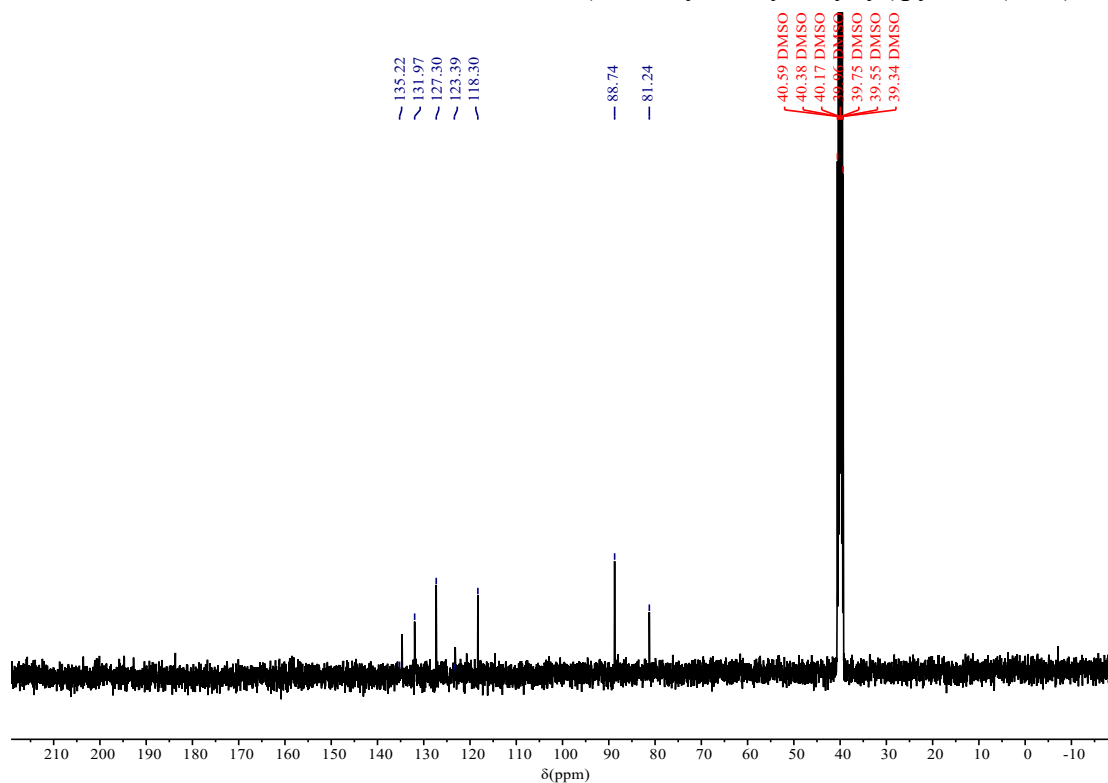


<sup>13</sup>C NMR (101 MHz, Chloroform-*d*) of 1,3,6,8-tetrakis(trimethylsilyl)ethynylpyrene

# 1,3,6,8-tetrakis(trimethylsilylethynyl)pyrene (TEP)

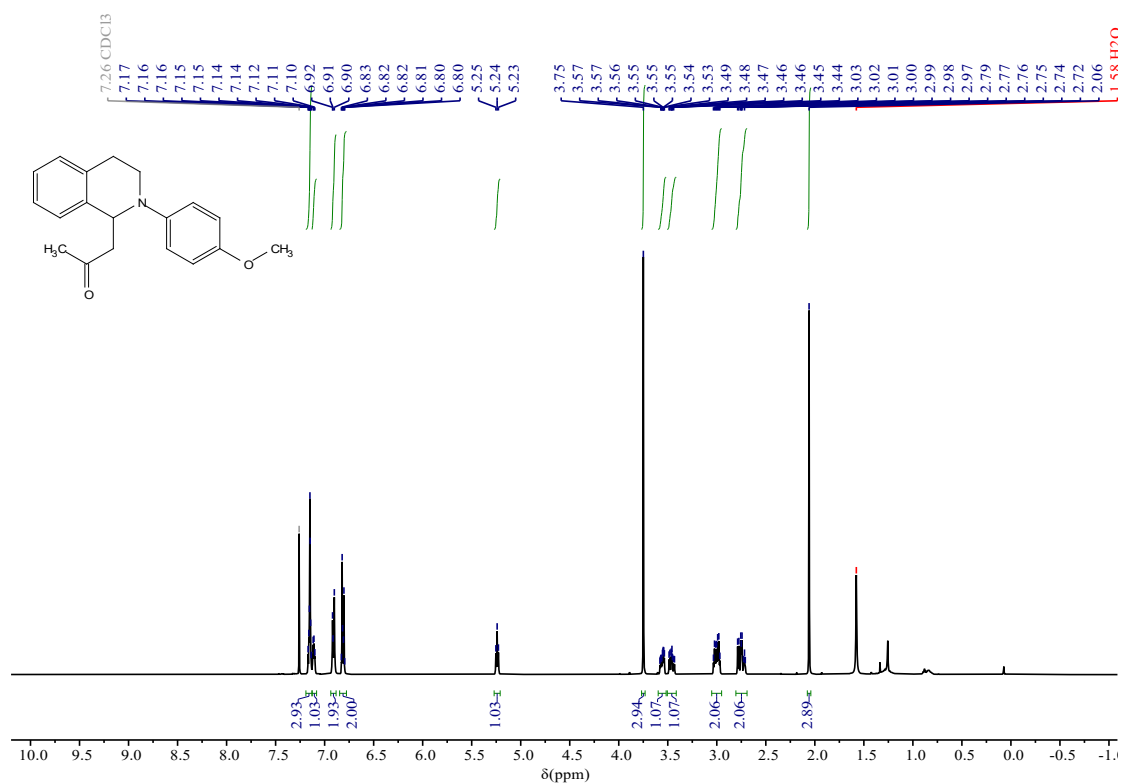


# $^{13}\text{C NMR}$ (101 MHz, $\text{DMSO-}d_6$ ) of 1,3,6,8-tetrakis(trimethylsilylethynyl)pyrene (TEP)

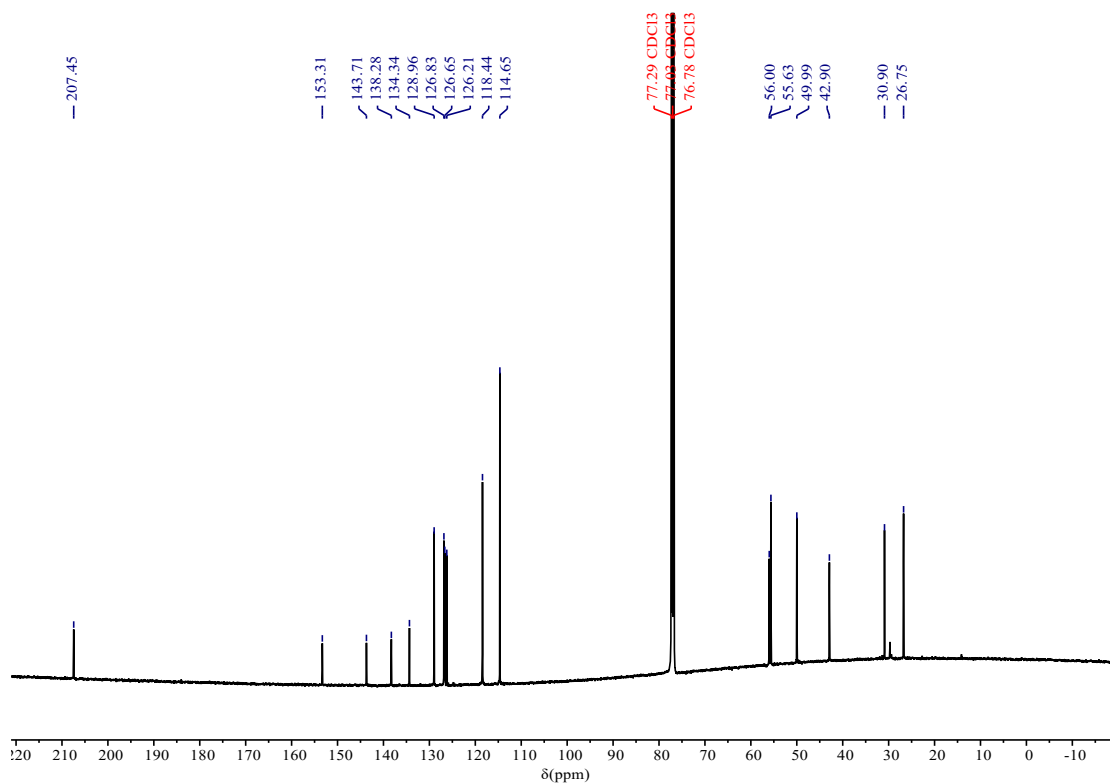




1-(2-(4-methoxyphenyl)-1,2,3,4-tetrahydroisoquinolin-1-yl)propan-2-one (2aa)

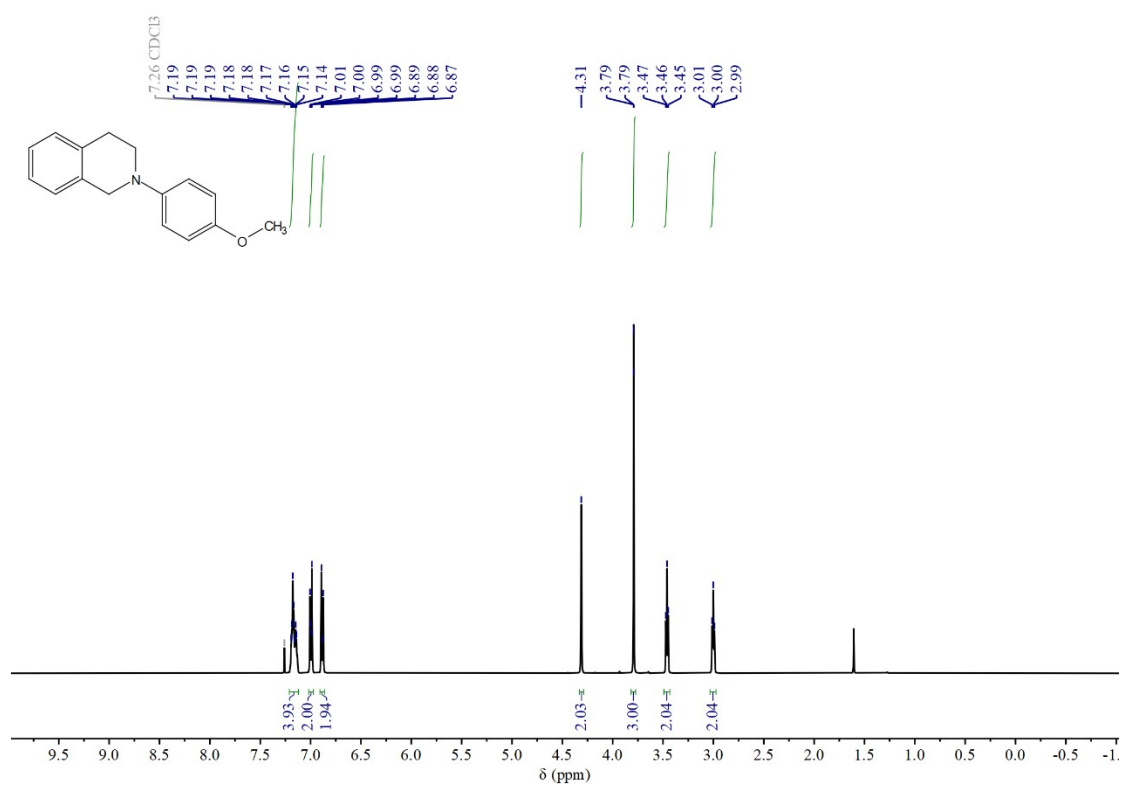


<sup>1</sup>H NMR (500 MHz, Chloroform-*d*) of 1-(2-(4-methoxyphenyl)-1,2,3,4-tetrahydroisoquinolin-1-yl)propan-2-one (2aa)

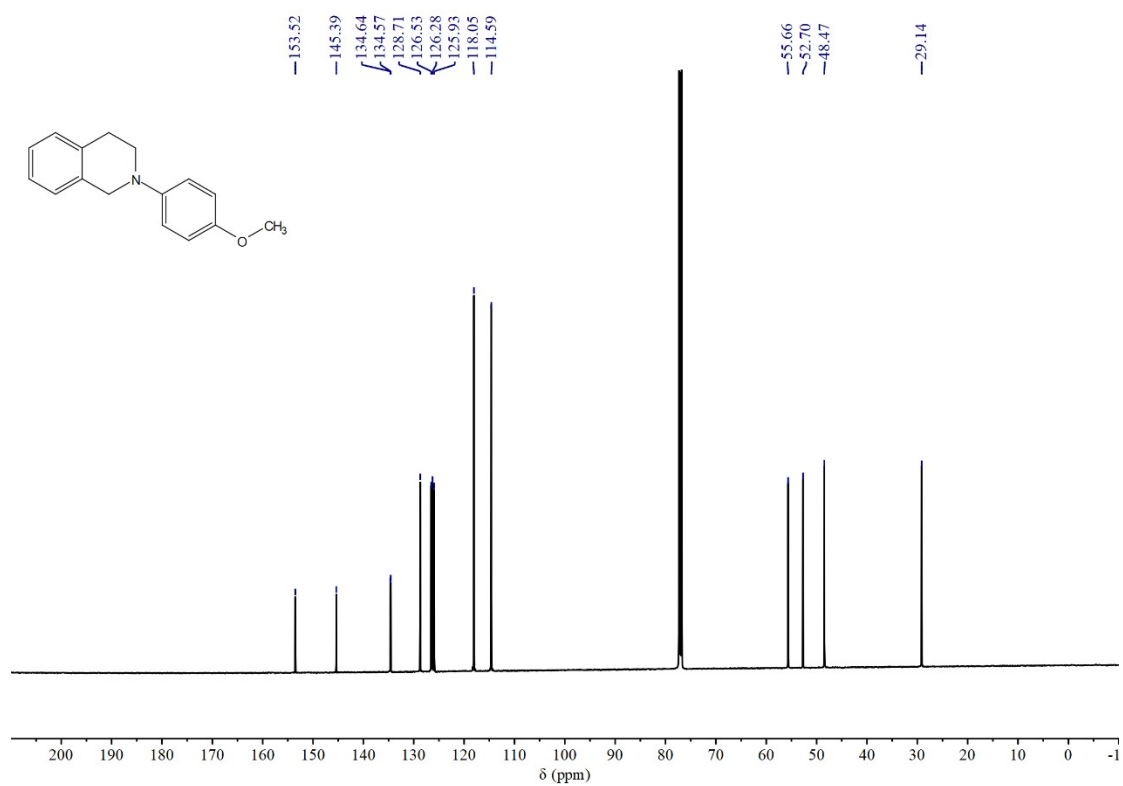


<sup>13</sup>C NMR (126 MHz, Chloroform-*d*) of 1-(2-(4-methoxyphenyl)-1,2,3,4-tetrahydroisoquinolin-1-yl)propan-2-one (2aa)

2-(4-methoxyphenyl)-1,2,3,4-tetrahydroisoquinoline (1a)

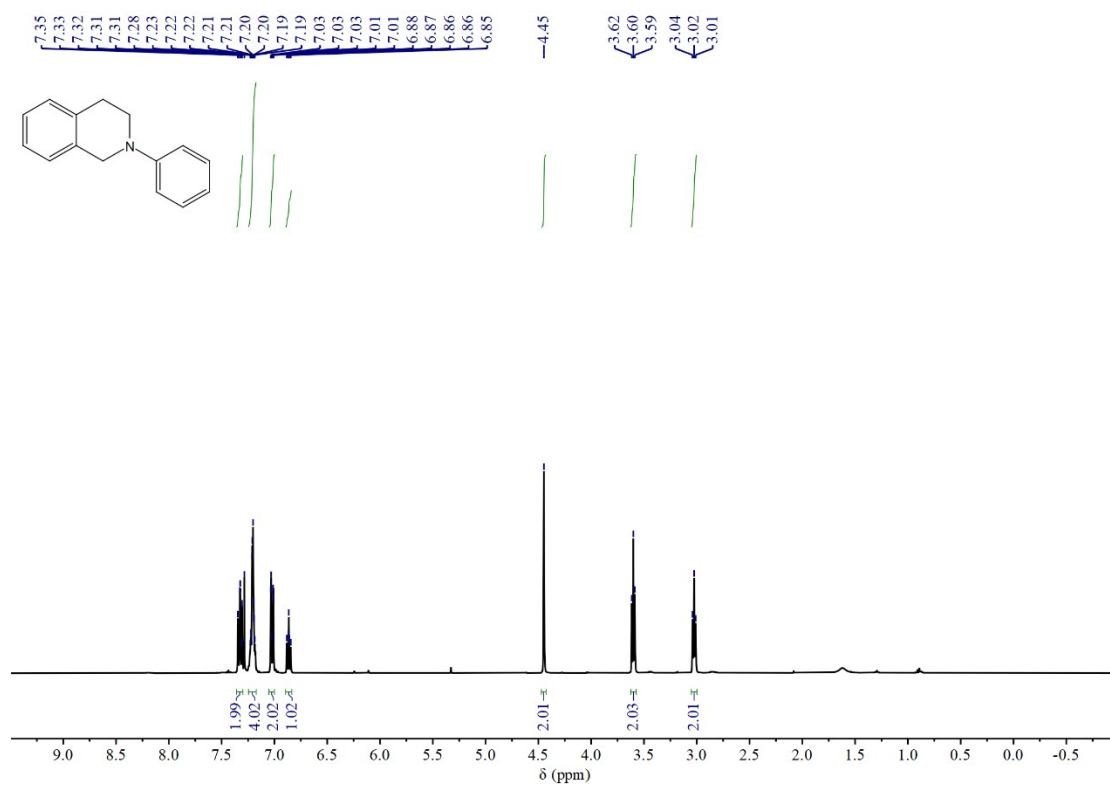


<sup>1</sup>H NMR (500 MHz, Chloroform-*d*) of 2-(4-methoxyphenyl)-1,2,3,4-tetrahydroisoquinoline (1a)

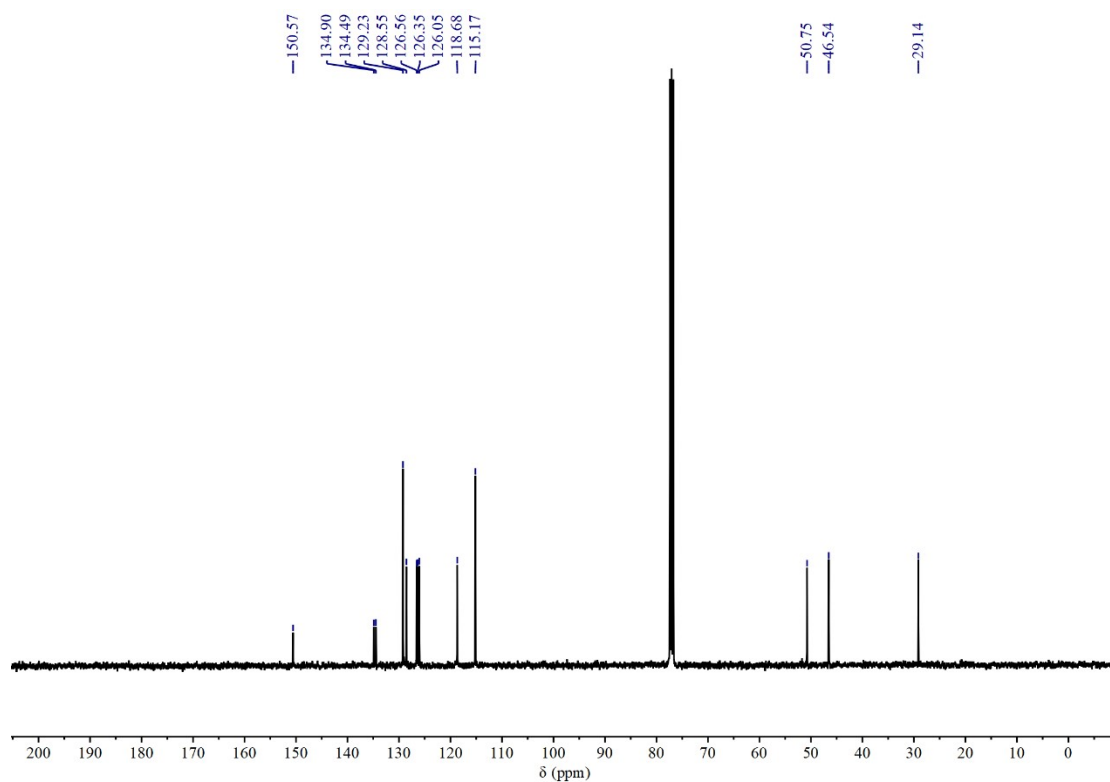


<sup>13</sup>C NMR (126 MHz, Chloroform-*d*) of 2-(4-methoxyphenyl)-1,2,3,4-tetrahydroisoquinoline (2a)

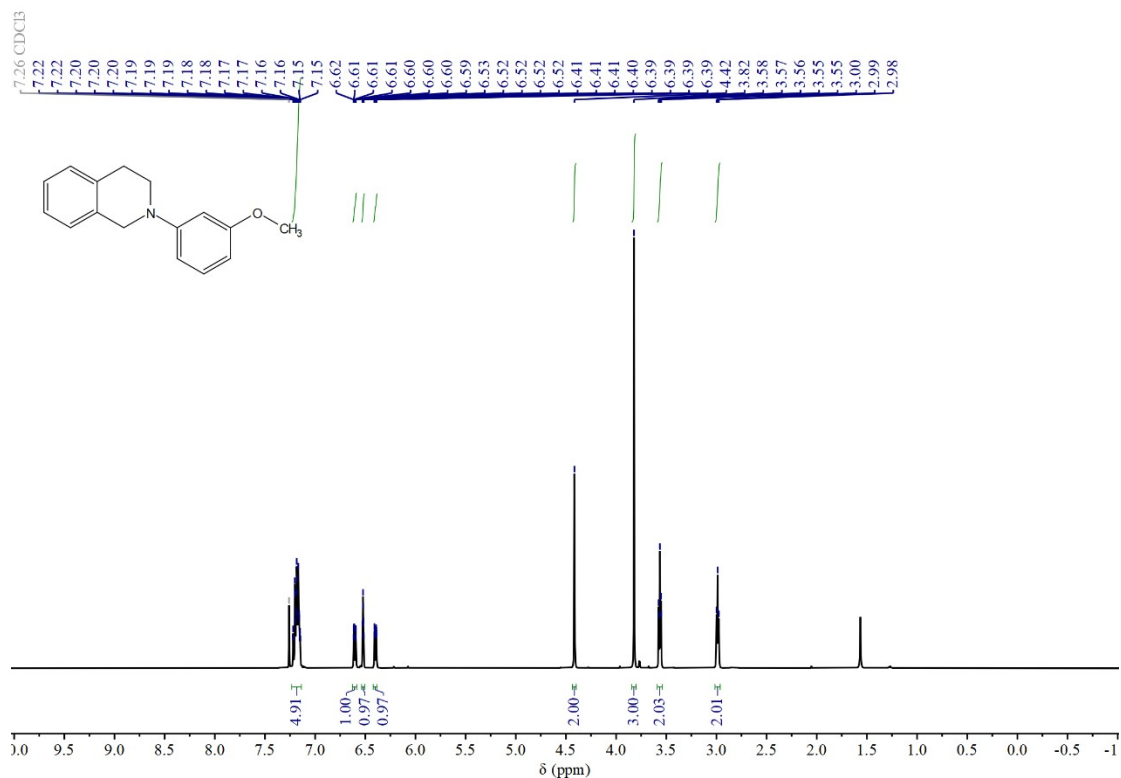
2-phenyl-1,2,3,4-tetrahydroisoquinoline (1b)



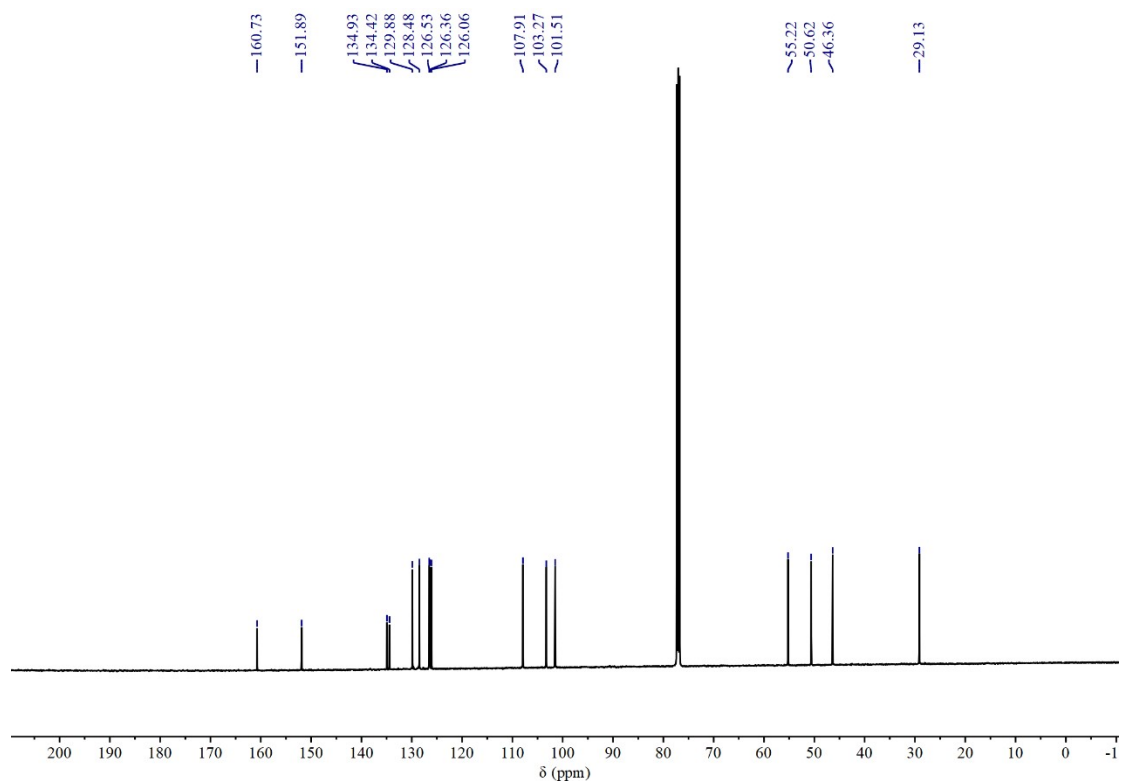
<sup>13</sup>C NMR (101 MHz, Chloroform-*d*) of 2-phenyl-1,2,3,4-tetrahydroisoquinoline (1b)



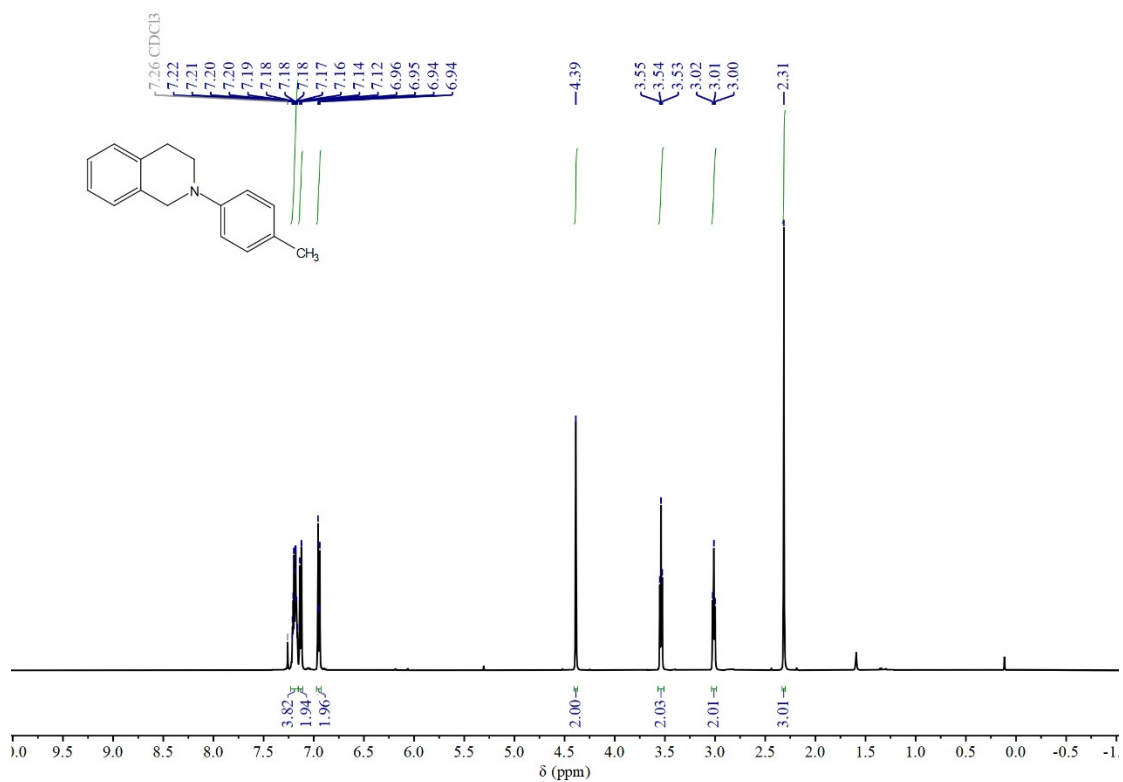
2-(3-methoxyphenyl)-1,2,3,4-tetrahydroisoquinoline (1c)



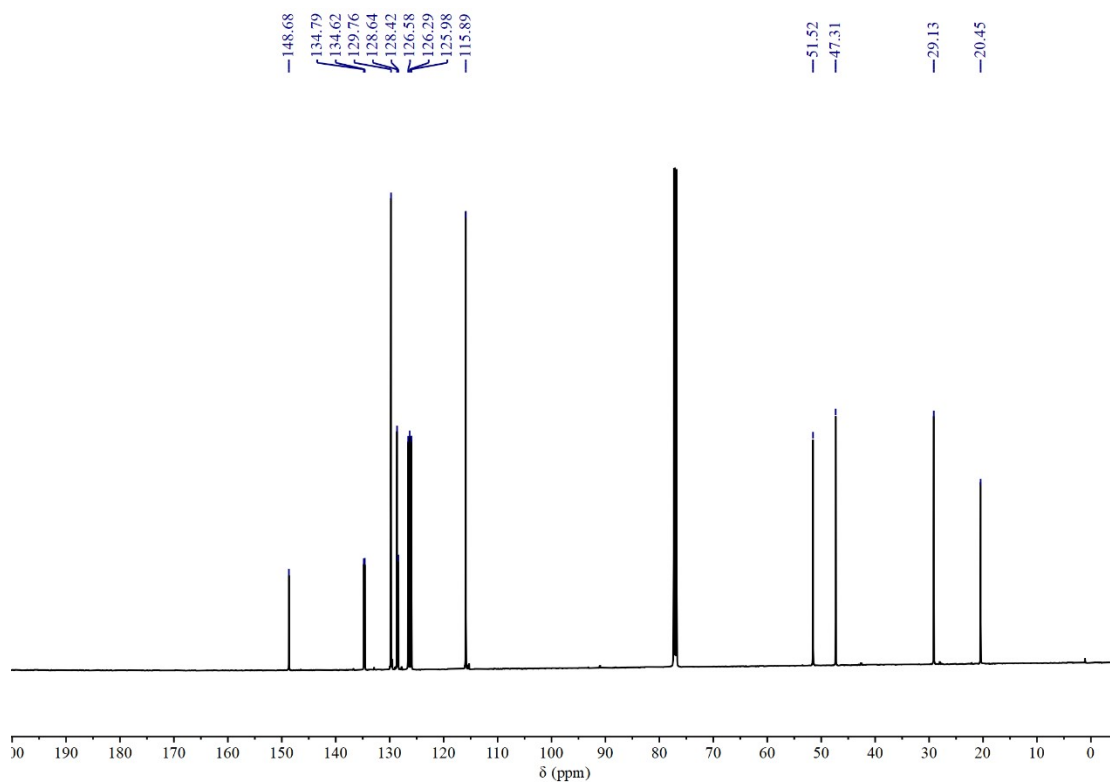
<sup>1</sup>H NMR (500 MHz, Chloroform-*d*) of 2-(3-methoxyphenyl)-1,2,3,4-tetrahydroisoquinoline (1c)



2-(*p*-tolyl)-1,2,3,4-tetrahydroisoquinoline (1d)

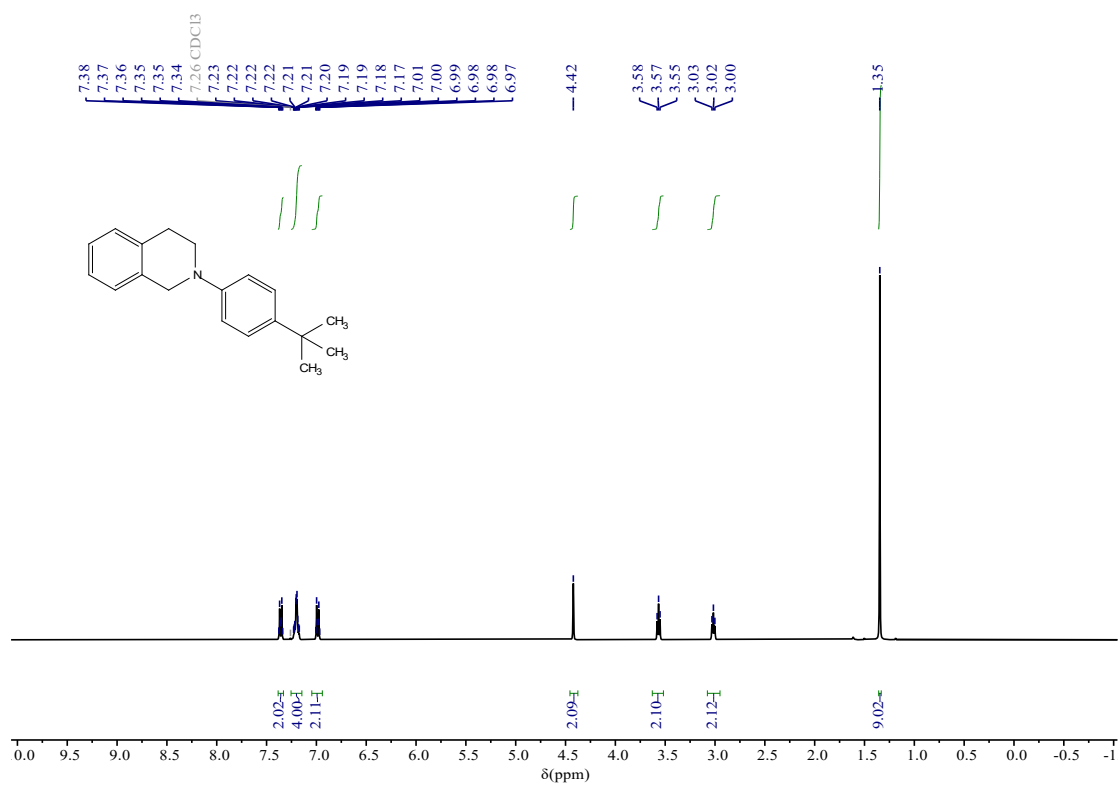


<sup>1</sup>H NMR (500 MHz, Chloroform-*d*) of 2-(*p*-tolyl)-1,2,3,4-tetrahydroisoquinoline (1d)

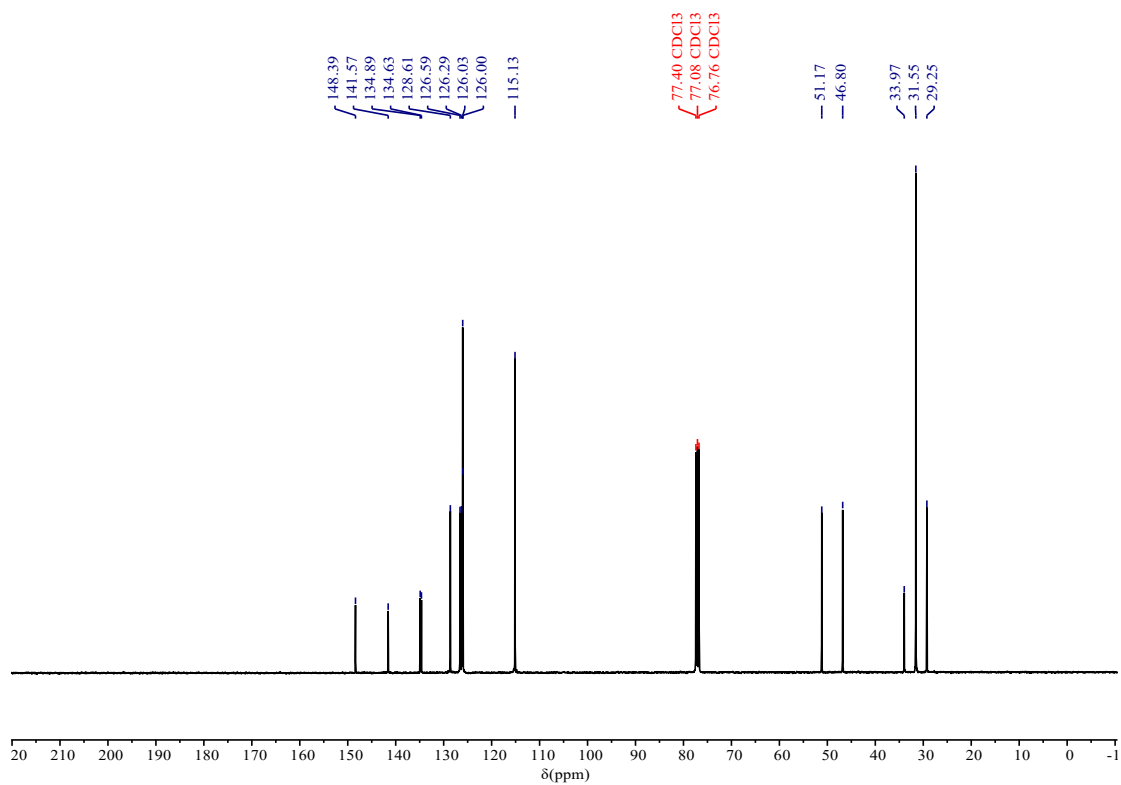


<sup>13</sup>C NMR (126 MHz, Chloroform-*d*) of 2-(*p*-tolyl)-1,2,3,4-tetrahydroisoquinoline (1d)

2-(4-(*tert*-butyl)phenyl)-1,2,3,4-tetrahydroisoquinoline (1e)

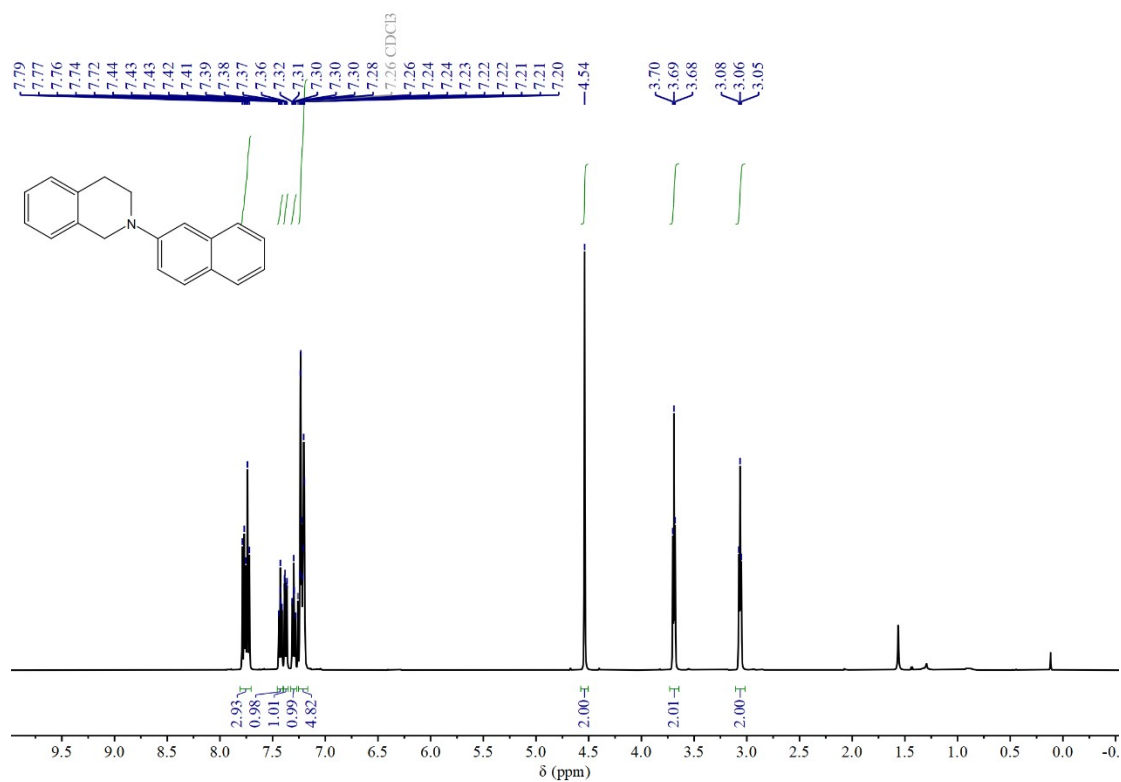


<sup>1</sup>H NMR (400 MHz, Chloroform-*d*) of 2-(4-(*tert*-butyl)phenyl)-1,2,3,4-tetrahydroisoquinoline (1e)

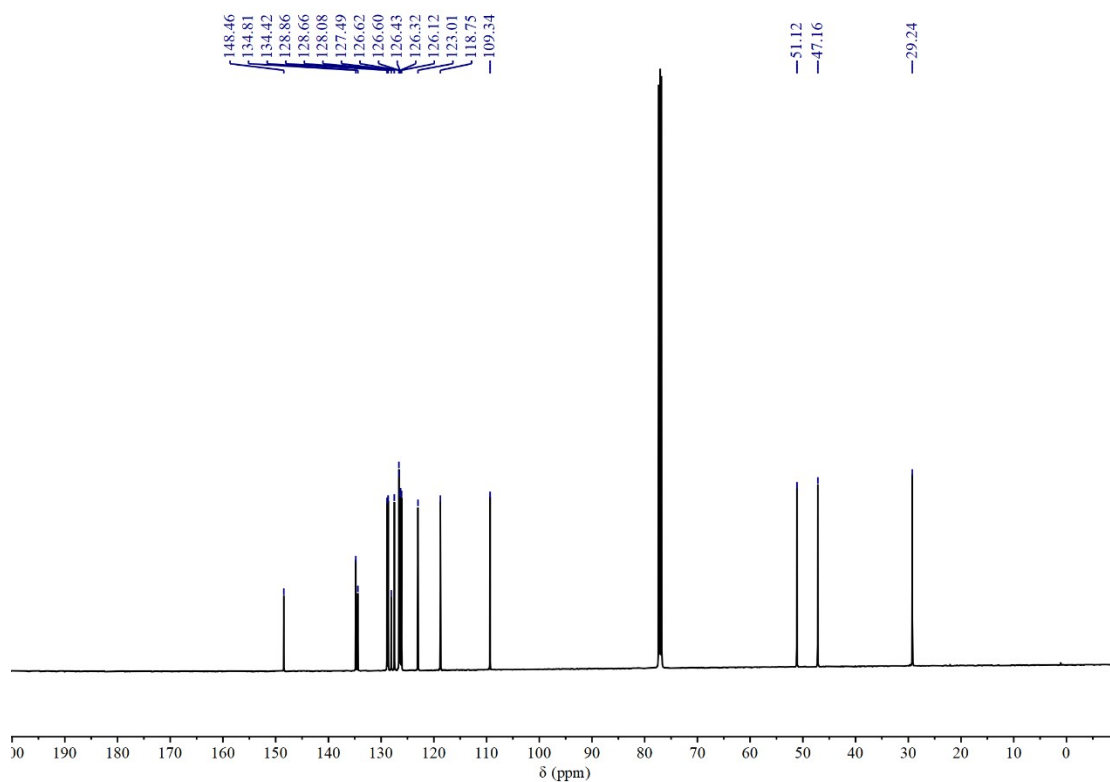


<sup>13</sup>C NMR (101 MHz, Chloroform-*d*) of 2-(4-(*tert*-butyl)phenyl)-1,2,3,4-tetrahydroisoquinoline (1e)

2-(naphthalen-2-yl)-1,2,3,4-tetrahydroisoquinoline (1f)

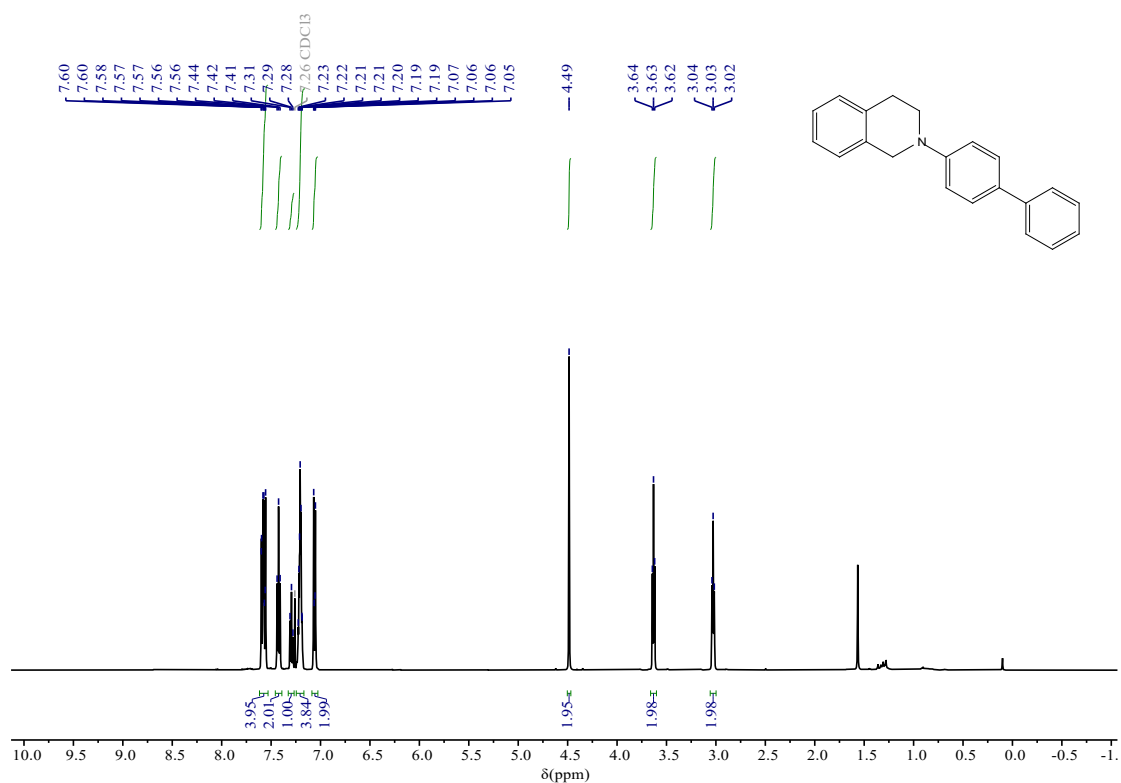


<sup>1</sup>H NMR (500 MHz, Chloroform-*d*) of 2-(naphthalen-2-yl)-1,2,3,4-tetrahydroisoquinoline (1f)

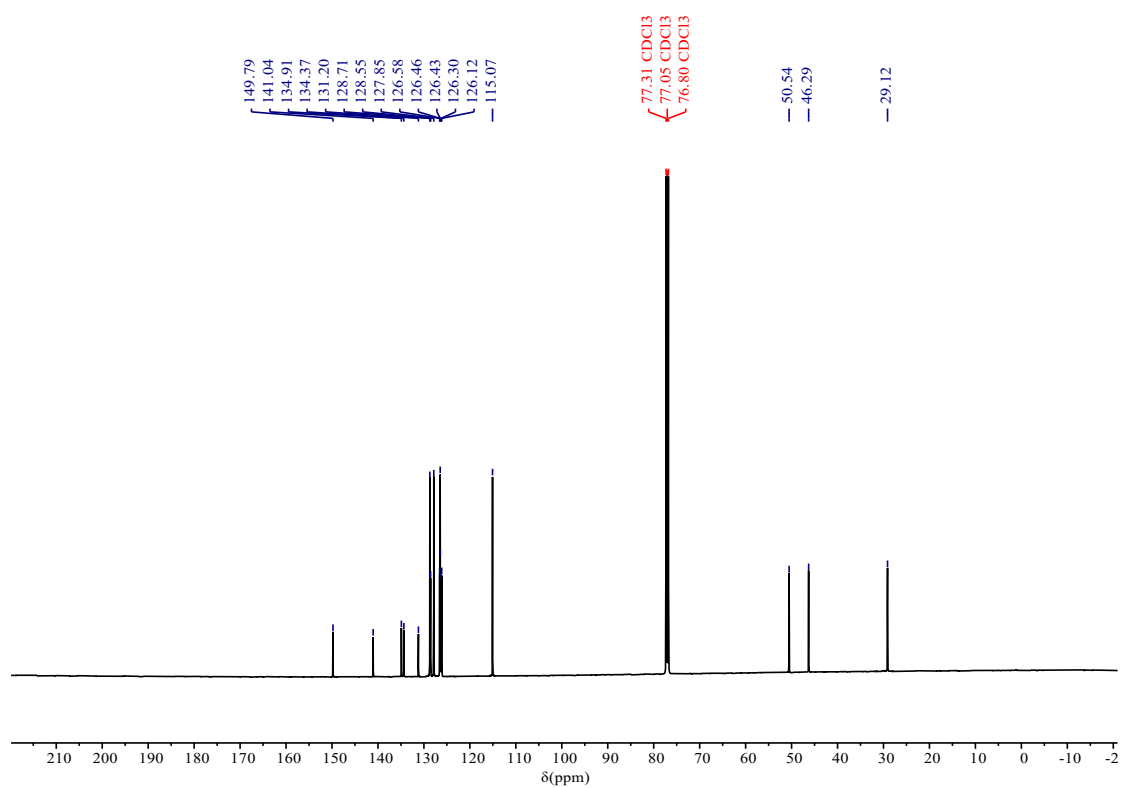


<sup>13</sup>C NMR (126 MHz, Chloroform-*d*) of 2-(naphthalen-2-yl)-1,2,3,4-tetrahydroisoquinoline (1f)

2-([1,1'-biphenyl]-4-yl)-1,2,3,4-tetrahydroisoquinoline (1g)



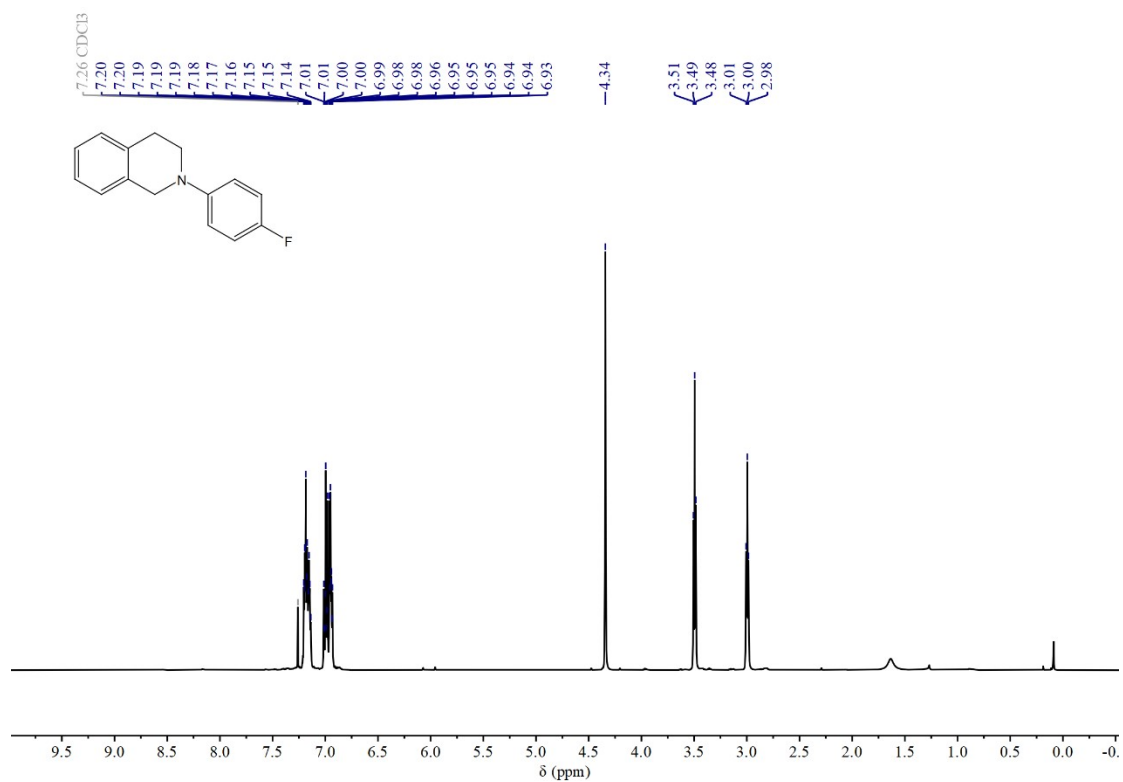
<sup>1</sup>H NMR (500 MHz, Chloroform-*d*) of 2-([1,1'-biphenyl]-4-yl)-1,2,3,4-tetrahydroisoquinoline (1g)



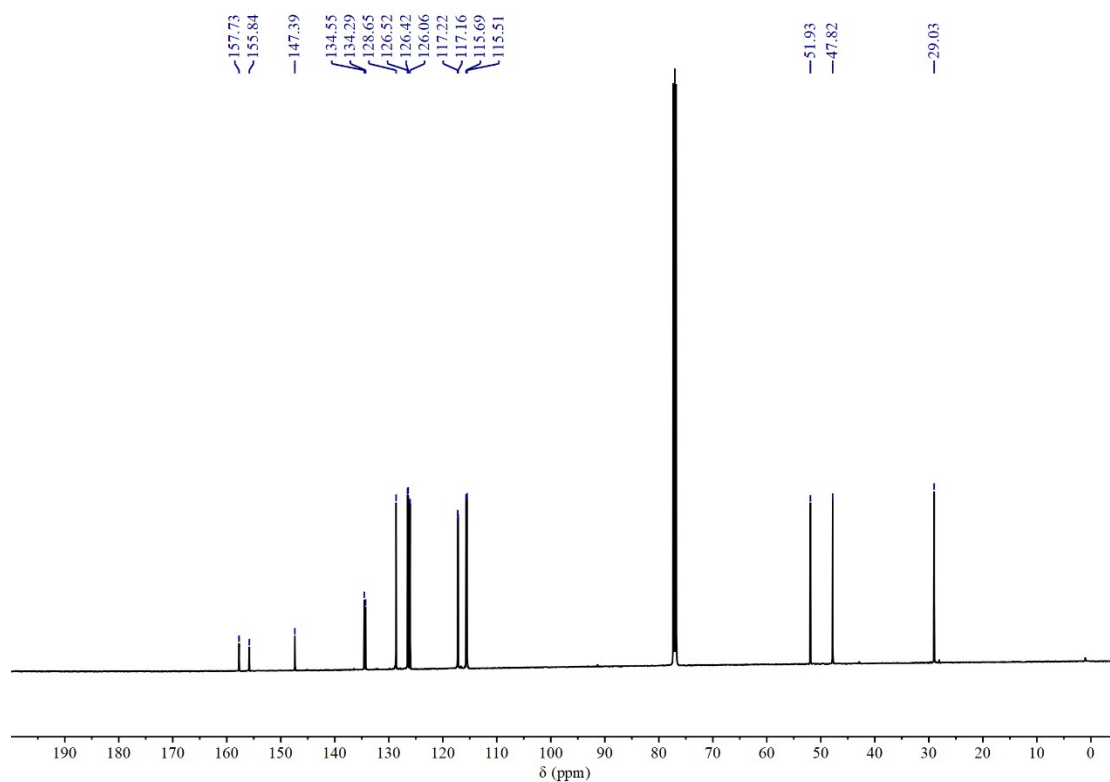
<sup>13</sup>C NMR (126 MHz, Chloroform-*d*) of 2-([1,1'-biphenyl]-4-yl)-1,2,3,4-tetrahydroisoquinoline (1g)



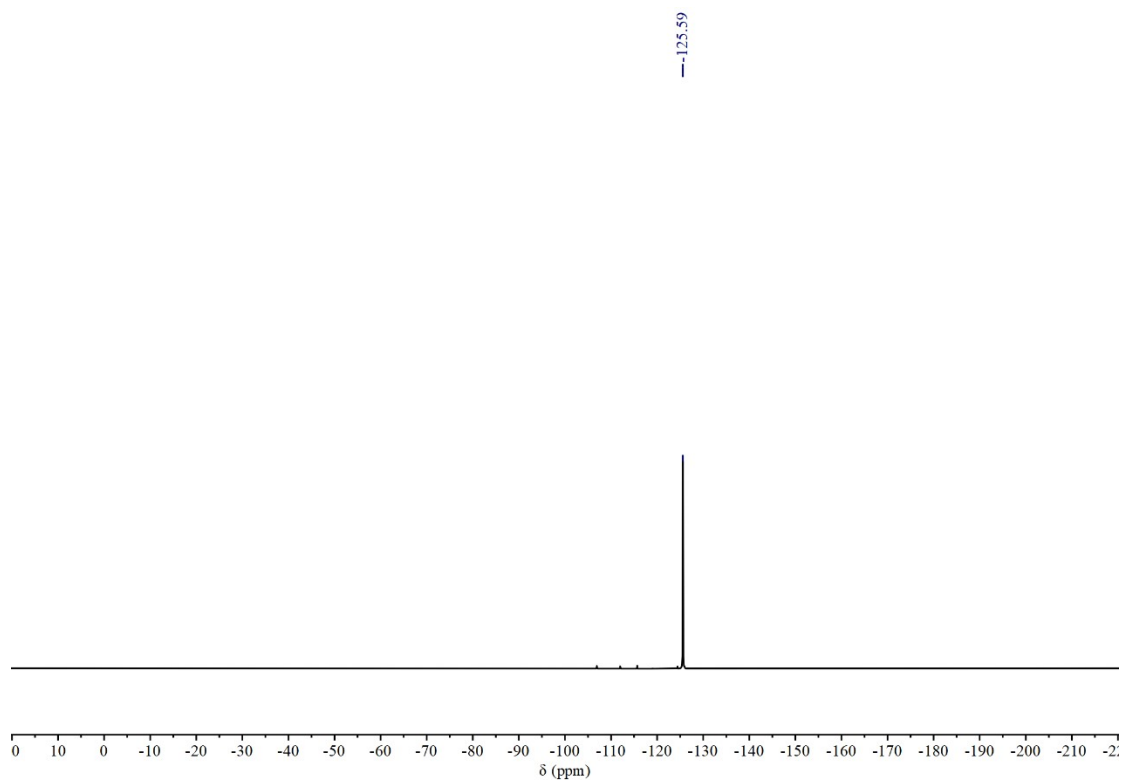
2-(4-fluorophenyl)-1,2,3,4-tetrahydroisoquinoline (1h)



<sup>1</sup>H NMR (500 MHz, Chloroform-*d*) of 2-(4-fluorophenyl)-1,2,3,4-tetrahydroisoquinoline (1h)

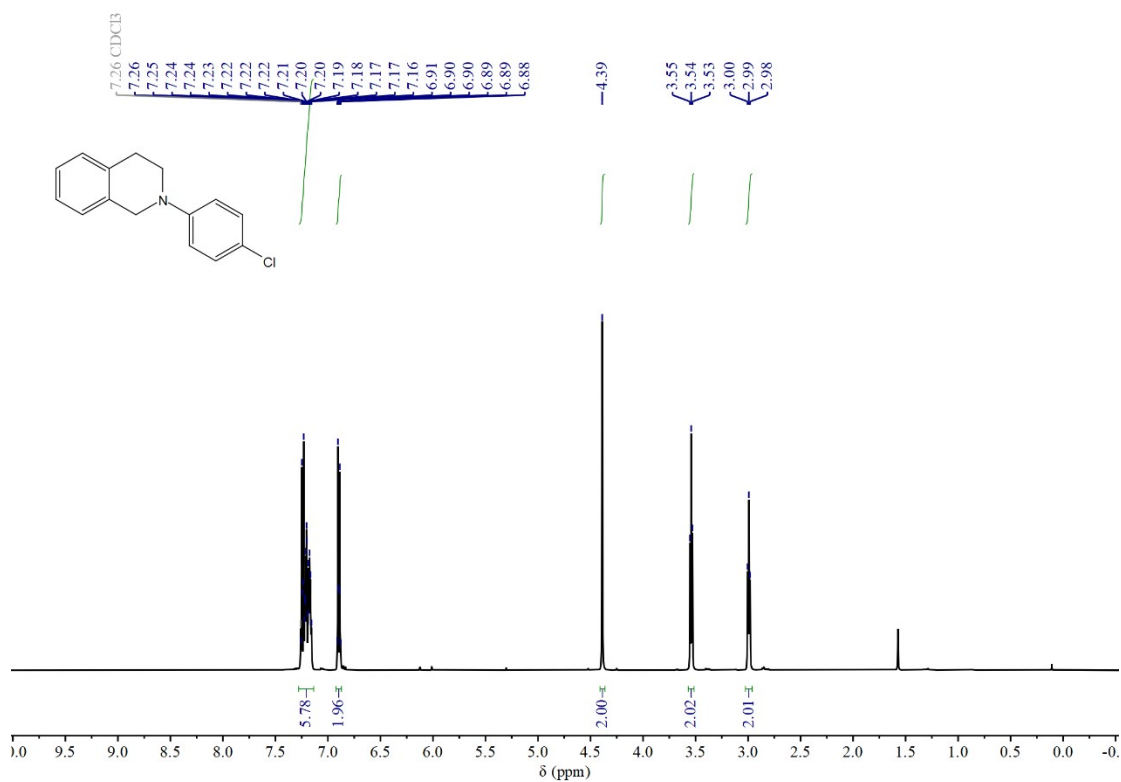


<sup>13</sup>C NMR (126 MHz, Chloroform-*d*) of 2-(4-fluorophenyl)-1,2,3,4-tetrahydroisoquinoline (1h)

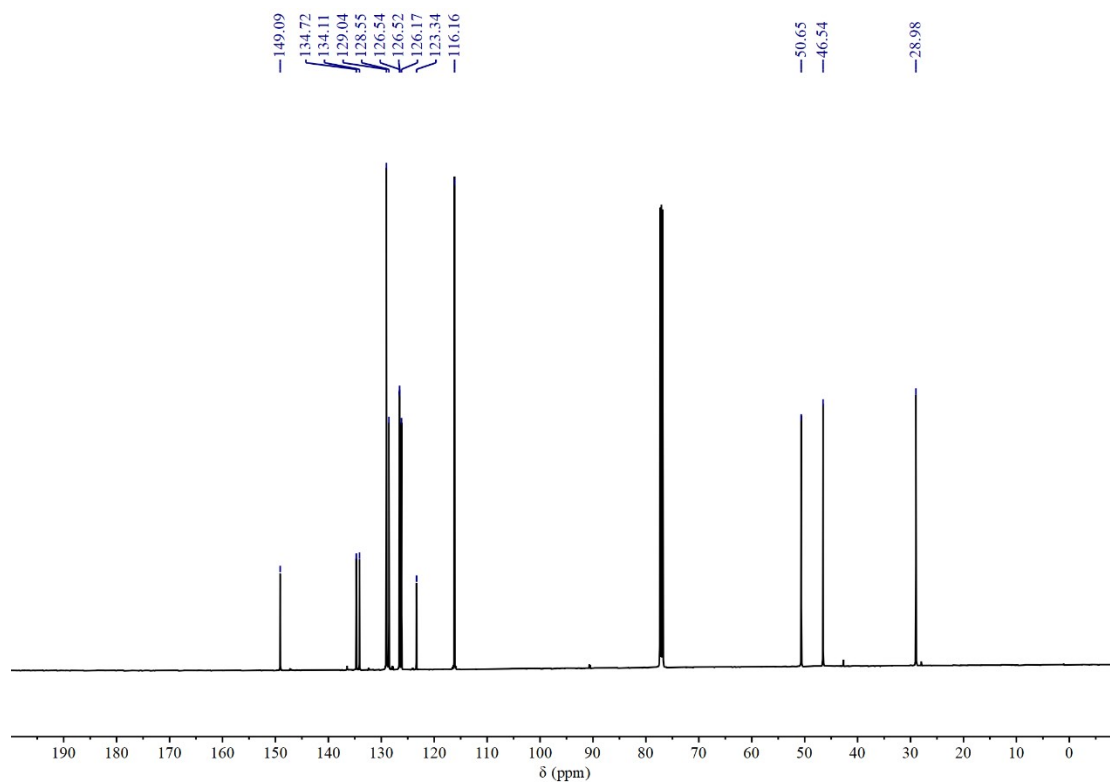


$^{19}\text{F}$  NMR (471 MHz, Chloroform-d) of 2-(4-fluorophenyl)-1,2,3,4-tetrahydroisoquinoline (1h)

2-(4-chlorophenyl)-1,2,3,4-tetrahydroisoquinoline (1i)

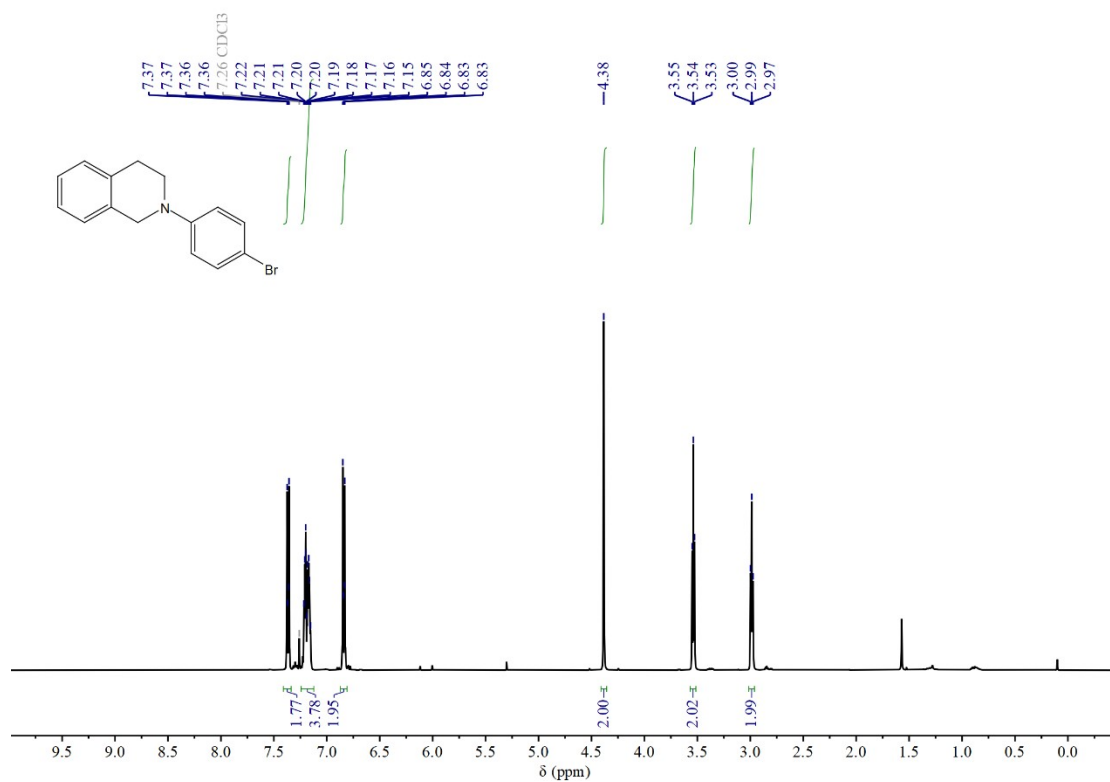


<sup>1</sup>H NMR (500 MHz, Chloroform-*d*) of 2-(4-chlorophenyl)-1,2,3,4-tetrahydroisoquinoline (1i)

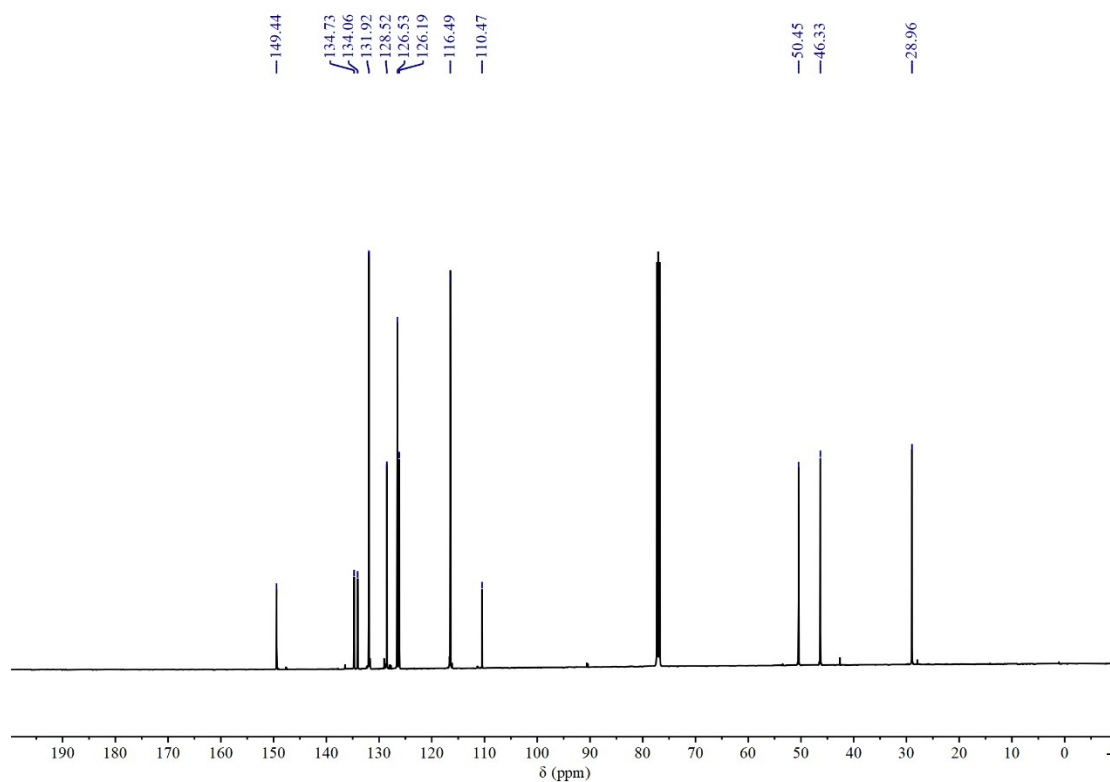


<sup>13</sup>C NMR (126 MHz, Chloroform-*d*) of 2-(4-chlorophenyl)-1,2,3,4-tetrahydroisoquinoline (1i)

2-(4-bromophenyl)-1,2,3,4-tetrahydroisoquinoline (1j)

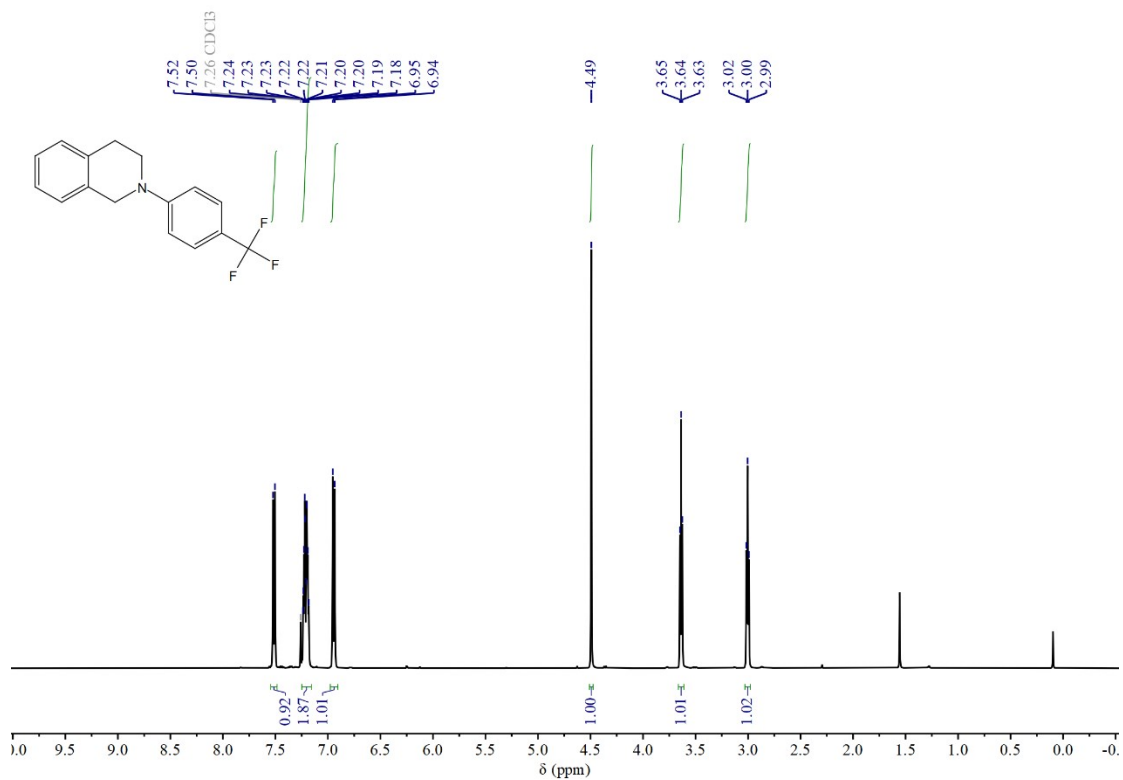


<sup>1</sup>H NMR (500 MHz, Chloroform-*d*) of 2-(4-bromophenyl)-1,2,3,4-tetrahydroisoquinoline (1j)

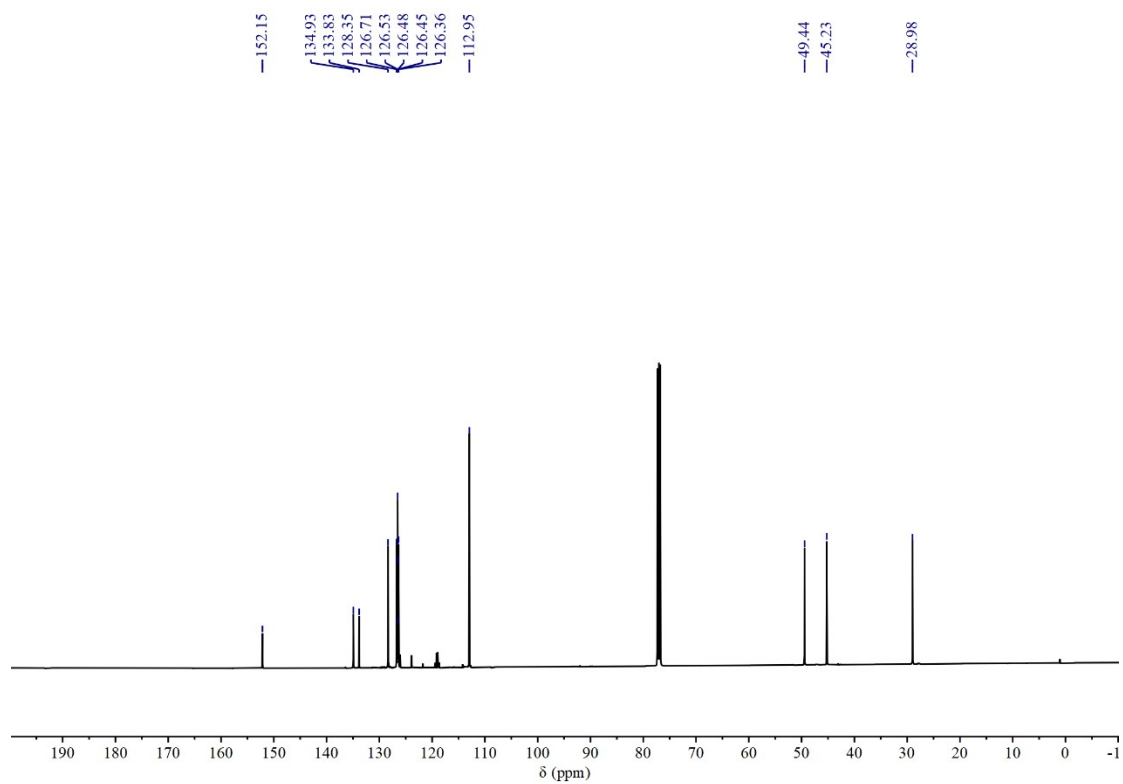


<sup>13</sup>C NMR (126 MHz, Chloroform-*d*) of 2-(4-bromophenyl)-1,2,3,4-tetrahydroisoquinoline (1j)

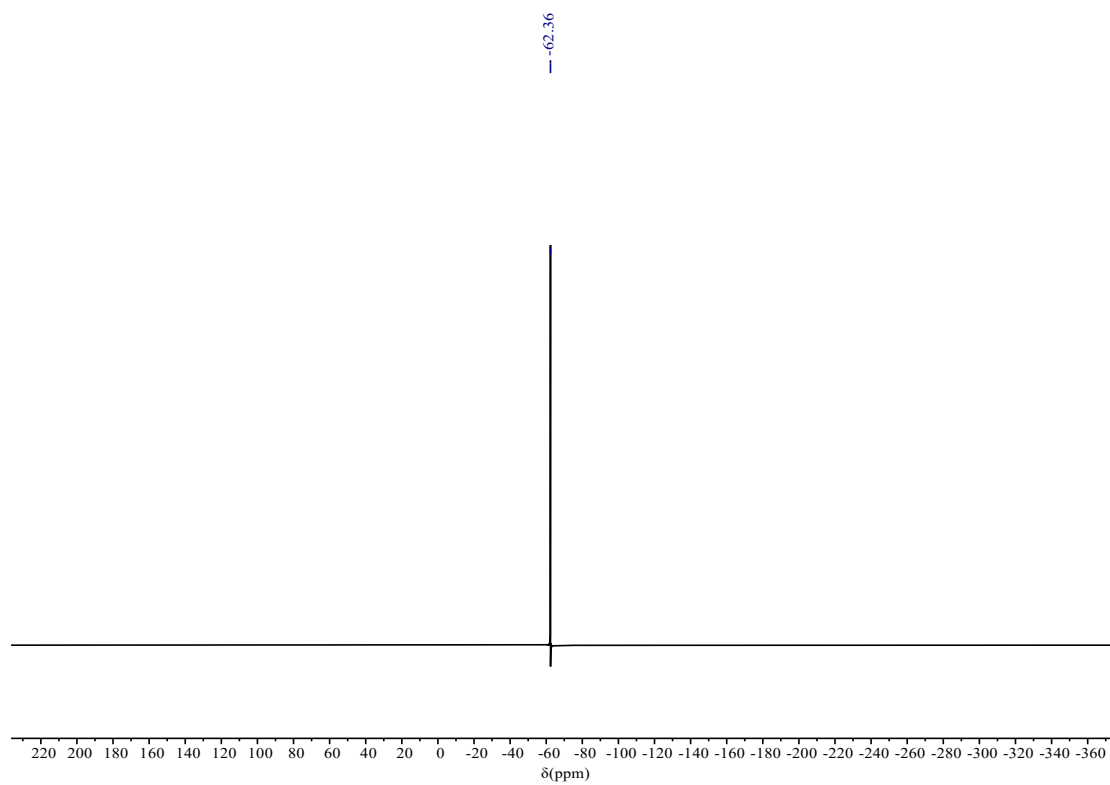
2-((p-trifluoromethyl)-phenyl)-1,2,3,4-tetrahydroisoquinoline (1k)



<sup>1</sup>H NMR (500 MHz, Chloroform-*d*) of 2-((p-trifluoromethyl)-phenyl)-1,2,3,4-tetrahydroisoquinoline (1k)

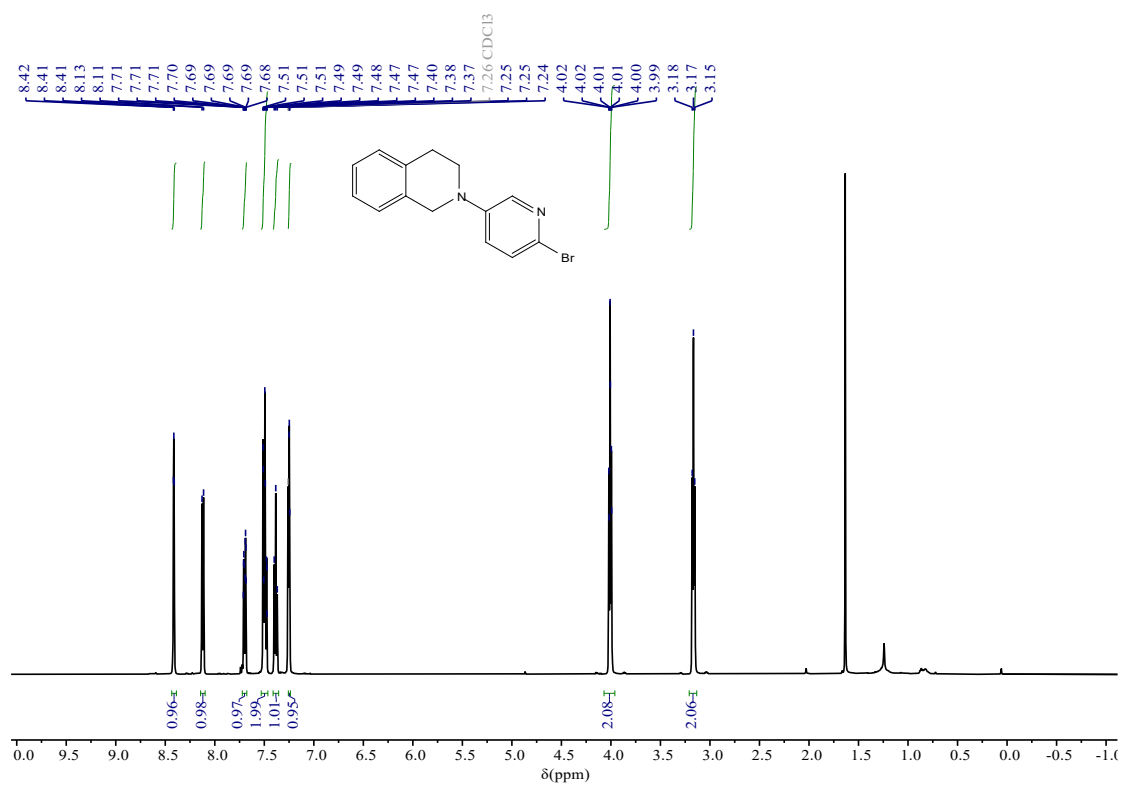


<sup>13</sup>C NMR (126 MHz, Chloroform-*d*) of 2-((p-trifluoromethyl)-phenyl)-1,2,3,4-tetrahydroisoquinoline (1k)

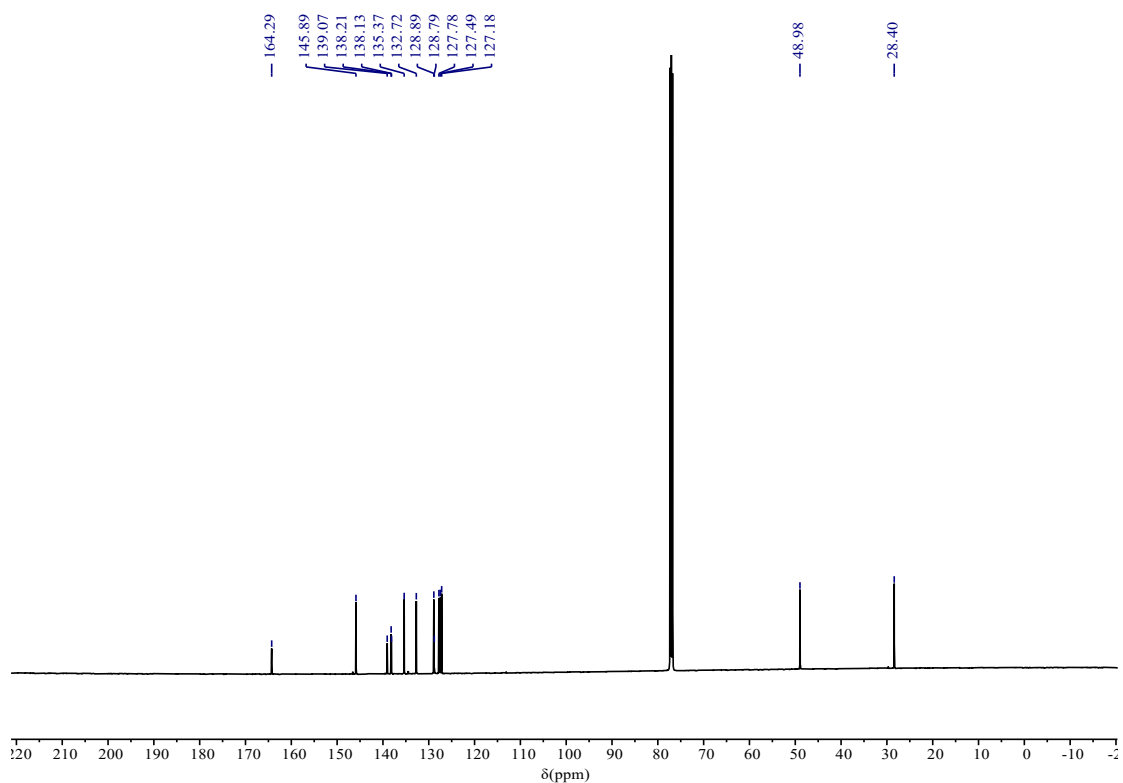


$^{19}\text{F}$  NMR (471 MHz, Chloroform- $d$ ) of 2-(( $p$ -trifluoromethyl)-phenyl)-1,2,3,4-tetrahydroisoquinoline (1k)

2-(6-bromopyridin-3-yl)-1,2,3,4-tetrahydroisoquinoline (11)

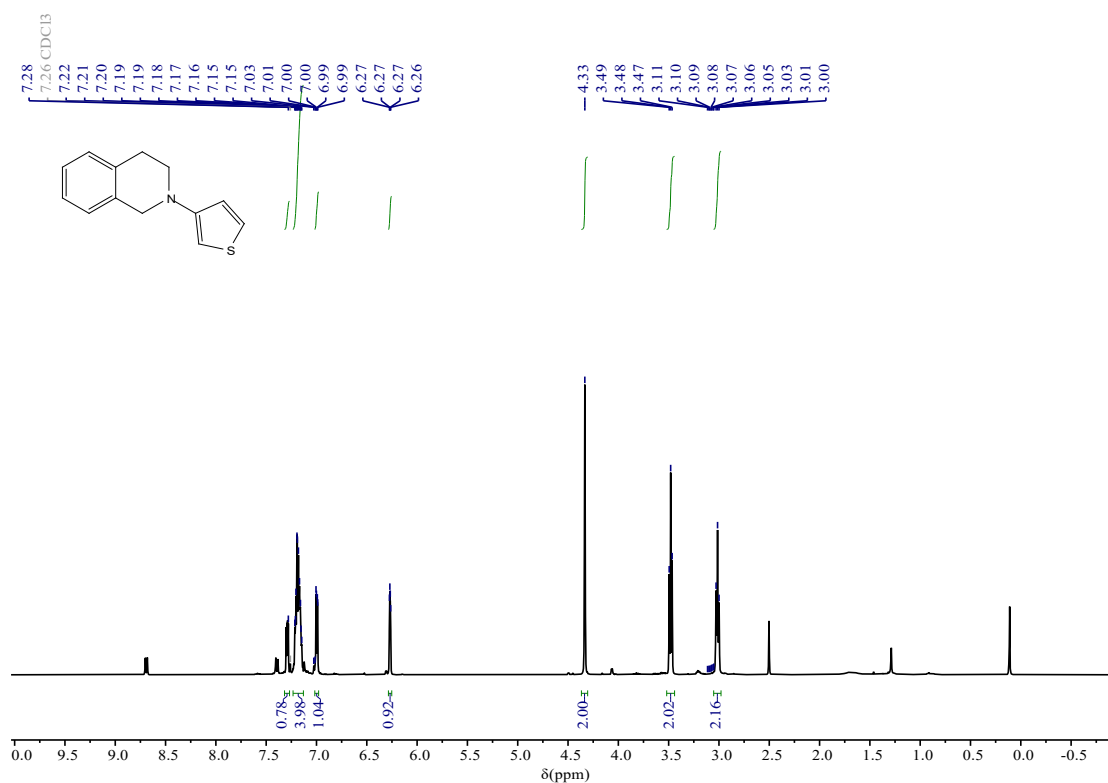


<sup>1</sup>H NMR (500 MHz, Chloroform-*d*) of 2-(6-bromopyridin-3-yl)-1,2,3,4-tetrahydroisoquinoline (11)

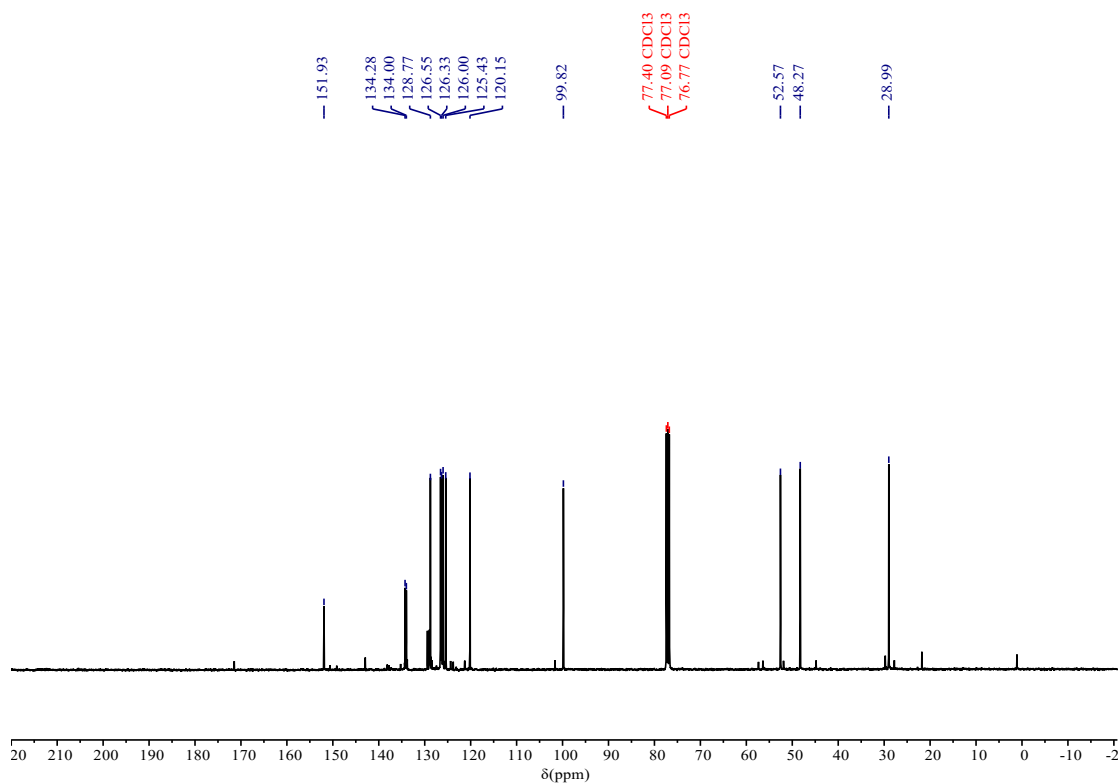


<sup>13</sup>C NMR (126 MHz, Chloroform-*d*) of 2-(6-bromopyridin-3-yl)-1,2,3,4-tetrahydroisoquinoline (11)

2-(thiophen-3-yl)-1,2,3,4-tetrahydroisoquinoline (1m)



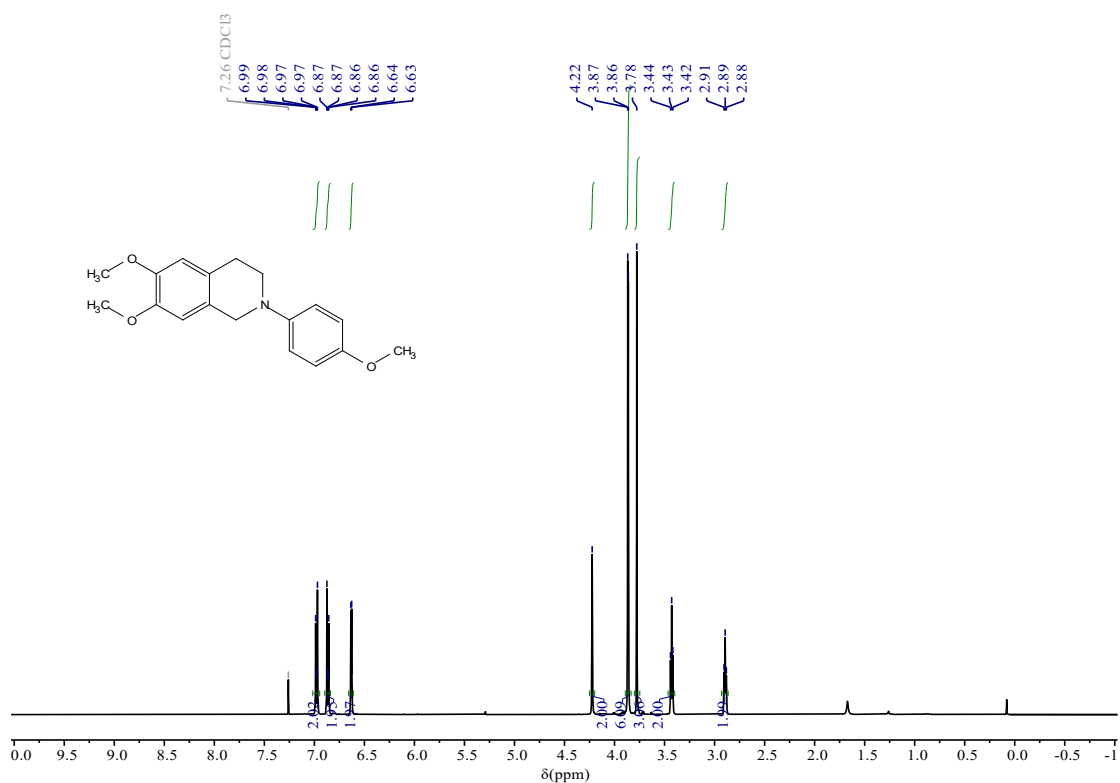
<sup>1</sup>H NMR (400 MHz, Chloroform-*d*) of 2-(thiophen-3-yl)-1,2,3,4-tetrahydroisoquinoline (1m)



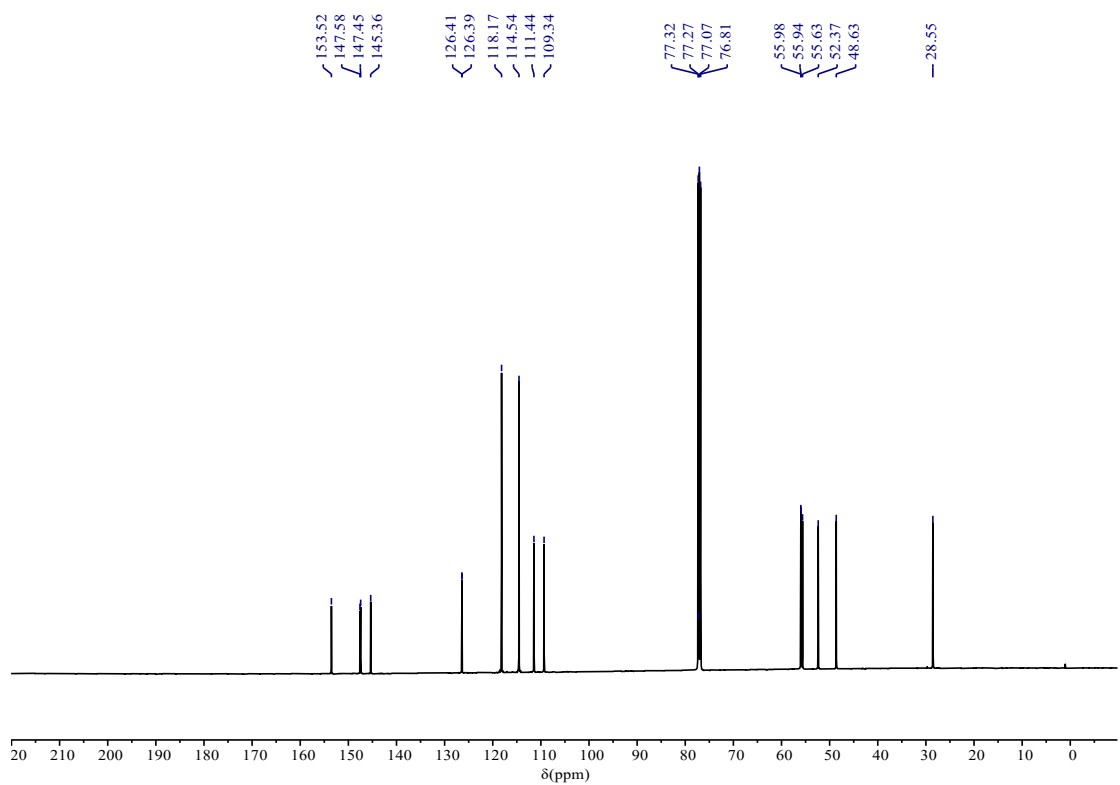
<sup>13</sup>C NMR (101 MHz, Chloroform-*d*) of 2-(thiophen-3-yl)-1,2,3,4-tetrahydroisoquinoline (1m)



6,7-dimethoxy-2-(4-methoxyphenyl)-1,2,3,4-tetrahydroisoquinoline (1n)

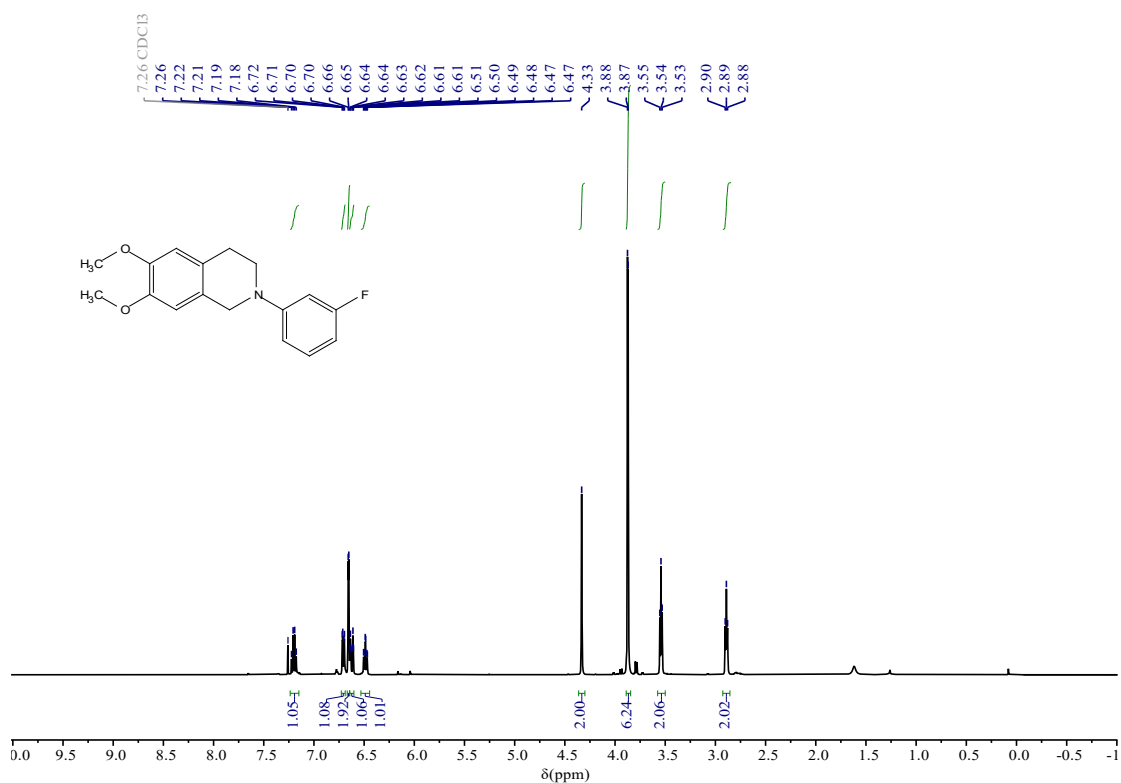


<sup>1</sup>H NMR (500 MHz, Chloroform-*d*) of 6,7-dimethoxy-2-(4-methoxyphenyl)-1,2,3,4-tetrahydroisoquinoline (1n)

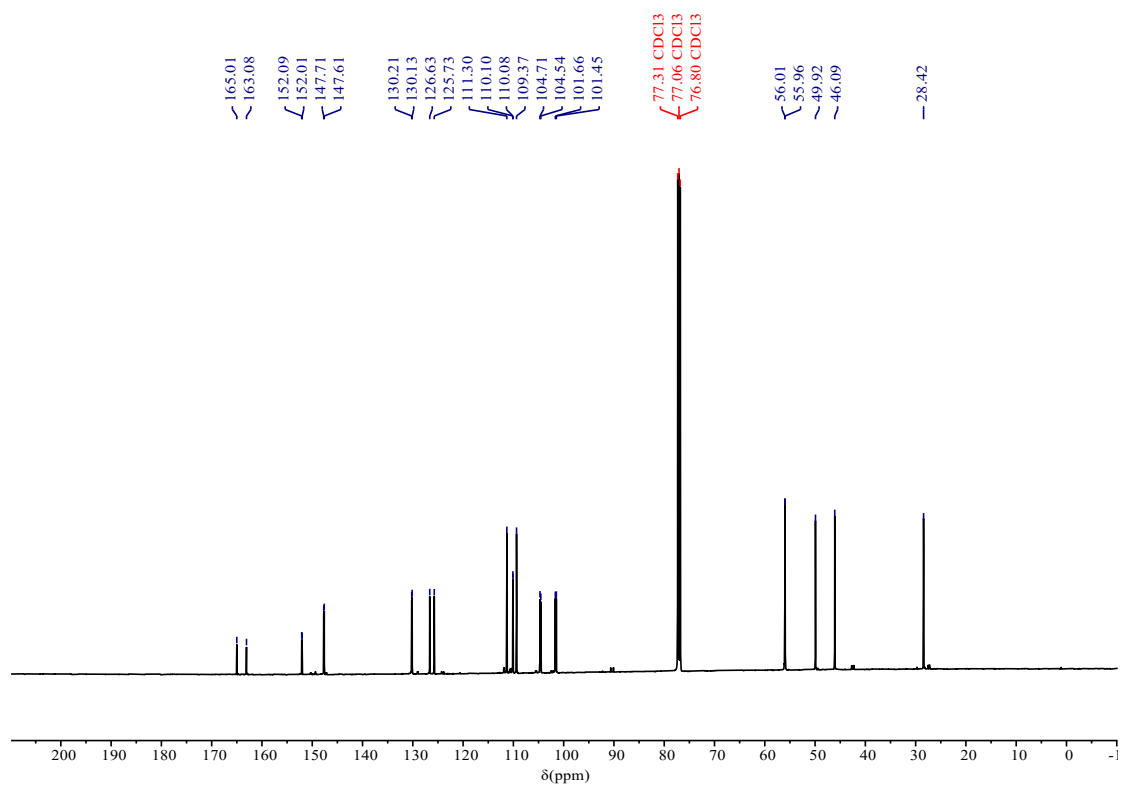


<sup>13</sup>C NMR (126 MHz, Chloroform-*d*) of 6,7-dimethoxy-2-(4-methoxyphenyl)-1,2,3,4-tetrahydroisoquinoline (1n)

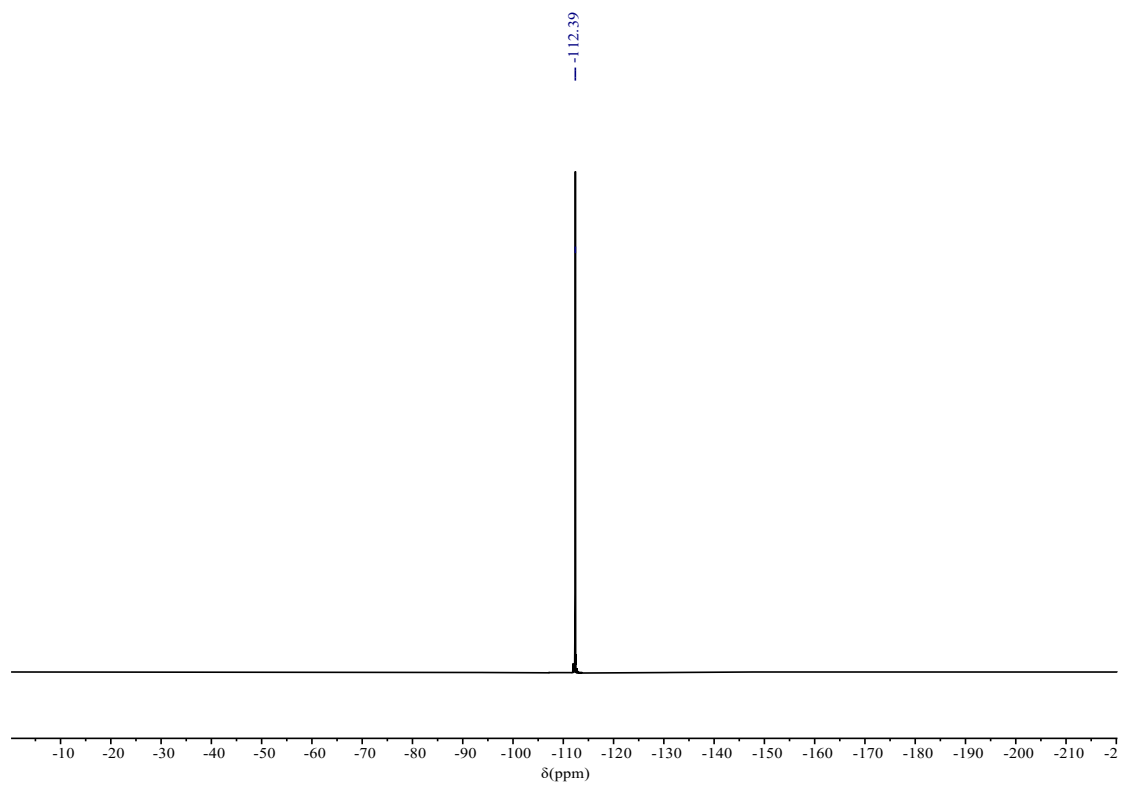
2-(3-fluorophenyl)-6,7-dimethoxy-1,2,3,4-tetrahydroisoquinoline (1o)



<sup>1</sup>H NMR (500 MHz, Chloroform-*d*) of 2-(3-fluorophenyl)-6,7-dimethoxy-1,2,3,4-tetrahydroisoquinoline (1o)

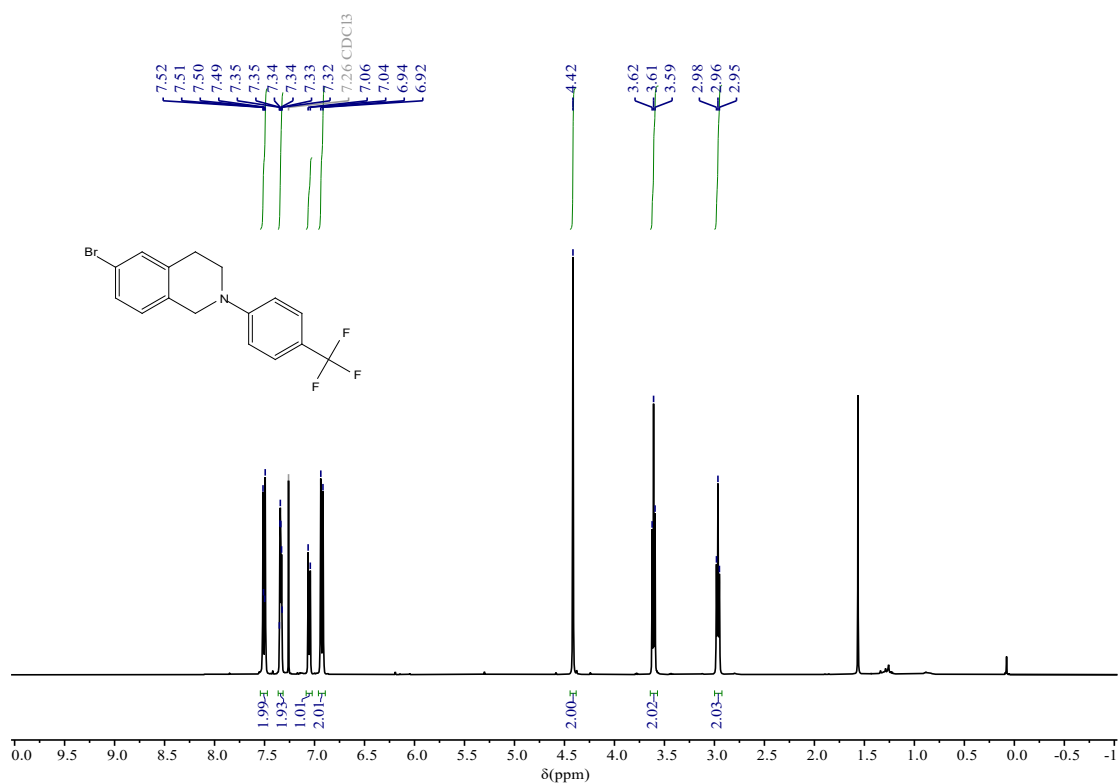


<sup>13</sup>C NMR (126 MHz, Chloroform-*d*) of 2-(3-fluorophenyl)-6,7-dimethoxy-1,2,3,4-tetrahydroisoquinoline (1o)

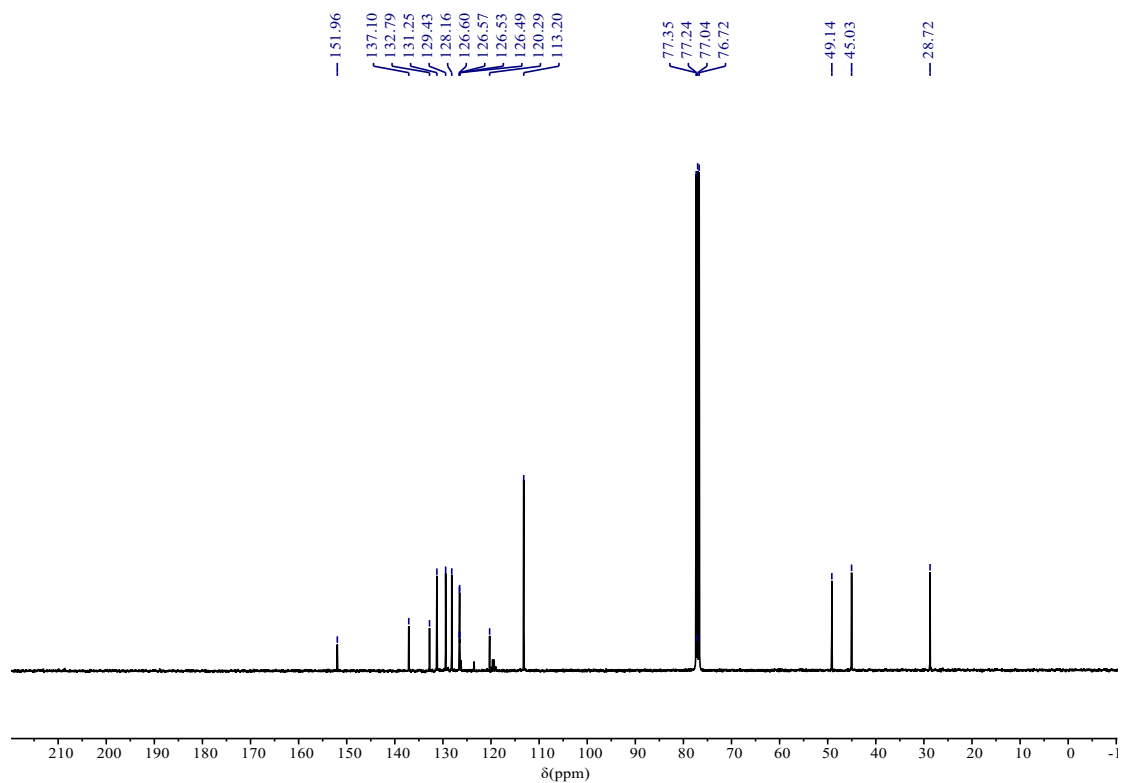


$^{19}\text{F}$  NMR (471 MHz, Chloroform-*d*) of 2-(3-fluorophenyl)-6,7-dimethoxy-1,2,3,4-tetrahydroisoquinoline (1o)

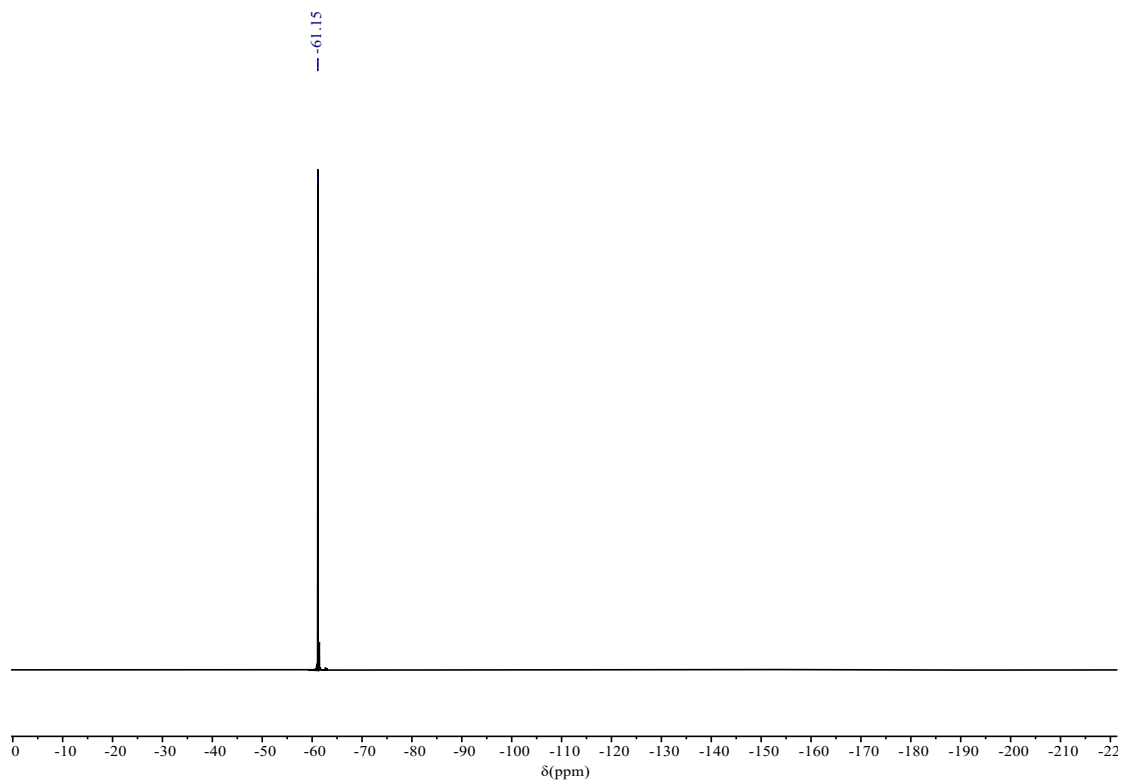
6-bromo-2-(4-(trifluoromethyl)phenyl)-1,2,3,4-tetrahydroisoquinoline (1p)



<sup>1</sup>H NMR (400 MHz, Chloroform-*d*) of 6-bromo-2-(4-(trifluoromethyl)phenyl)-1,2,3,4-tetrahydroisoquinoline (1p)

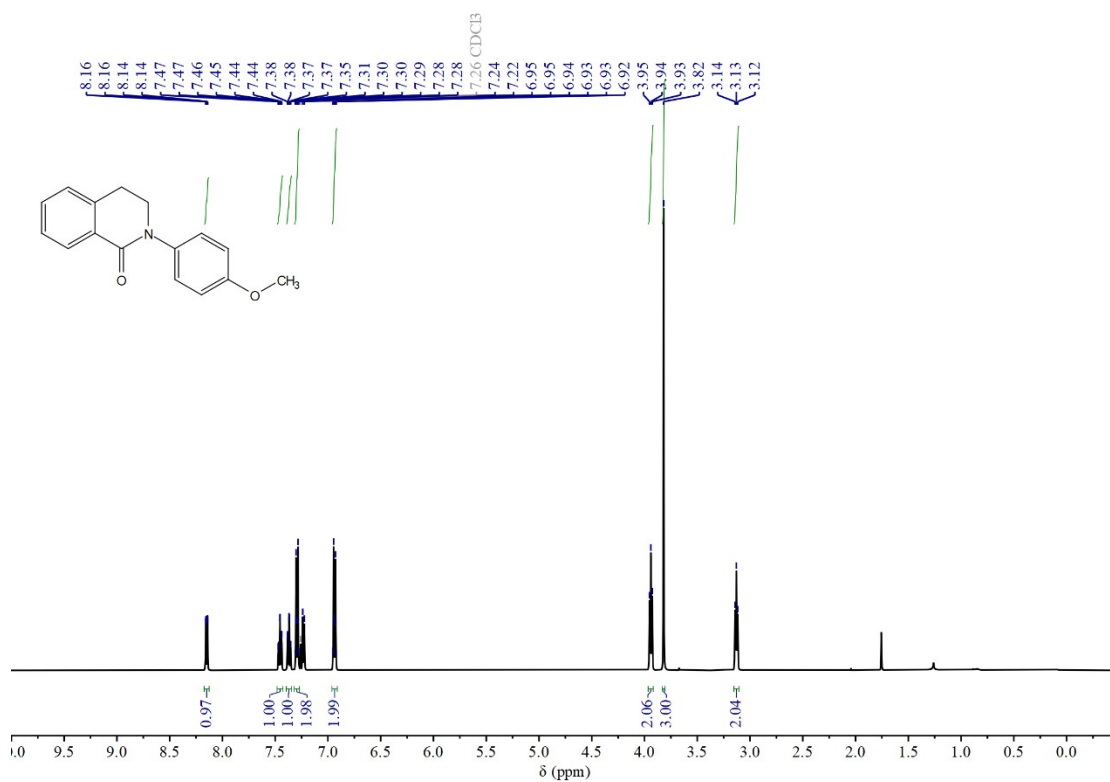


<sup>13</sup>C NMR (101 MHz, Chloroform-*d*) of 6-bromo-2-(4-(trifluoromethyl)phenyl)-1,2,3,4-tetrahydroisoquinoline (1p)

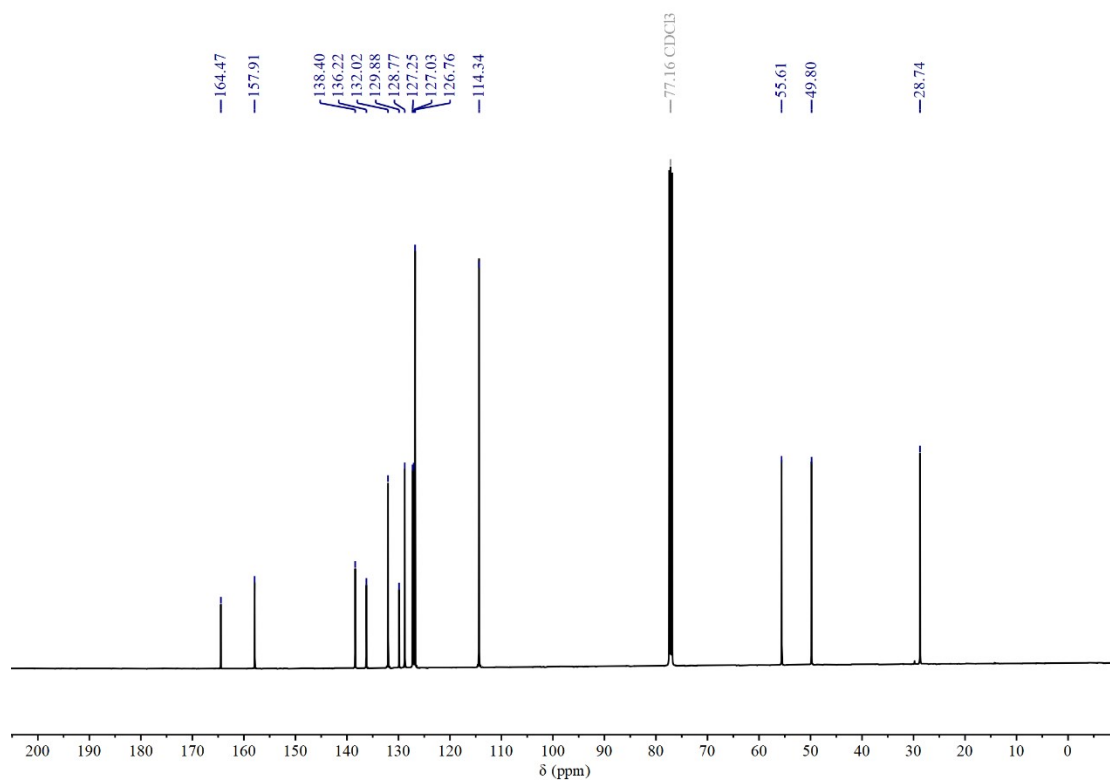


$^{19}\text{F}$  NMR (377 MHz, Chloroform-*d*) of 6-bromo-2-(4-(trifluoromethyl)phenyl)-1,2,3,4-tetrahydroisoquinoline (1p)

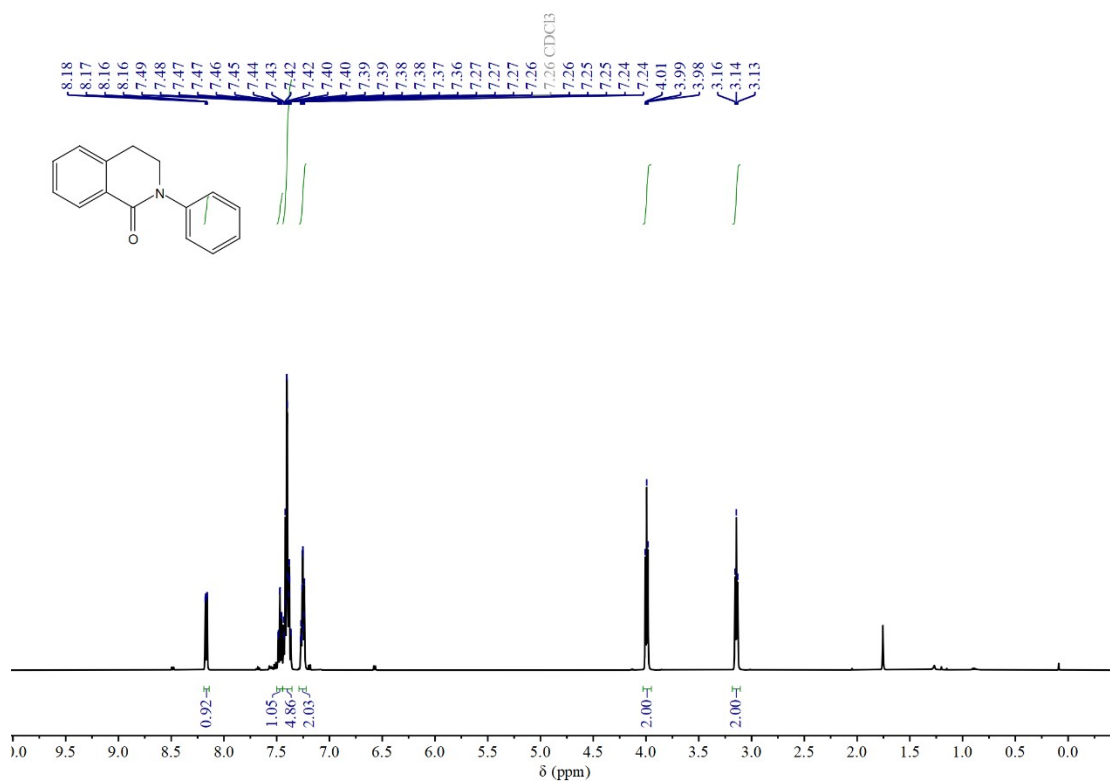
2-(4-methoxyphenyl)-3,4-dihydroisoquinolin-1(2H)-one (2a)



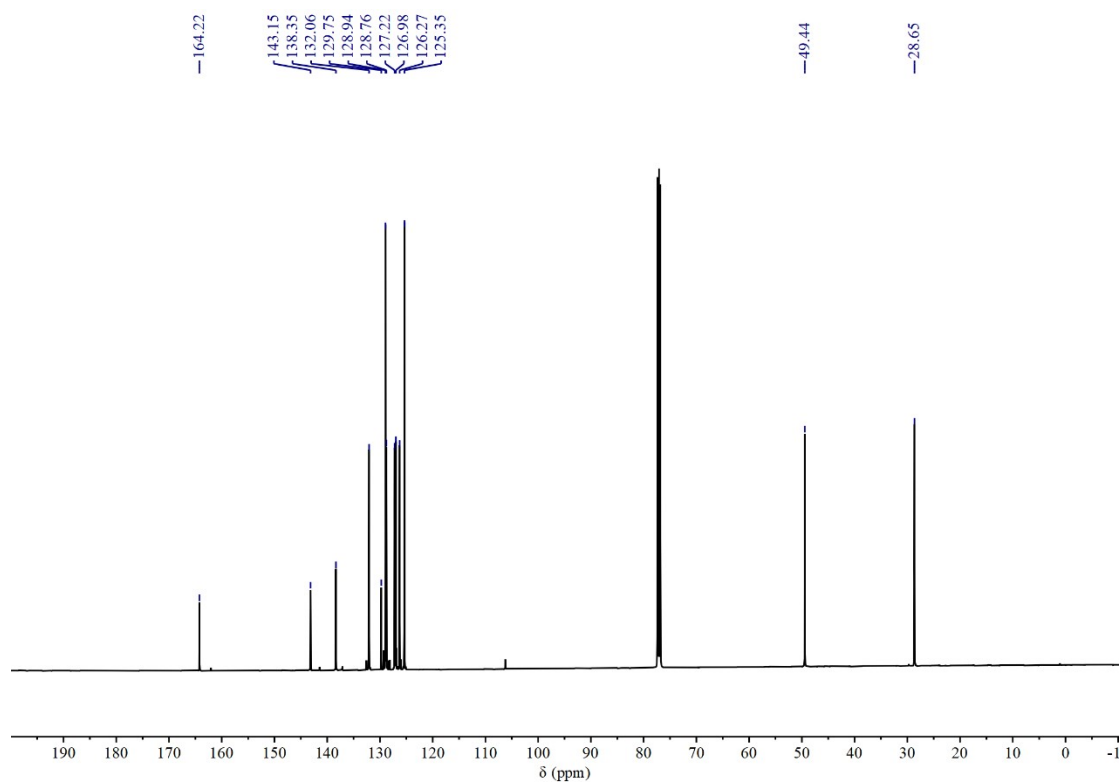
<sup>1</sup>H NMR (500 MHz, Chloroform-*d*) of 2-(4-methoxyphenyl)-3,4-dihydroisoquinolin-1(2H)-one (2a)



2-phenyl-3,4-dihydroisoquinolin-1(2H)-one (2b)

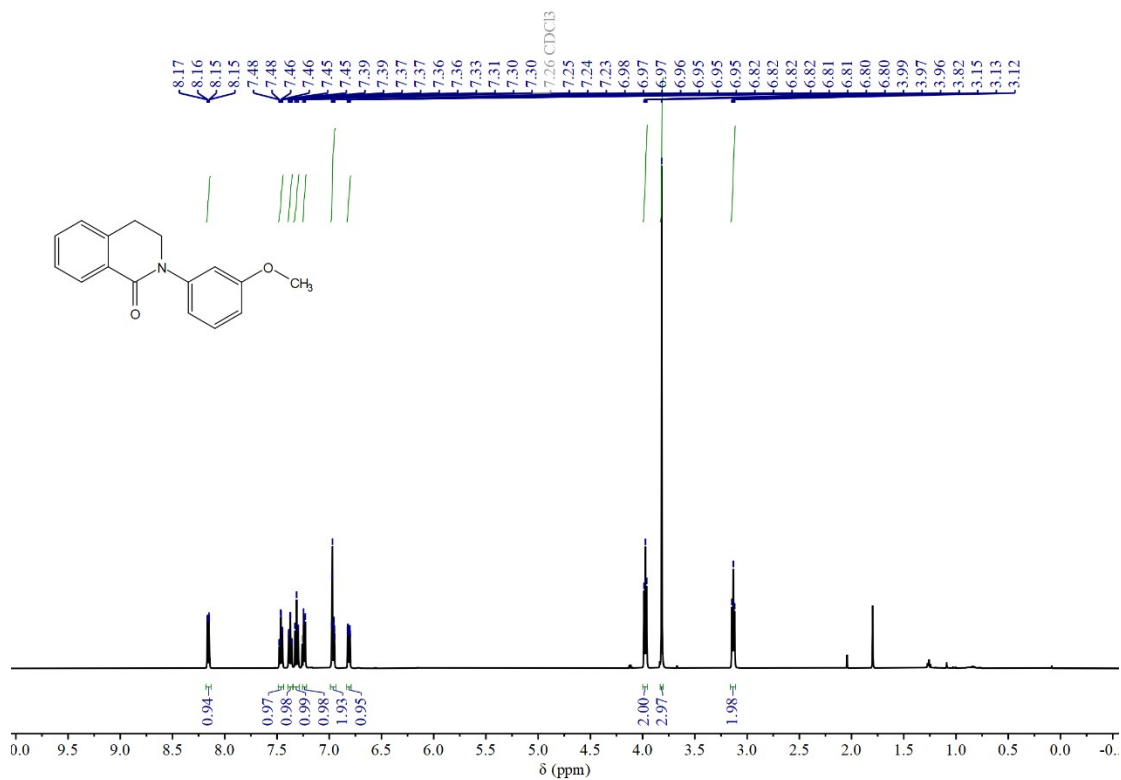


<sup>1</sup>H NMR (500 MHz, Chloroform-*d*) of 2-phenyl-3,4-dihydroisoquinolin-1(2H)-one (2b)

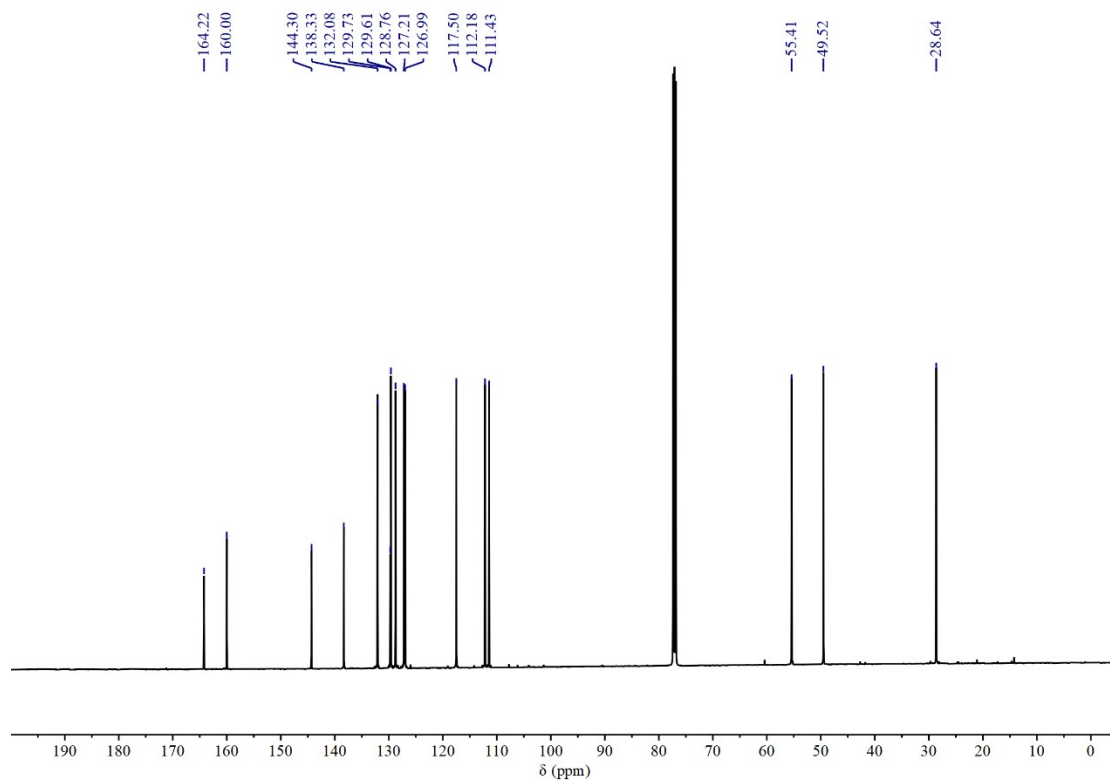


<sup>13</sup>C NMR (126 MHz, Chloroform-*d*) of 2-phenyl-3,4-dihydroisoquinolin-1(2H)-one (2b)

2-(3-methoxyphenyl)-3,4-dihydroisoquinolin-1(2H)-one (2c)



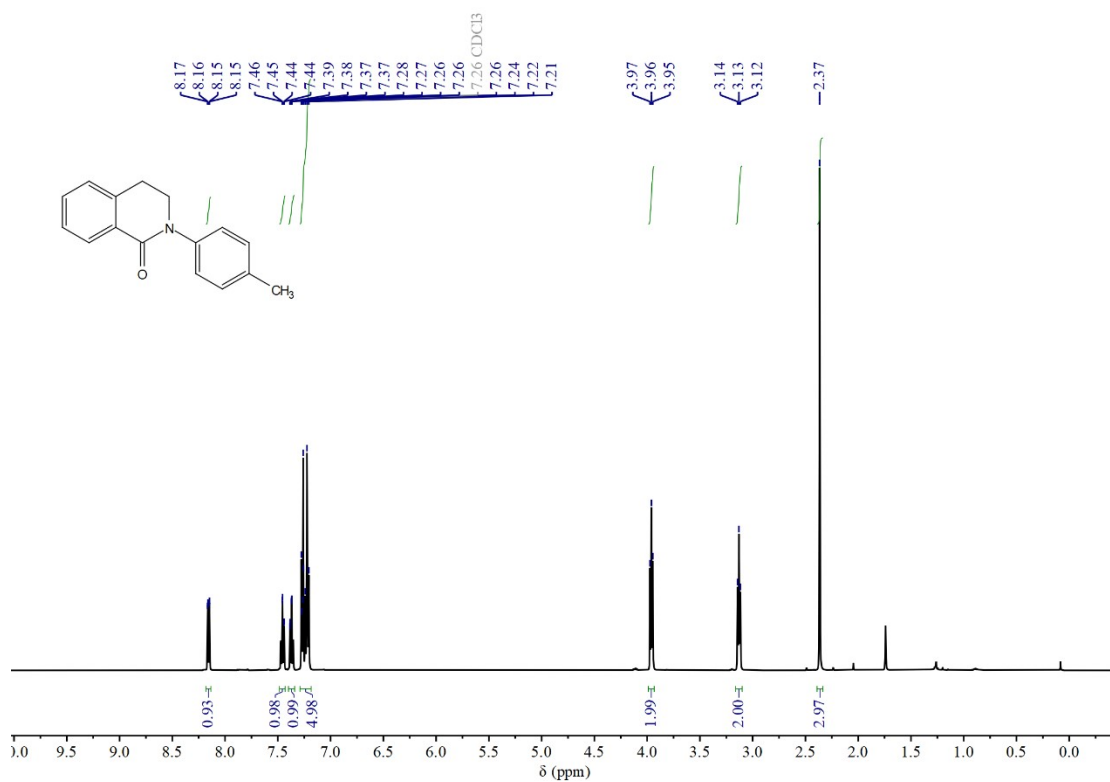
<sup>1</sup>H NMR (500 MHz, Chloroform-*d*) of 2-(3-methoxyphenyl)-3,4-dihydroisoquinolin-1(2H)-one (2c)



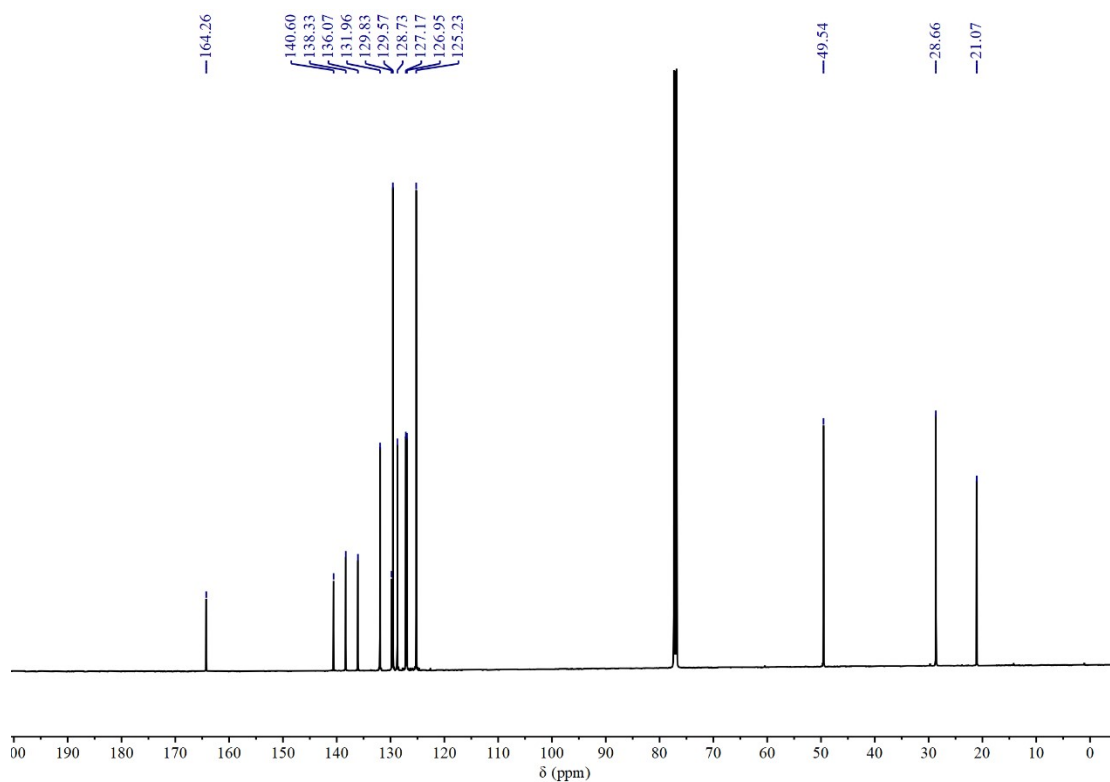
<sup>13</sup>C NMR (126 MHz, Chloroform-*d*) of 2-(3-methoxyphenyl)-3,4-dihydroisoquinolin-1(2H)-one (2c)



2-(*p*-tolyl)-3,4-dihydroisoquinolin-1(2*H*)-one (2d)

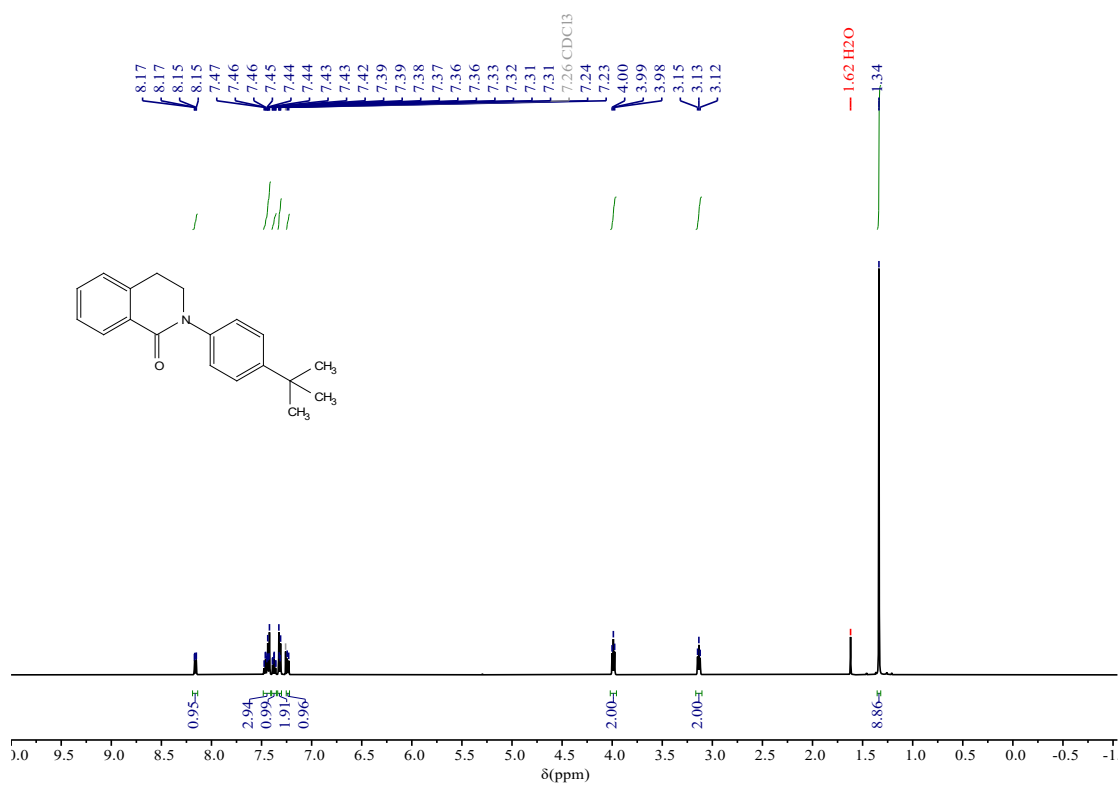


<sup>1</sup>H NMR (500 MHz, Chloroform-*d*) of 2-(*p*-tolyl)-3,4-dihydroisoquinolin-1(2*H*)-one (2d)

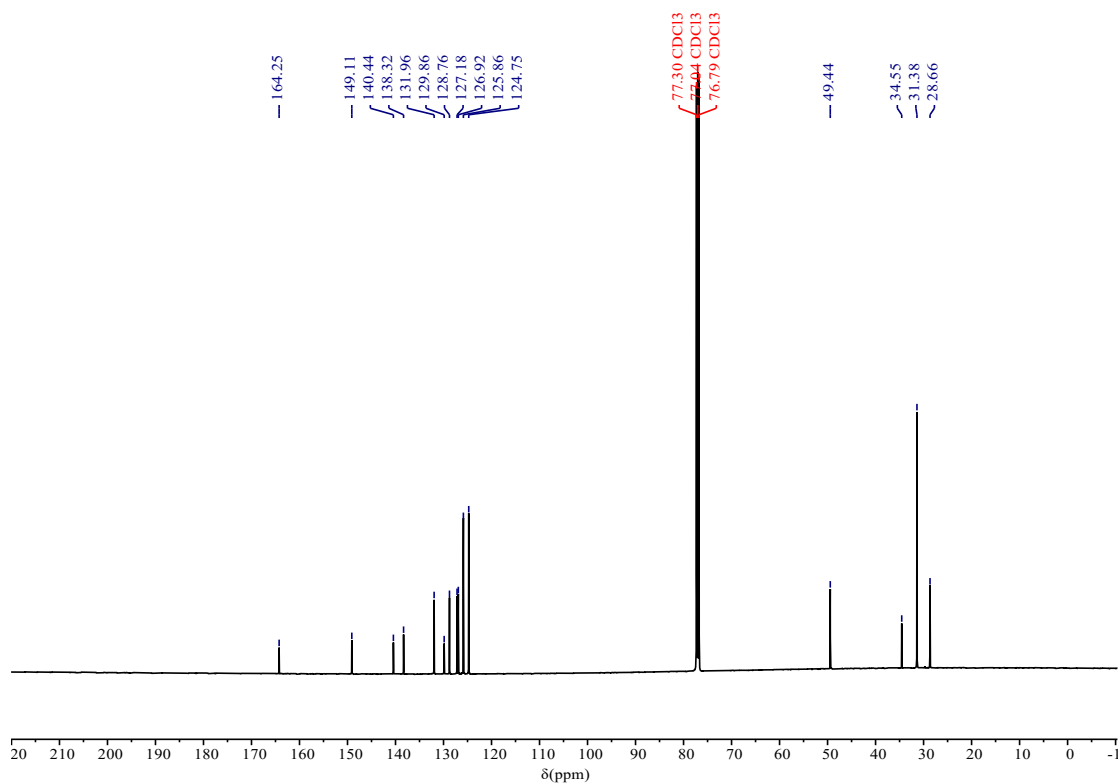


<sup>13</sup>C NMR (126 MHz, Chloroform-*d*) of 2-(*p*-tolyl)-3,4-dihydroisoquinolin-1(2*H*)-one (2d)

2-(4-(*tert*-butyl)phenyl)-3,4-dihydroisoquinolin-1(2*H*)-one (2e)



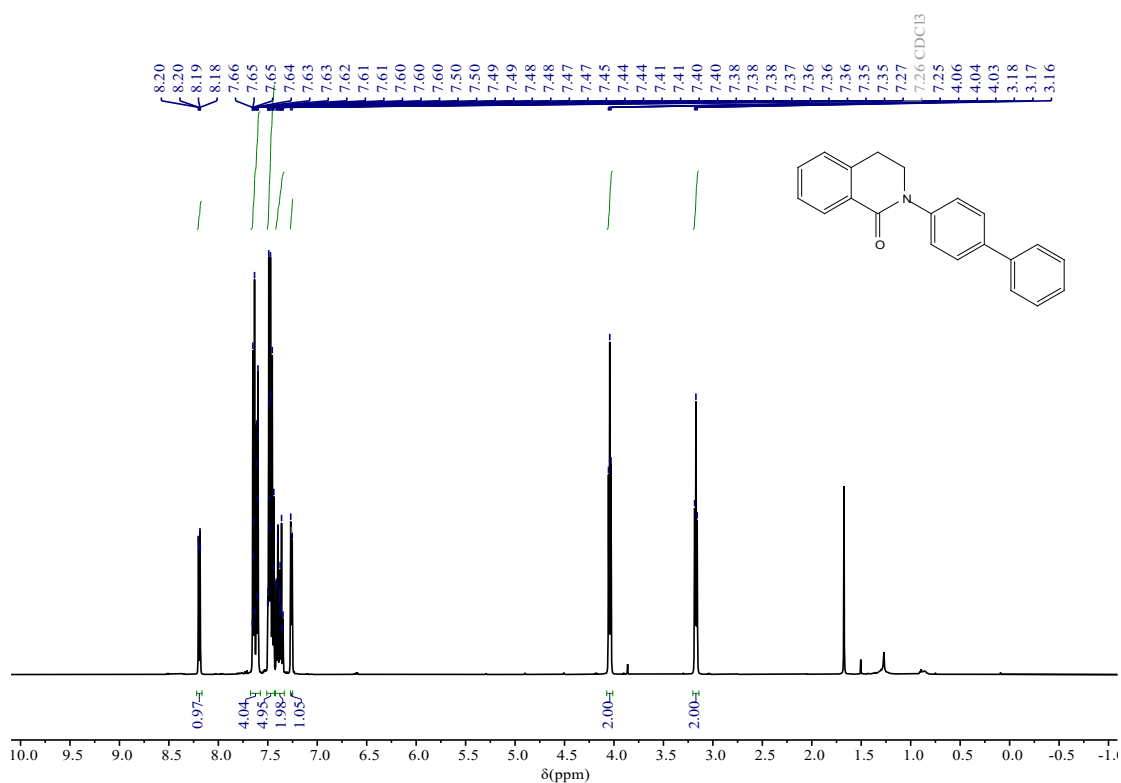
<sup>1</sup>H NMR (500 MHz, Chloroform-*d*) of 2-(4-(*tert*-butyl)phenyl)-3,4-dihydroisoquinolin-1(2*H*)-one (2e)



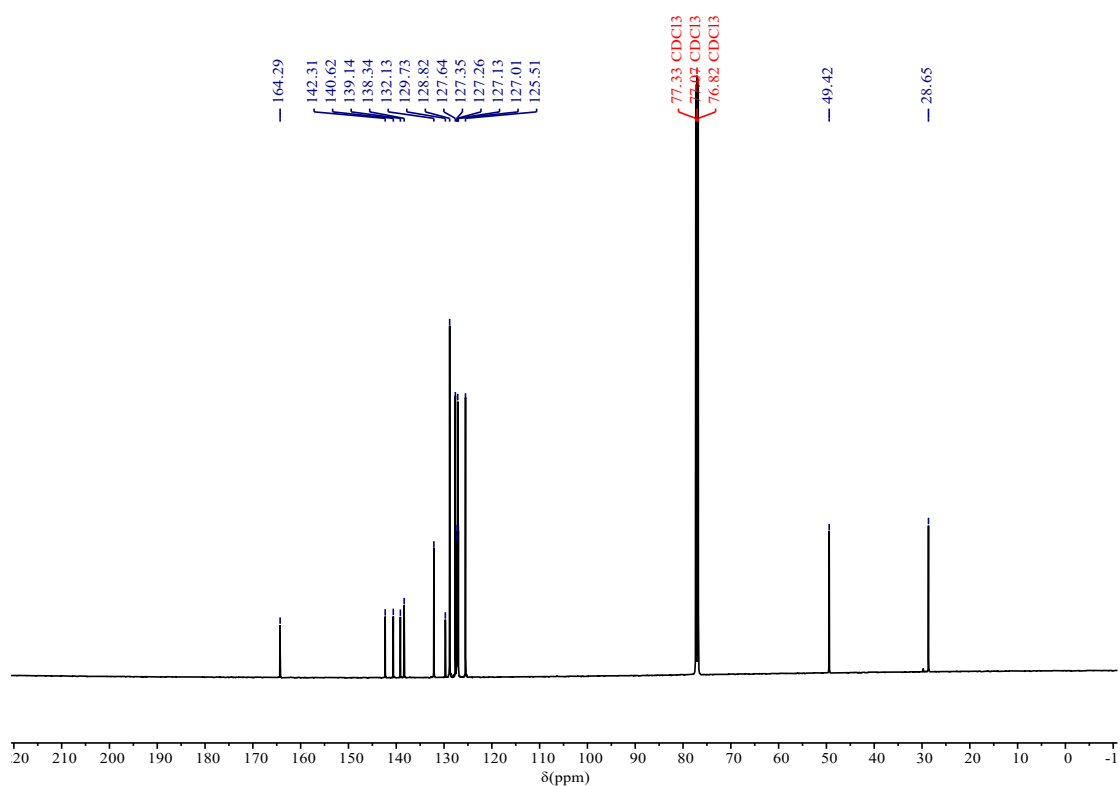
<sup>13</sup>C NMR (126 MHz, Chloroform-*d*) of 2-(4-(*tert*-butyl)phenyl)-3,4-dihydroisoquinolin-1(2*H*)-one (2e)



2-([1,1'-biphenyl]-4-yl)-3,4-dihydroisoquinolin-1(2H)-one (2g)

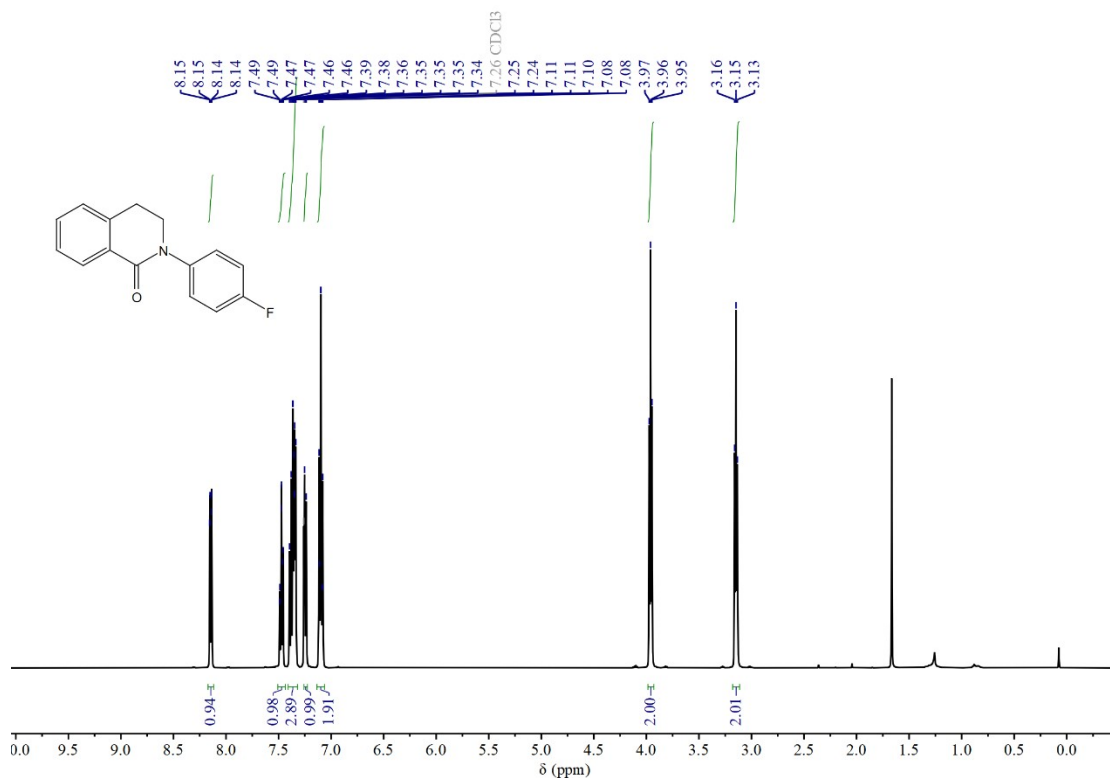


<sup>1</sup>H NMR (500 MHz, Chloroform-*d*) of 2-([1,1'-biphenyl]-4-yl)-3,4-dihydroisoquinolin-1(2H)-one (2g)

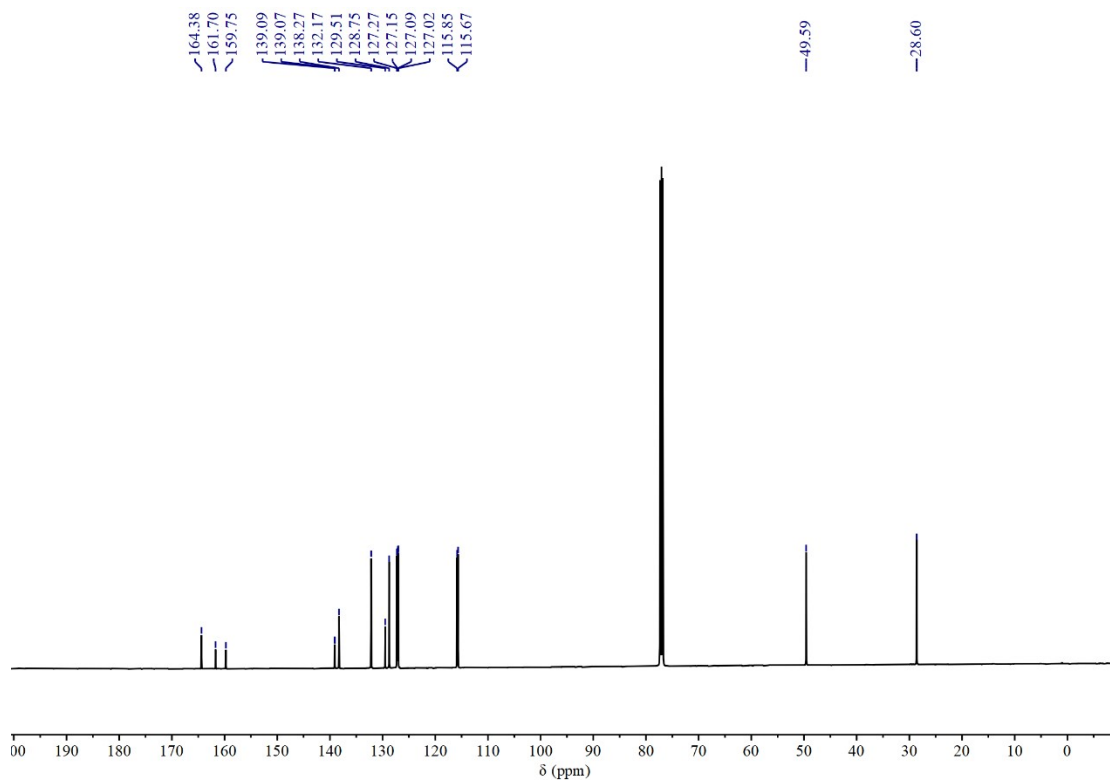


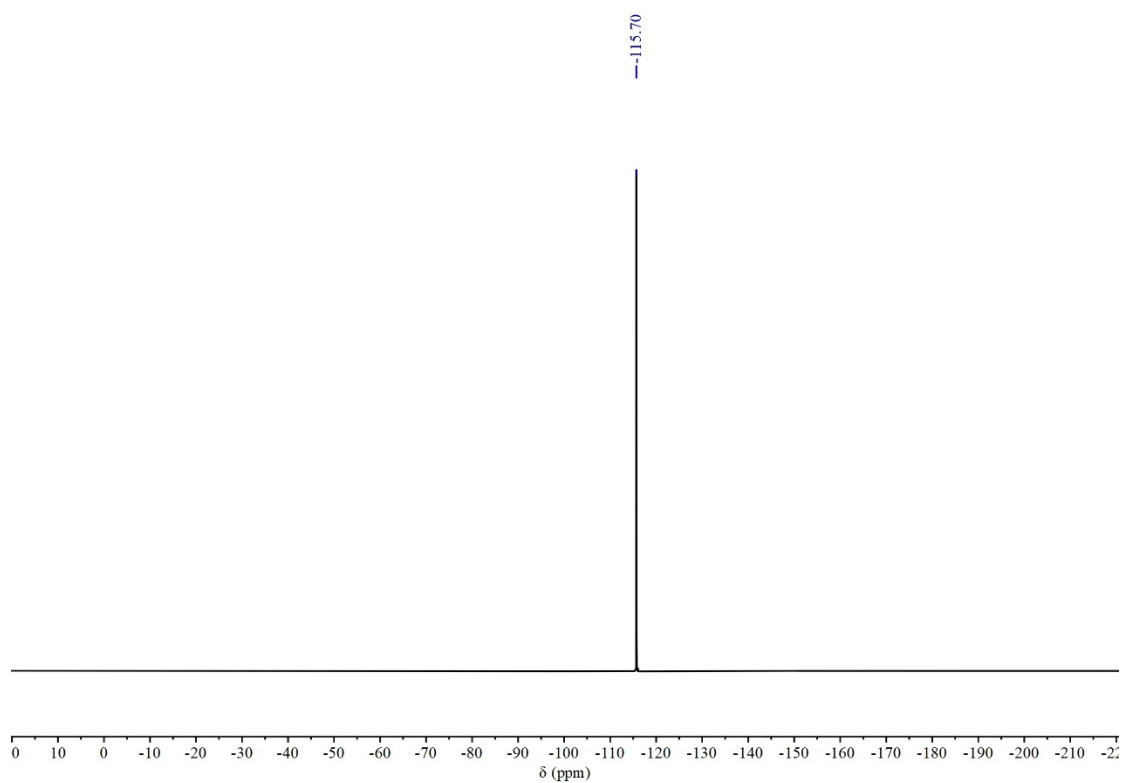
<sup>13</sup>C NMR (126 MHz, Chloroform-*d*) of 2-([1,1'-biphenyl]-4-yl)-3,4-dihydroisoquinolin-1(2H)-one (2g)

2-(4-fluorophenyl)-3,4-dihydroisoquinolin-1(2H)-one (2h)



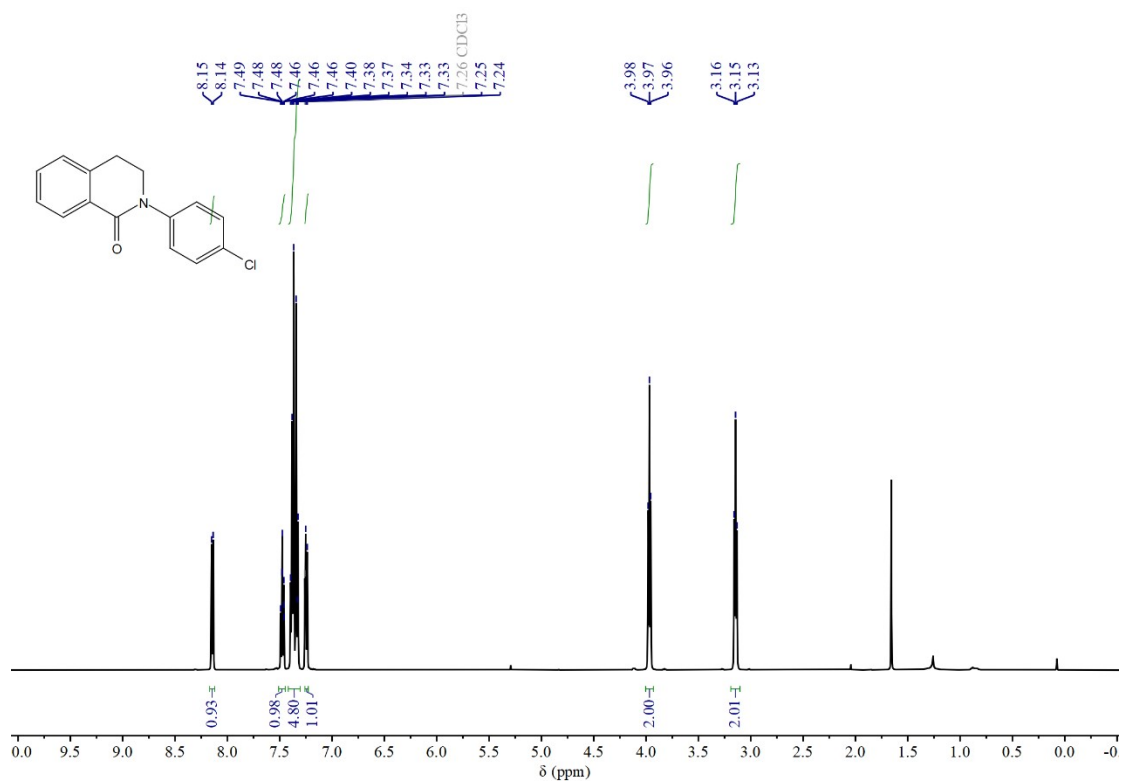
<sup>1</sup>H NMR (500 MHz, Chloroform-*d*) of 2-(4-fluorophenyl)-3,4-dihydroisoquinolin-1(2H)-one (2h)



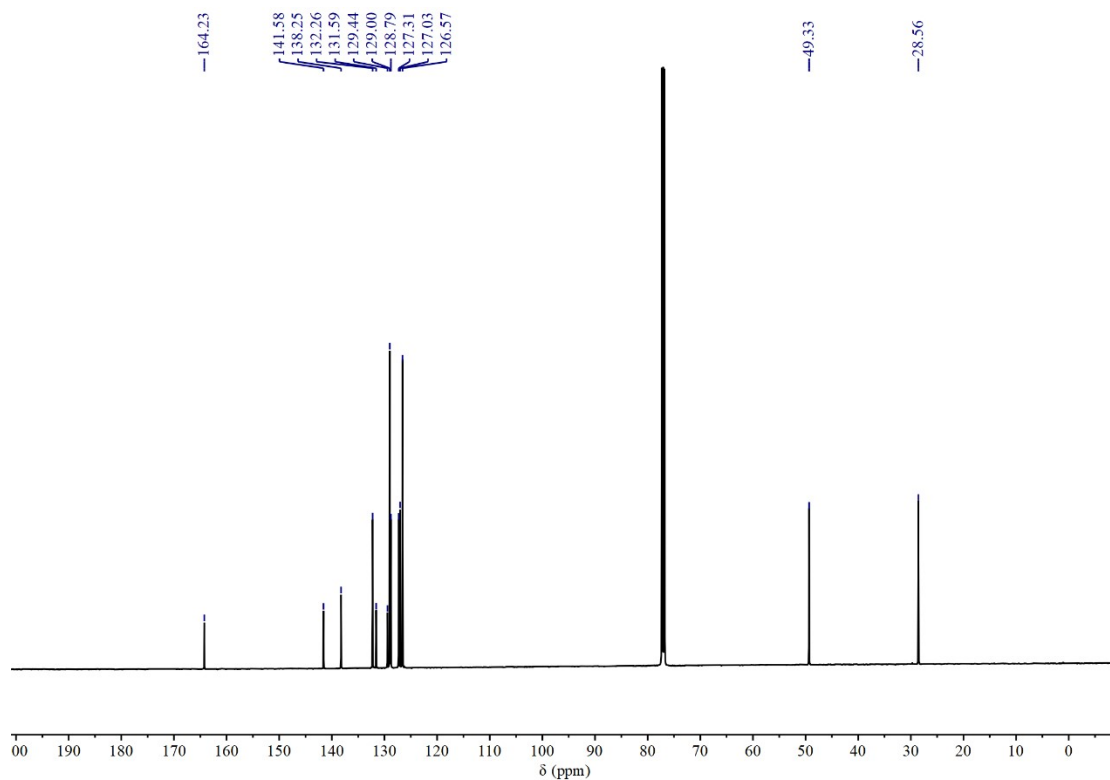


$^{19}\text{F}$  NMR (471 MHz, Chloroform-d) of 2-(4-fluorophenyl)-3,4-dihydroisoquinolin-1(2*H*)-one (2h)

2-(4-chlorophenyl)-3,4-dihydroisoquinolin-1(2H)-one (2i)

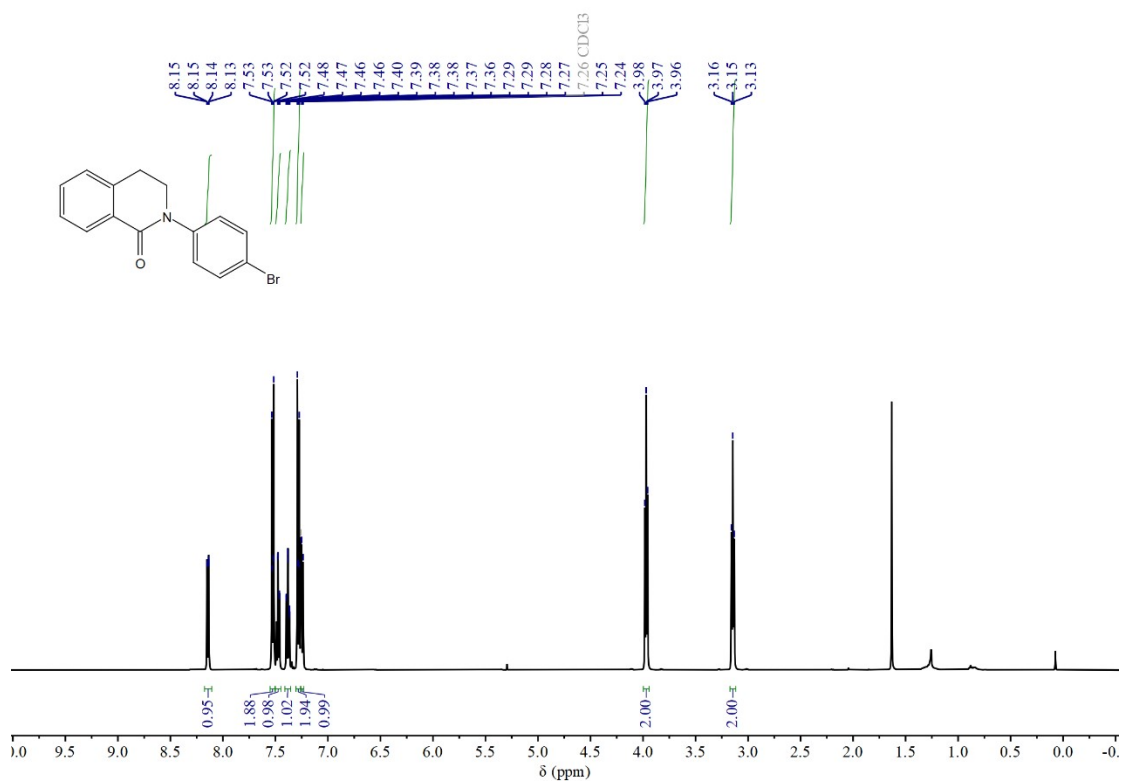


<sup>1</sup>H NMR (500 MHz, Chloroform-*d*) of 2-(4-chlorophenyl)-3,4-dihydroisoquinolin-1(2H)-one (2i)

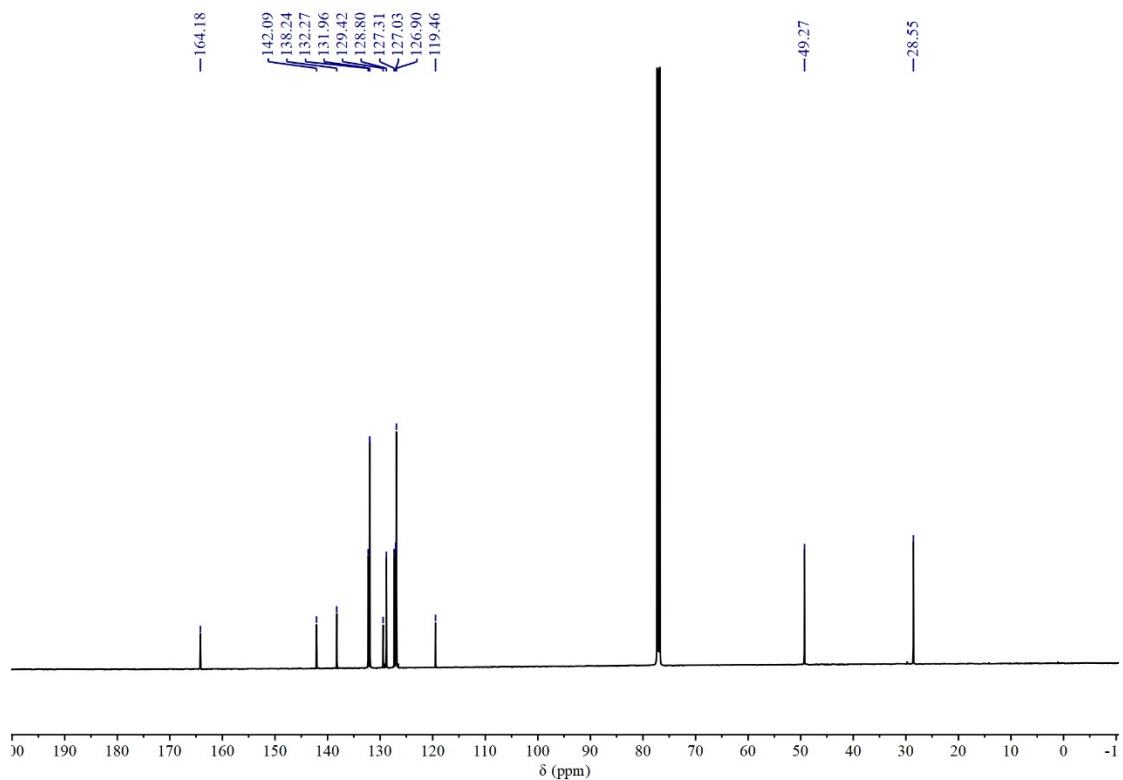


<sup>13</sup>C NMR (126 MHz, Chloroform-*d*) of 2-(4-chlorophenyl)-3,4-dihydroisoquinolin-1(2H)-one (2i)

2-(4-bromophenyl)-3,4-dihydroisoquinolin-1(2H)-one (2j)



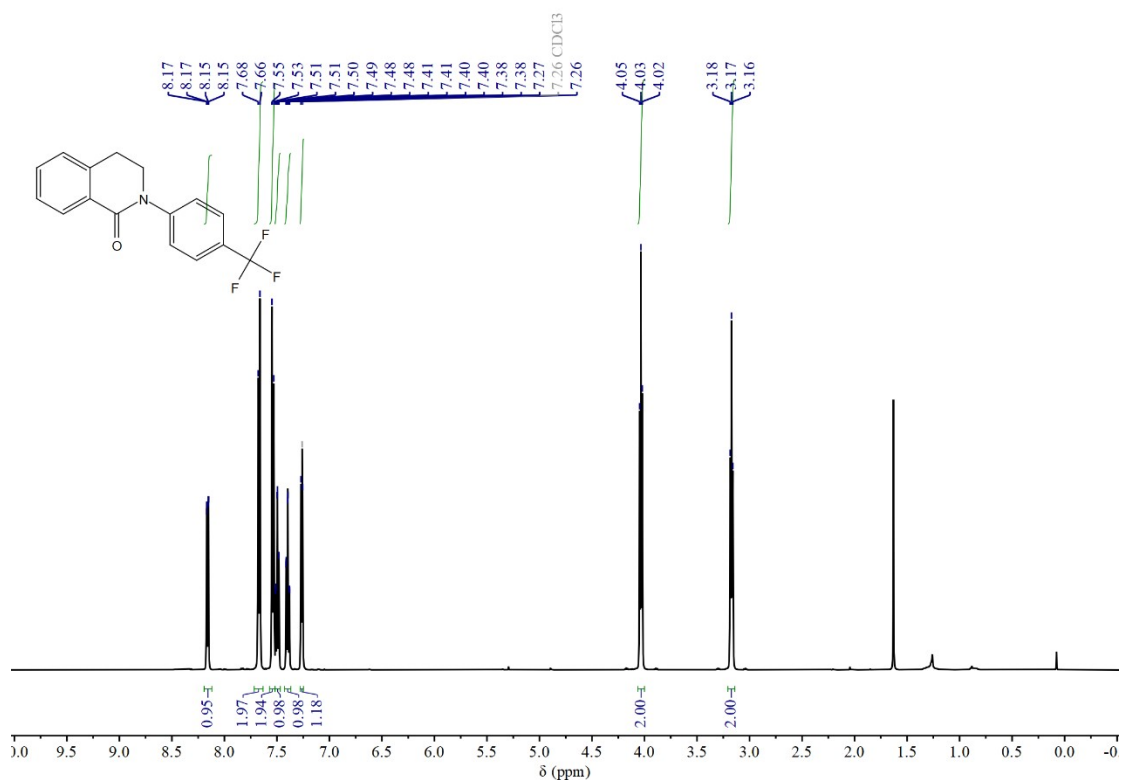
<sup>1</sup>H NMR (500 MHz, Chloroform-*d*) of 2-(4-bromophenyl)-3,4-dihydroisoquinolin-1(2H)-one (2j)



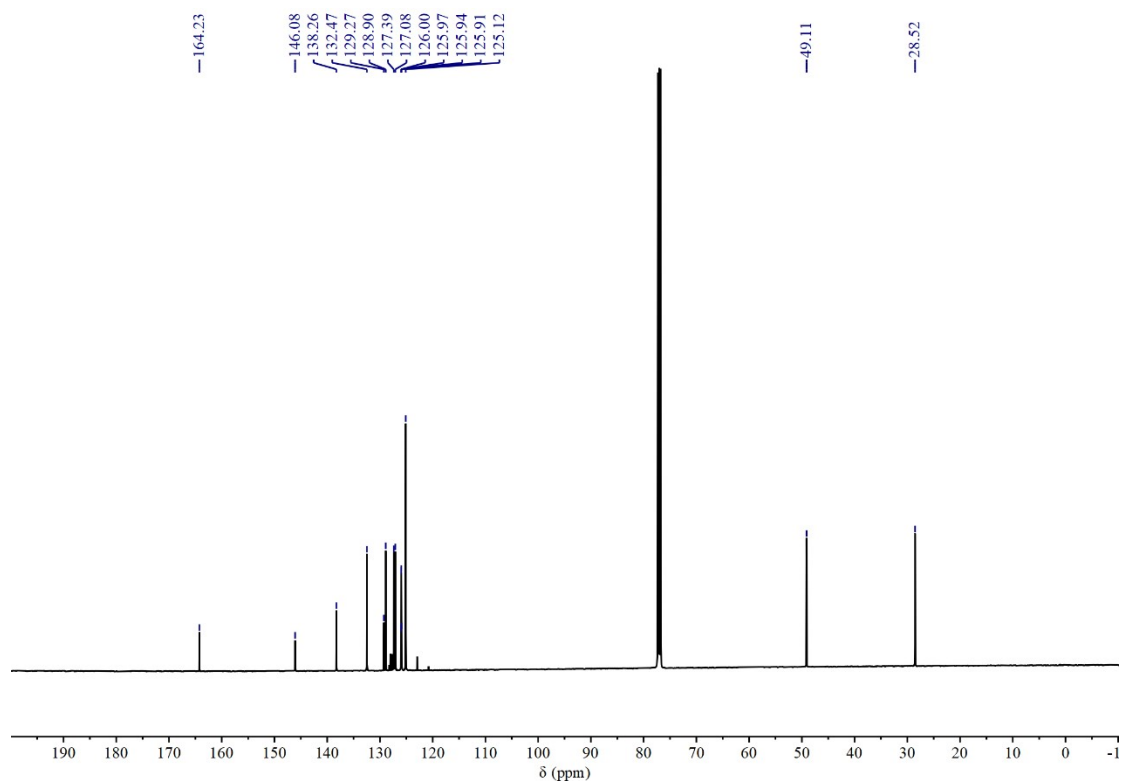
<sup>13</sup>C NMR (126 MHz, Chloroform-*d*) of 2-(4-bromophenyl)-3,4-dihydroisoquinolin-1(2H)-one (2j)



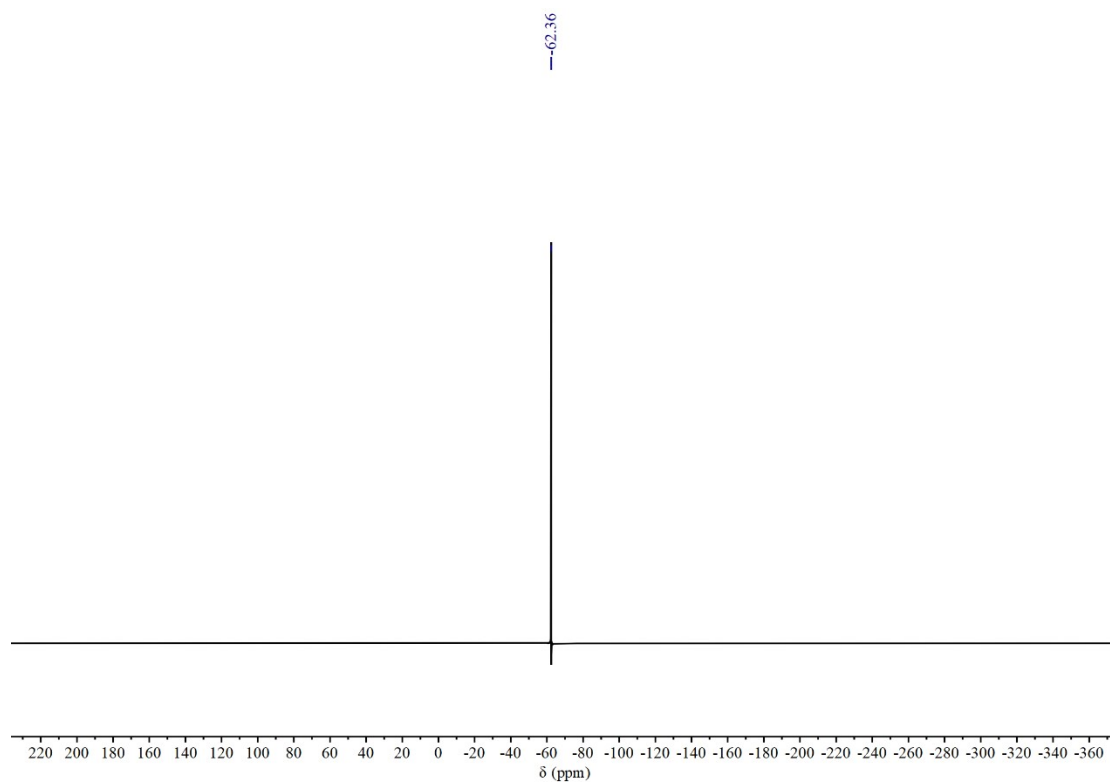
2-(4-(trifluoromethyl)phenyl)-3,4-dihydroisoquinolin-1(2H)-one (2k)



<sup>1</sup>H NMR (500 MHz, Chloroform-*d*) of 2-(4-(trifluoromethyl)phenyl)-3,4-dihydroisoquinolin-1(2H)-one (2k)

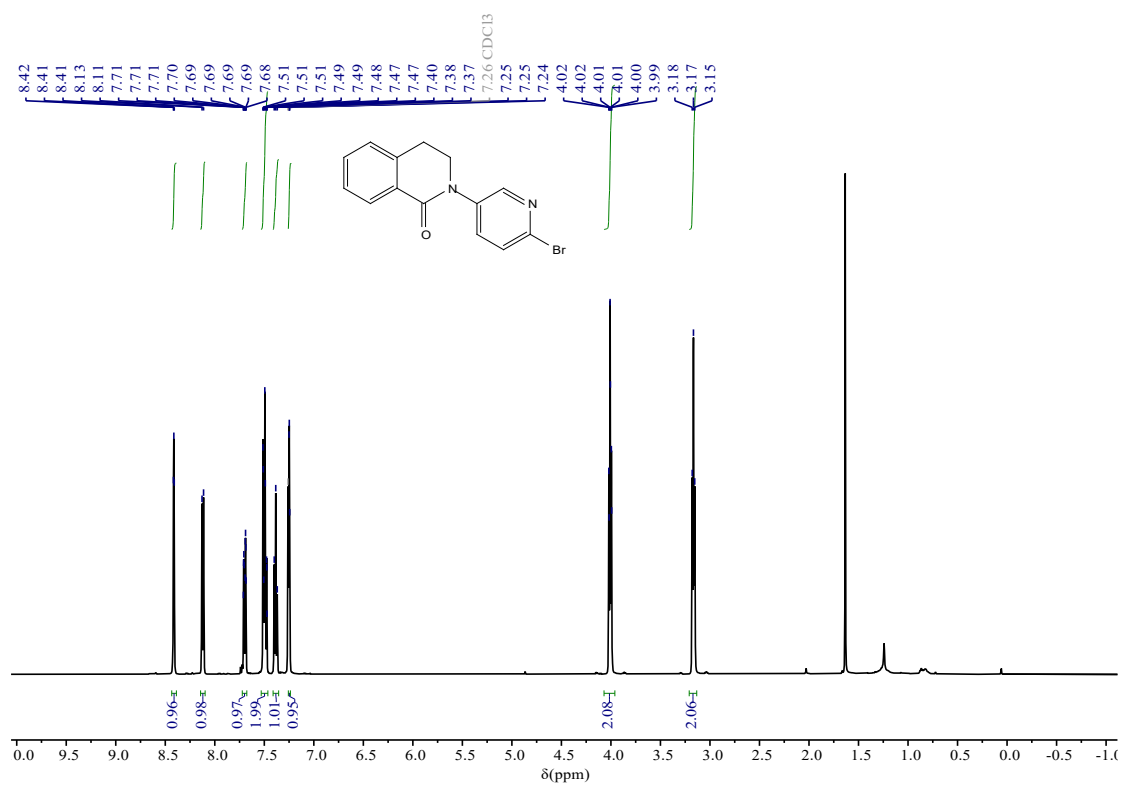


<sup>13</sup>C NMR (126 MHz, Chloroform-*d*) of 2-(4-(trifluoromethyl)phenyl)-3,4-dihydroisoquinolin-1(2H)-one (2k)

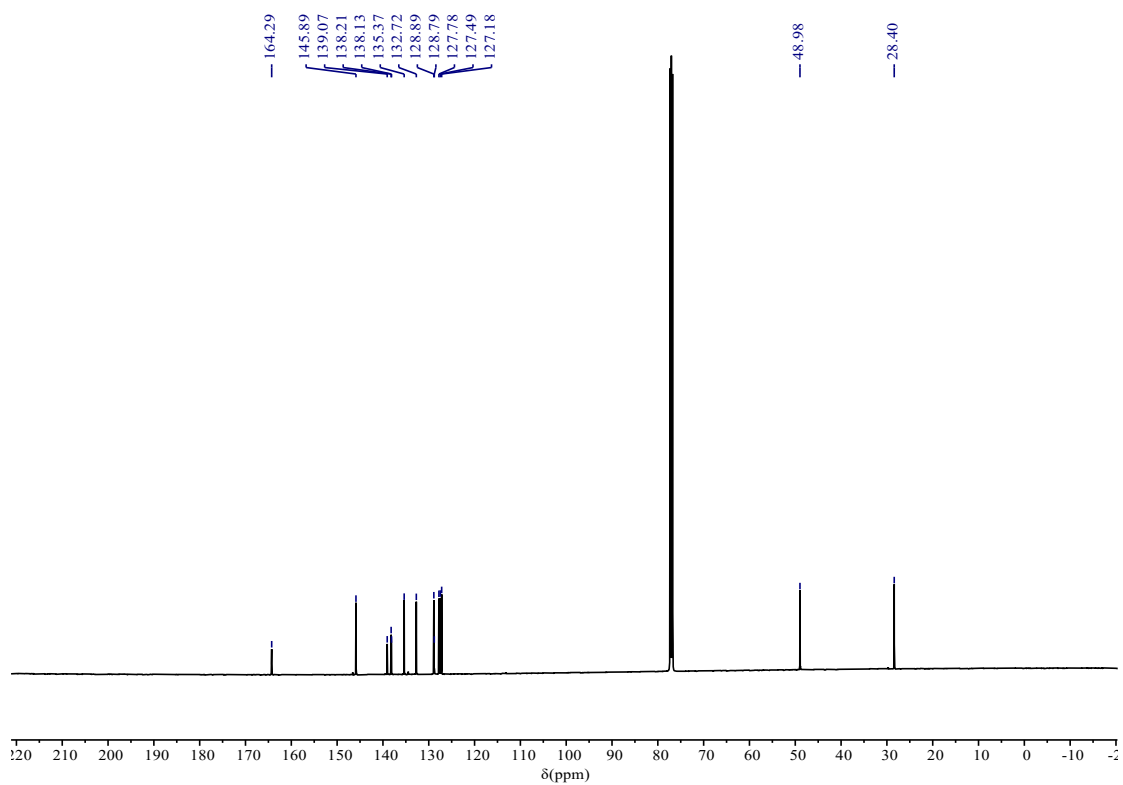


$^{19}\text{F}$  NMR (471 MHz, Chloroform-d) of 2-(4-(trifluoromethyl)phenyl)-3,4-dihydroisoquinolin-1(2*H*)-one (2k)

2-(6-bromopyridin-3-yl)-3,4-dihydroisoquinolin-1(2H)-one (2l)

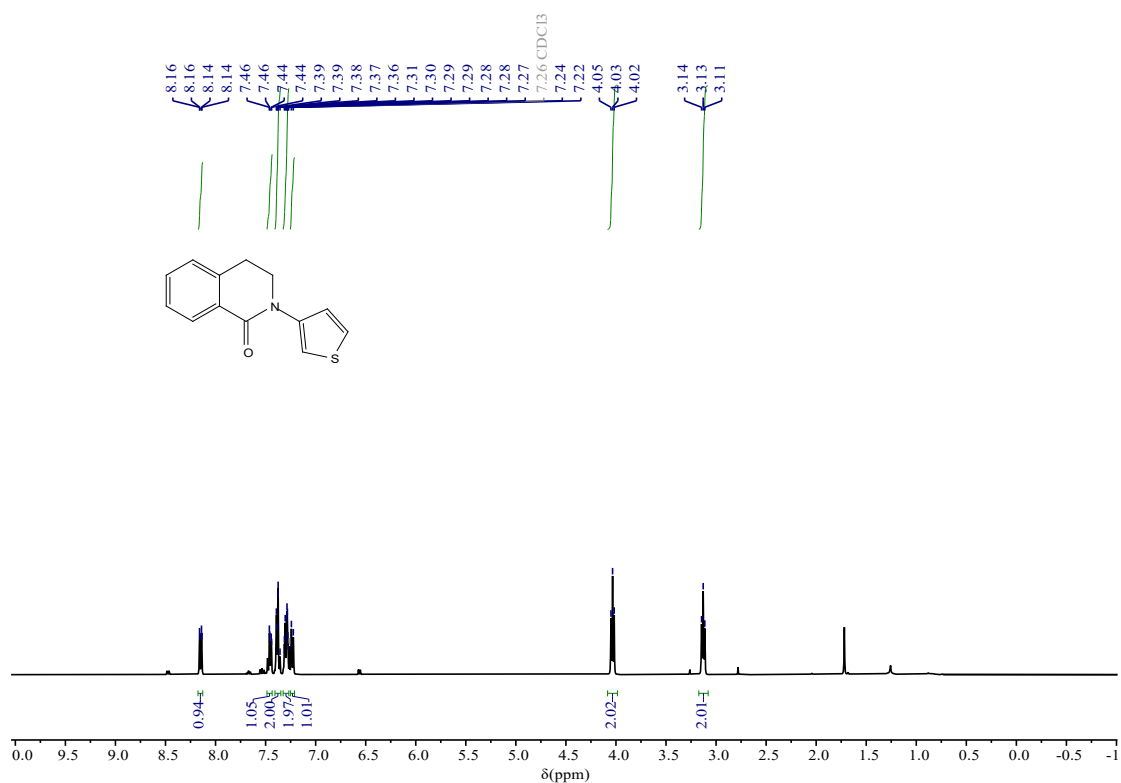


<sup>1</sup>H NMR (500 MHz, Chloroform-*d*) of 2-(6-bromopyridin-3-yl)-3,4-dihydroisoquinolin-1(2H)-one (2l)

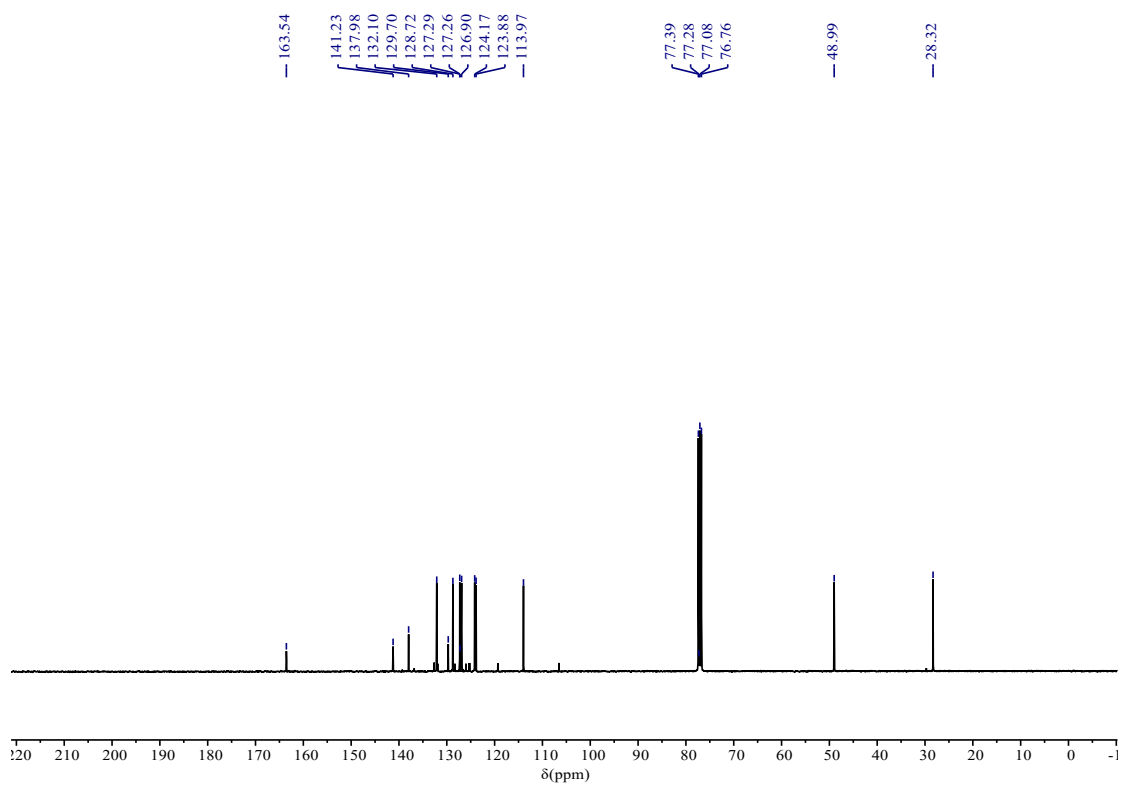


<sup>13</sup>C NMR (126 MHz, Chloroform-*d*) of 2-(6-bromopyridin-3-yl)-3,4-dihydroisoquinolin-1(2H)-one (2l)

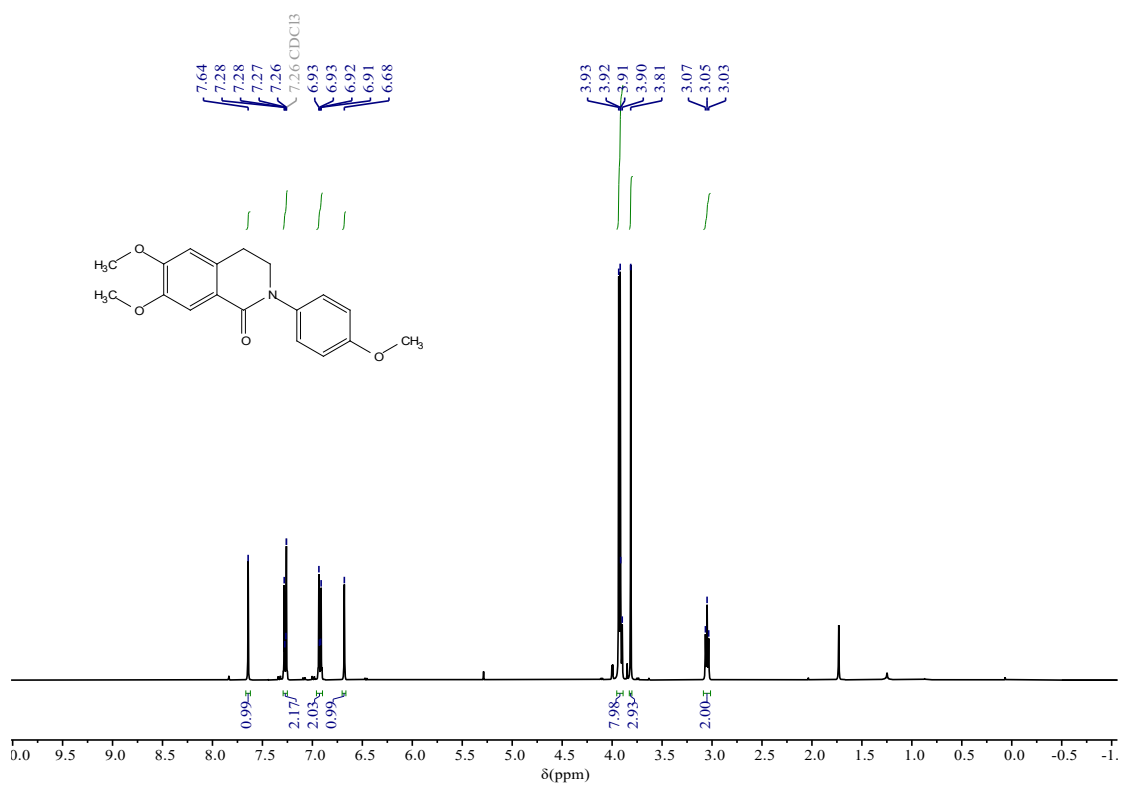
2-(thiophen-3-yl)-3,4-dihydroisoquinolin-1(2H)-one (2m)



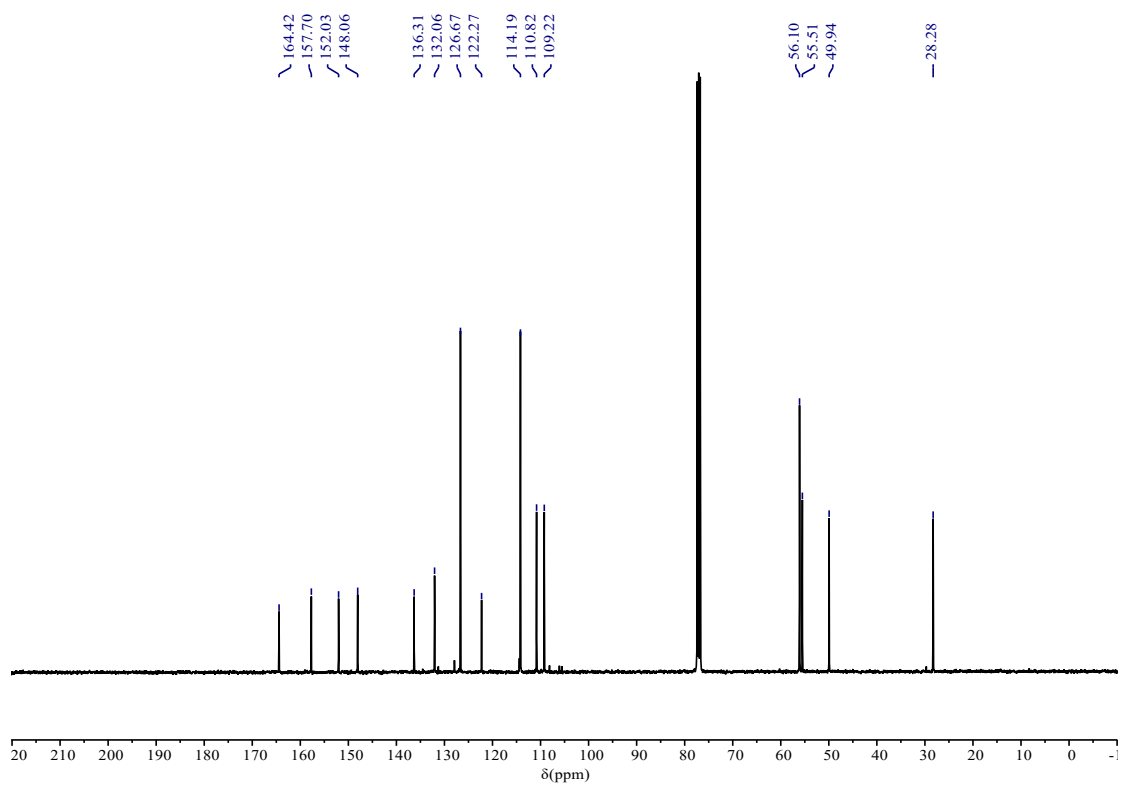
<sup>1</sup>H NMR (500 MHz, Chloroform-*d*) of 2-(thiophen-3-yl)-3,4-dihydroisoquinolin-1(2H)-one (2m)



6,7-dimethoxy-2-(4-methoxyphenyl)-3,4-dihydroisoquinolin-1(2H)-one (2n)

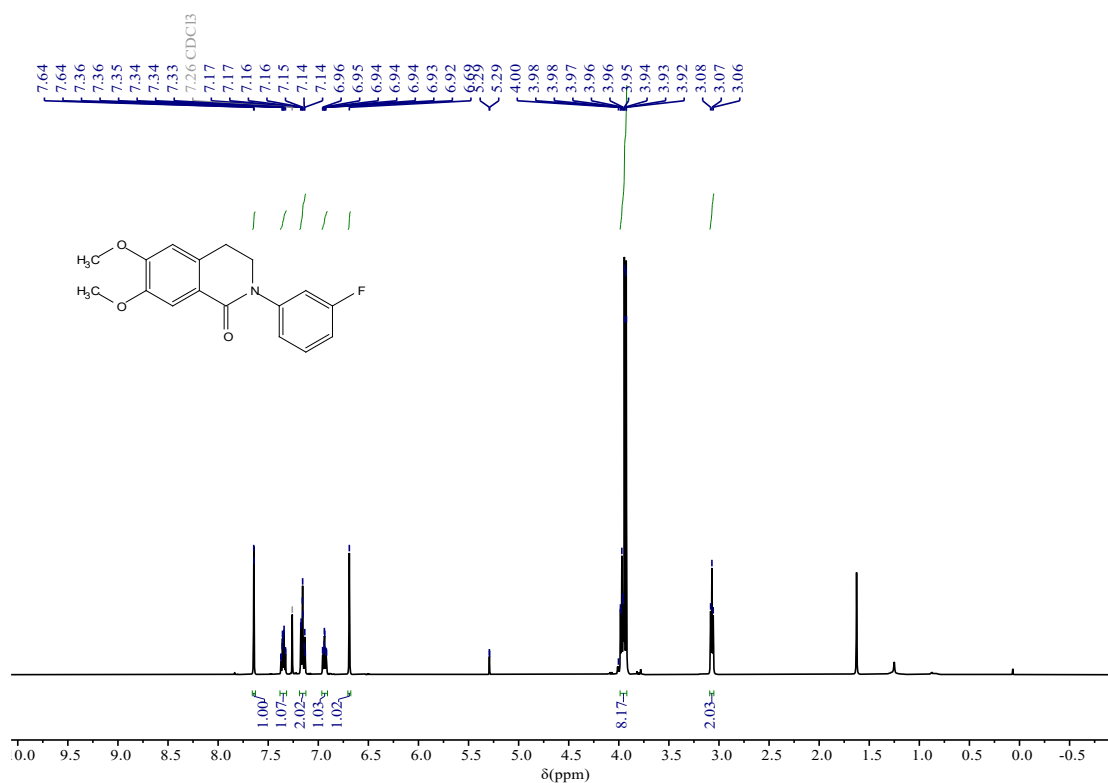


<sup>1</sup>H NMR (500 MHz, Chloroform-*d*) of 6,7-dimethoxy-2-(4-methoxyphenyl)-3,4-dihydroisoquinolin-1(2H)-one (2n)

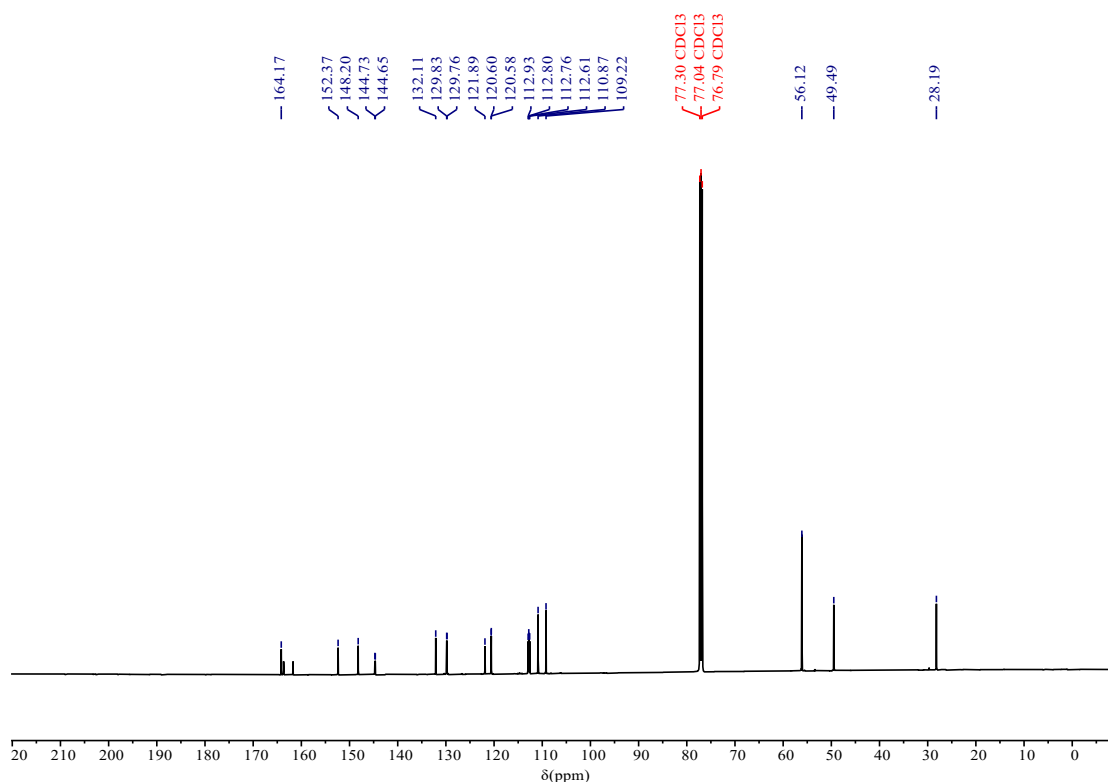


<sup>13</sup>C NMR (126 MHz, Chloroform-*d*) of 6,7-dimethoxy-2-(4-methoxyphenyl)-3,4-dihydroisoquinolin-1(2H)-one (2n)

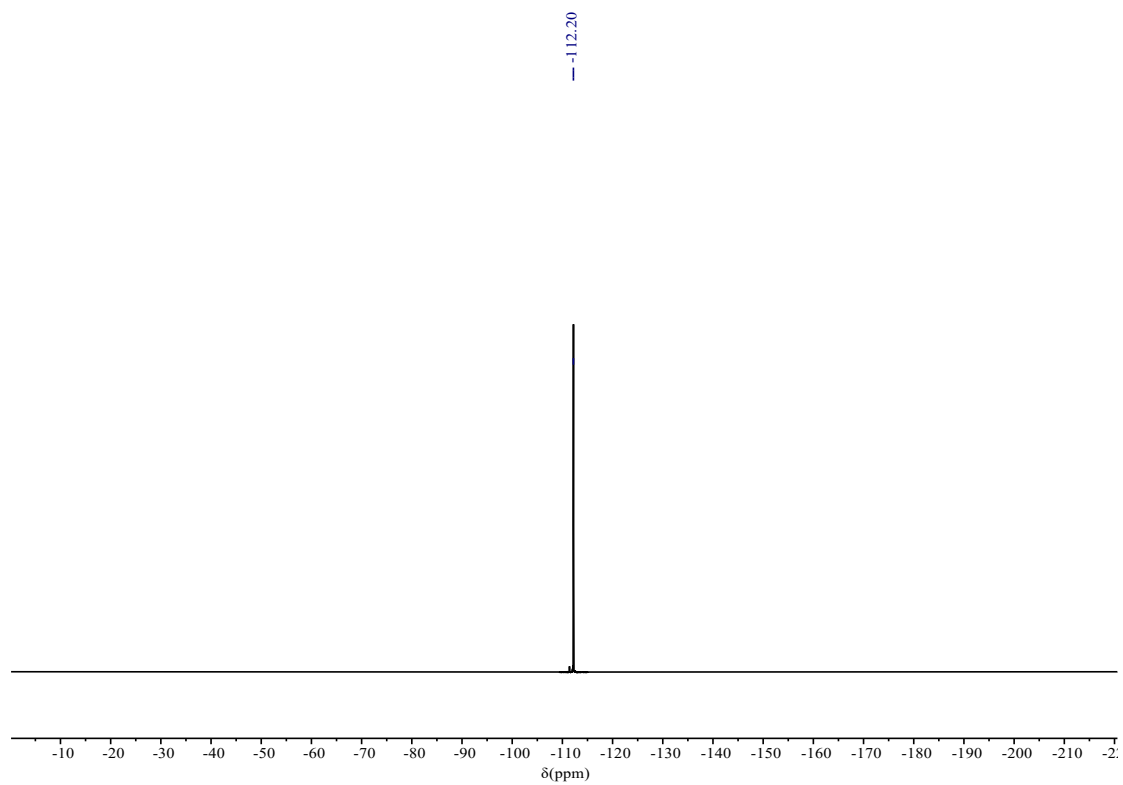
2-(3-fluorophenyl)-6,7-dimethoxy-3,4-dihydroisoquinolin-1(2H)-one (2o)



<sup>1</sup>H NMR (500 MHz, Chloroform-*d*) of 2-(3-fluorophenyl)-6,7-dimethoxy-3,4-dihydroisoquinolin-1(2H)-one (2o)

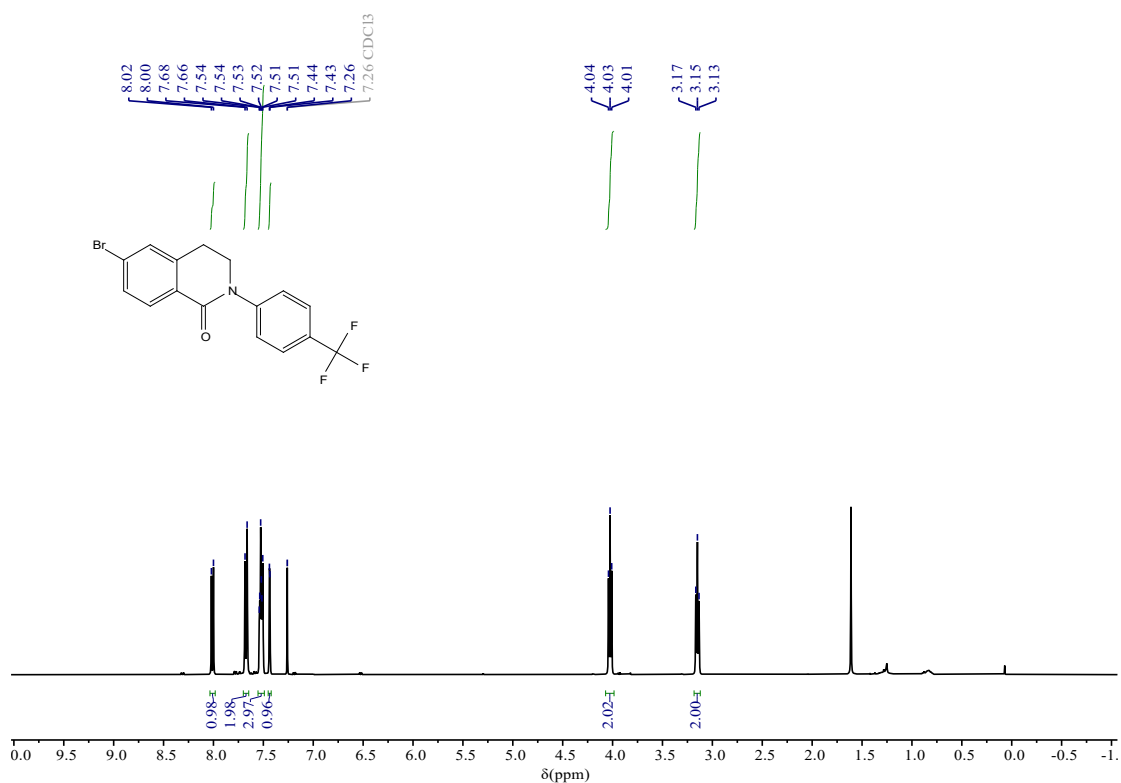


<sup>13</sup>C NMR (126 MHz, Chloroform-*d*) of 2-(3-fluorophenyl)-6,7-dimethoxy-3,4-dihydroisoquinolin-1(2H)-one (2o)

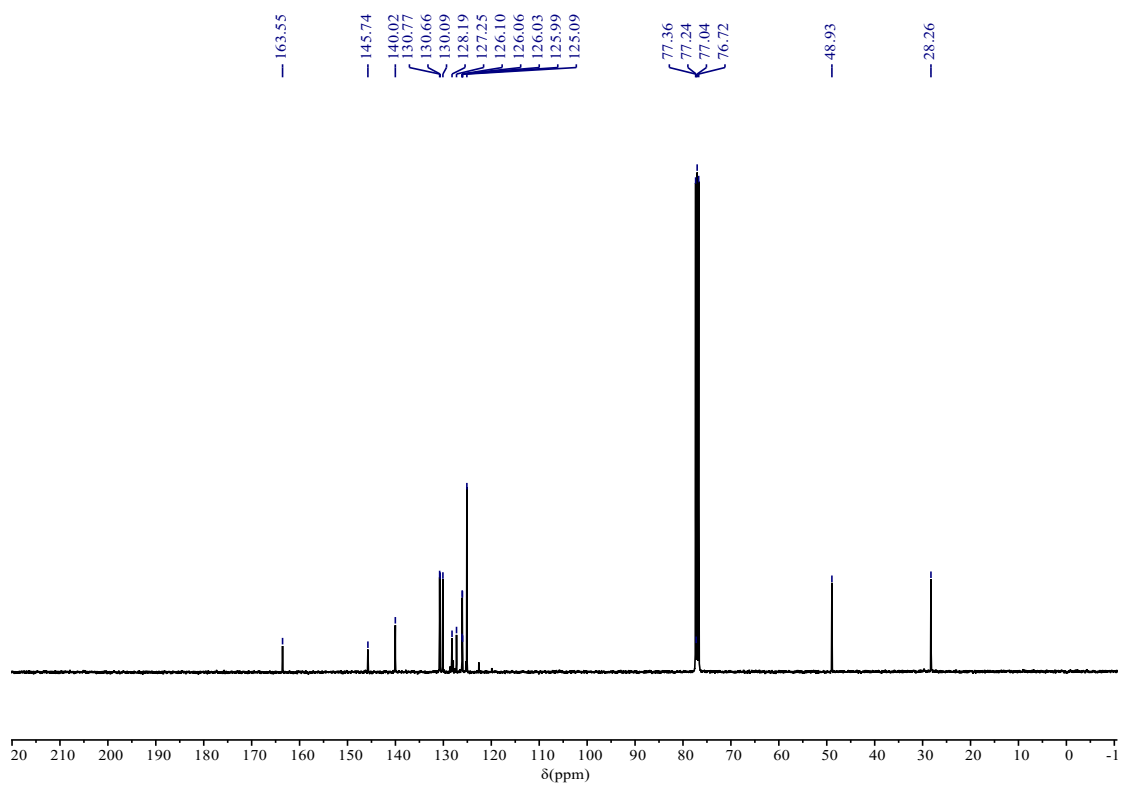


$^{19}\text{F}$  NMR (471 MHz, Chloroform- $d$ ) of 2-(3-fluorophenyl)-6,7-dimethoxy-3,4-dihydroisoquinolin-1(2*H*)-one (2o)

6-bromo-2-(4-(trifluoromethyl)phenyl)-3,4-dihydroisoquinolin-1(2H)-one (2p)

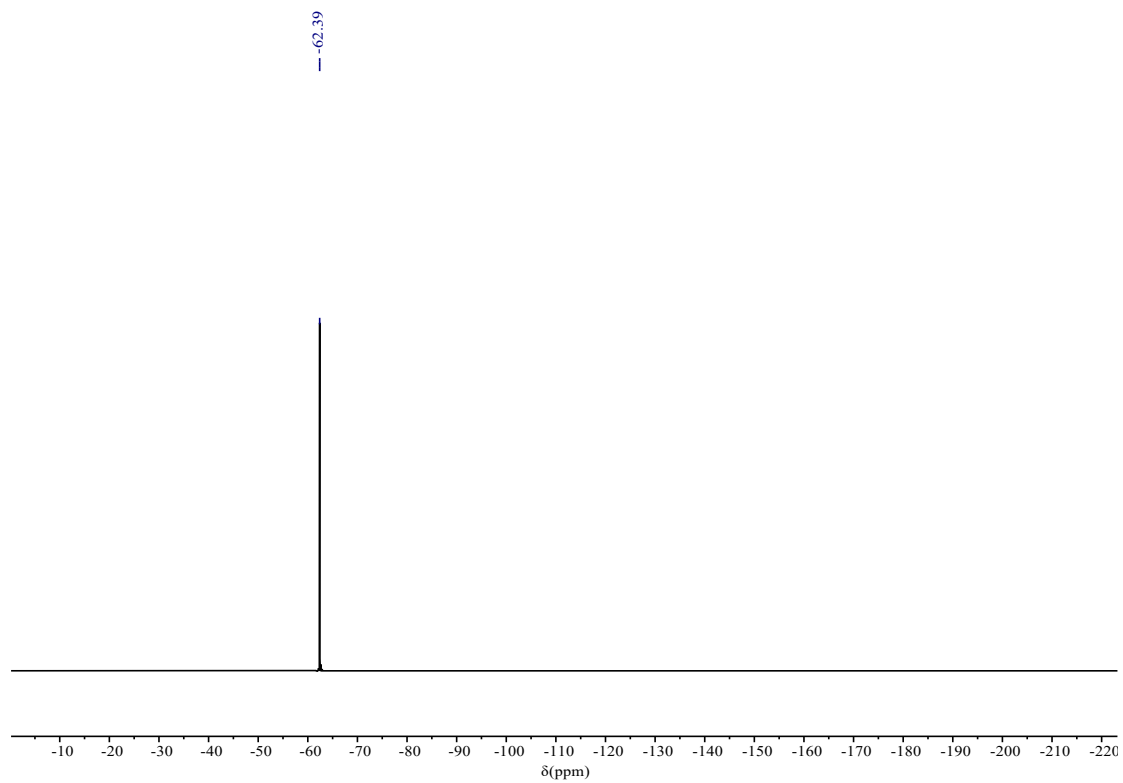


<sup>1</sup>H NMR (500 MHz, Chloroform-*d*) of 6-bromo-2-(4-(trifluoromethyl)phenyl)-3,4-dihydroisoquinolin-1(2H)-one (2p)



<sup>13</sup>C NMR (126 MHz, Chloroform-*d*) of 6-bromo-2-(4-(trifluoromethyl)phenyl)-3,4-dihydroisoquinolin-1(2H)-one (2p)





$^{19}\text{F}$  NMR (471 MHz, Chloroform- $d$ ) of 6-bromo-2-(4-(trifluoromethyl)phenyl)-3,4-dihydroisoquinolin-1(2*H*)-one (2p)